AD-A066 092 GENERAL ELECTRIC CO CINCINNATI OHIO AIRCRAFT ENGINE GROUP F/G 21/5
TURBINE DESIGN SYSTEM.(U)
NOV 78 R R WYSONG, T C PRINCE, D T LENAHAN F33615-75-C-2073
UNCLASSIFIED R78AEG XXX AFAPL-TR-78-92 NL

1 OF 3
ADA
066092

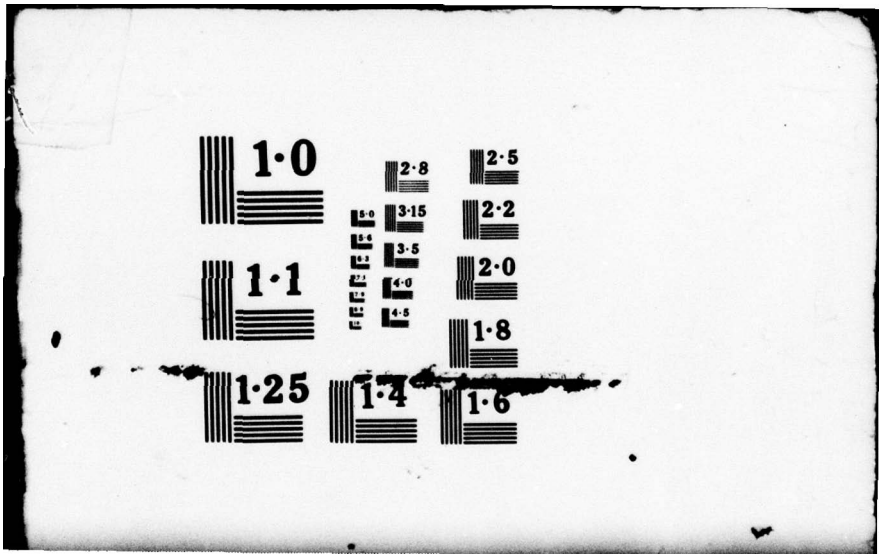
1·0
1·1
1·25
2·8
3·15
3·5
4·0
4·5
2·5
2·2
2·0
1·8
1·4
1·6

AFAPL-TR-78-92

LEVEL II

TURBINE DESIGN SYSTEM

R. R. WYSONG
T. C. PRINCE
D. T. LENAHAN, et al

GENERAL ELECTRIC COMPANY
AIRCRAFT ENGINE GROUP
CINCINNATI, OHIO 45215

NOVEMBER 1978

TECHNICAL REPORT AFAPL-TR-78-92
Final Report 1 November 1975 – 30 November 1977

AIR FORCE AERO PROPULSION LABORATORY
AIR FORCE WRIGHT AERONAUTICAL LABORATORIES
AIR FORCE SYSTEMS COMMAND
WRIGHT-PATTERSON AIR FORCE BASE, OHIO 45433

NOTICE

When Government drawings, specifications, or other data are used for any purpose other than in connection with a definitely related Government procurement operation, the United States Government thereby incurs no responsibility nor any obligation whatsoever; and the fact that the government may have formulated, furnished, or in any way supplied the said drawings, specifications, or other data, is not to be regarded by implication or otherwise as in any manner licensing the holder or any other person or corporation, or conveying any rights or permission to manufacture, use, or sell any patented invention that may in any way be related thereto.

This report has been reviewed by the Information Office (OI) and is releasable to the National Technical Information Service (NTIS). At NTIS, it will be available to the general public, including foreign nations.

This technical report has been reviewed and is approved for publication.

KERVYN D. MACH
Aerospace Engineer

JOSEPH C. HURST, Major, USAF
Chief, Components Branch
Turbine Engine Division

FOR THE COMMANDER

ERNEST C. SIMPSON
Director, Turbine Engine Division

"If your address has changed, if you wish to be removed from our mailing list, or if the addressee is no longer employed by your organization please notify AFAPL/TBC, W-PAFB, OH 45433 to help us maintain a current mailing list".

Copies of this report should not be returned unless return is required by security considerations, contractual obligations, or notice on a specific document.

AIR FORCE/56780/16 February 1979 — 75

UNCLASSIFIED

SECURITY CLASSIFICATION OF THIS PAGE (When Data Entered)

REPORT DOCUMENTATION PAGE

READ INSTRUCTIONS BEFORE COMPLETING FORM

1. REPORT NUMBER: AFAPL-TR-78-92	2. GOVT ACCESSION NO.
3. RECIPIENT'S CATALOG NUMBER	
4. TITLE (and Subtitle): TURBINE DESIGN SYSTEM	5. TYPE OF REPORT & PERIOD COVERED: Final Technical Report, 1 Nov 1975 - 30 Nov 1977
6. PERFORMING ORG. REPORT NUMBER: R78AEGXXX	
7. AUTHOR(s): R.R. Wysong, T.C. Prince, D.T. Lenahan, R.D. Caney, J.S. Keith, D.H. Landis, and L.J. Kues	8. CONTRACT OR GRANT NUMBER(s): F33615-75-C-2073
9. PERFORMING ORGANIZATION NAME AND ADDRESS: General Electric Company, Aircraft Engine Group, Cincinnati, Ohio 45215	10. PROGRAM ELEMENT, PROJECT, TASK AREA & WORK UNIT NUMBERS: 3066-06-26
11. CONTROLLING OFFICE NAME AND ADDRESS: Air Force Aero Propulsion Laboratory (TBC), Air Force Wright Aeroanutical Laboratories, Wright-Patterson AFB, Ohio 45433	12. REPORT DATE: November 1978 13. NUMBER OF PAGES: 177 (213 p.)
14. MONITORING AGENCY NAME & ADDRESS (if different from Controlling Office)	15. SECURITY CLASS. (of this report): Unclassified 15a. DECLASSIFICATION/DOWNGRADING SCHEDULE

16. DISTRIBUTION STATEMENT (of this Report)

Approved for public release; distribution unlimited.

17. DISTRIBUTION STATEMENT (of the abstract entered in Block 20, if different from Report)

18. SUPPLEMENTARY NOTES

19. KEY WORDS (Continue on reverse side if necessary and identify by block number)

Turbine	Cascade Analysis
Preliminary Design	Turbine Blade Section Interpolation
Flowpath	Turbine Blade Heat Transfer Analysis
Axisymmetric Analysis	Turbine Blade Stress Analysis
Turbine Blade Design	Mission Life Analysis (continued)

20. ABSTRACT (Continue on reverse side if necessary and identify by block number)

A time-sharing computer system has been developed which provides for the interactive design and analytical performance evaluation of aircraft engine turbines. The sytem is modularized to permit the user to deal with one functional aspect of the design at a time; twelve modules are employed to encompass the turbine aerodynamic, heat transfer, and mechanical design. The analytical and numerical methods employed in each module, and their theoretical basis, are presented in this report.

DD FORM 1 JAN 73 1473 EDITION OF 1 NOV 65 IS OBSOLETE

UNCLASSIFIED

SECURITY CLASSIFICATION OF THIS PAGE (When Data Entered)

403 468

79 03 19 054

19. (concluded)

Computer Program
Data Base
Time-Sharing

FOREWORD

This final report describes computer program development effort conducted by personnel of the General Electric Company, Aircraft Engine Group, Cincinnati, Ohio, under Contract F33615-75-C-2073, Project 3066, with the Air Force Aero Propulsion Laboratory, Wright-Patterson Air Force Base, Ohio. Dr. Kervyn D. Mach (AFAPL/TBC) was the Air Force Project Engineer.

The work reported herein was performed during the period 1 November 1975 to 30 November 1977. The report was released by the authors in December 1977.

The General Electric Program Manager was A.L. Meyer, the Technical Program Manager was J.S. Keith; the Principal Investigator was R.R. Wysong, who compiled this report. Authors of the sections of the report which describe the various program modules are as follows:

R.R. Wysong	-	Preliminary Flowpath Design, Blade Design, Blade Stacking
T.C. Prince	-	Axisymmetric Analysis
D.T. Lenahan	-	Interstage Gas Temperature Profiles, Blade Heat Flux Potential, Cooling Flow Rate Prediction
R.D. Caney and J.S. Keith	-	Airfoil Pressure Distribution
W.E. Miller and D.H. Landis	-	Airfoil Properties, Airfoil Stress, Mission Life
L.J. Kues	-	Integrated Data Base

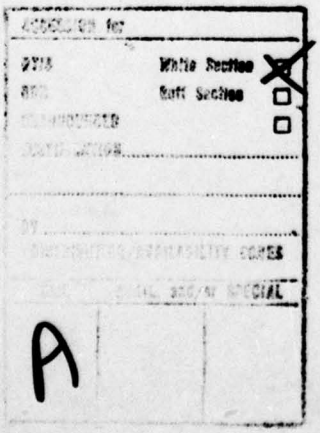

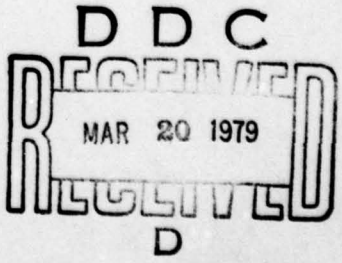

TABLE OF CONTENTS

TABLE OF CONTENTS (Continued)

TABLE OF CONTENTS (Continued)

TABLE OF CONTENTS (Continued)

TABLE OF CONTENTS (Concluded)

LIST OF ILLUSTRATIONS

LIST OF ILLUSTRATIONS (Concluded)

1.0 INTRODUCTION

Modern turbine engine design has evolved into an extremely complex science. Aerodynamic, heat transfer, and structural analyses are continually being developed, refined, and integrated into comprehensive component and engine design systems. As the analyses have advanced, they generally become more detailed and extensive; therefore, in the interest of productivity they have been programmed for solution by digital computer.

Individual, batch-type computer programs for each facet of the analysis yield a tremendous saving in human labor, but they still require someone to prepare the data, punch the input cards, interpret the output, and repeat the process for the next program. The actual computation may require a few seconds or minutes while the human labor is measured in hours or days and the possibility of an error being introduced is always present.

The time sharing and data handling facilities available on modern computer systems provide the capability to greatly reduce or even eliminate the labor involved in generating the information necessary for final design decisions, thereby freeing the engineer to do what he was hired to do: to make decisions. Sophisticated data storage and retrieval systems exist which will handle the transfer of data from one program to another. Interactive programming via a time sharing terminal enables the user to monitor the results of each step, change the input if he wishes, and guide the computation through the sequence of steps appropriate to the problem. The potential improvement in productivity is tremendous.

The purpose of the Turbine Design System (hereafter referred to as TDS) is to provide a system for the interactive design and performance evaluation of aircraft engine turbines. The system is oriented toward preliminary design and offers "quick look" calculations of flowpath configuration, design point and off-design point performance analyses of this configuration, blade and vane airfoil contour design, blade-to-blade flowfield analysis, intermediate blade section interpolation, heat transfer analysis to the point of identifying the coolant system technology level required for each blade row, and stress analysis and mission life capability for each blade row. A central, unifying feature of the system is the Integrated Data Base, a sophisticated data storage and retreival facility which can maintain the pertinent information on either a day-to-day or archival basis. Special support software has been developed to enhance input and output data file manipulation. The system is modularized to permit the user to deal with one functional aspect of the design process at a time.

Figure 1 shows the overall TDS module structure. This report describes the analytical and, where necessary, the numerical methods employed in each of the modules. A User's Manual devoted to the detailed execution of the system modules is a companion volume to this report.

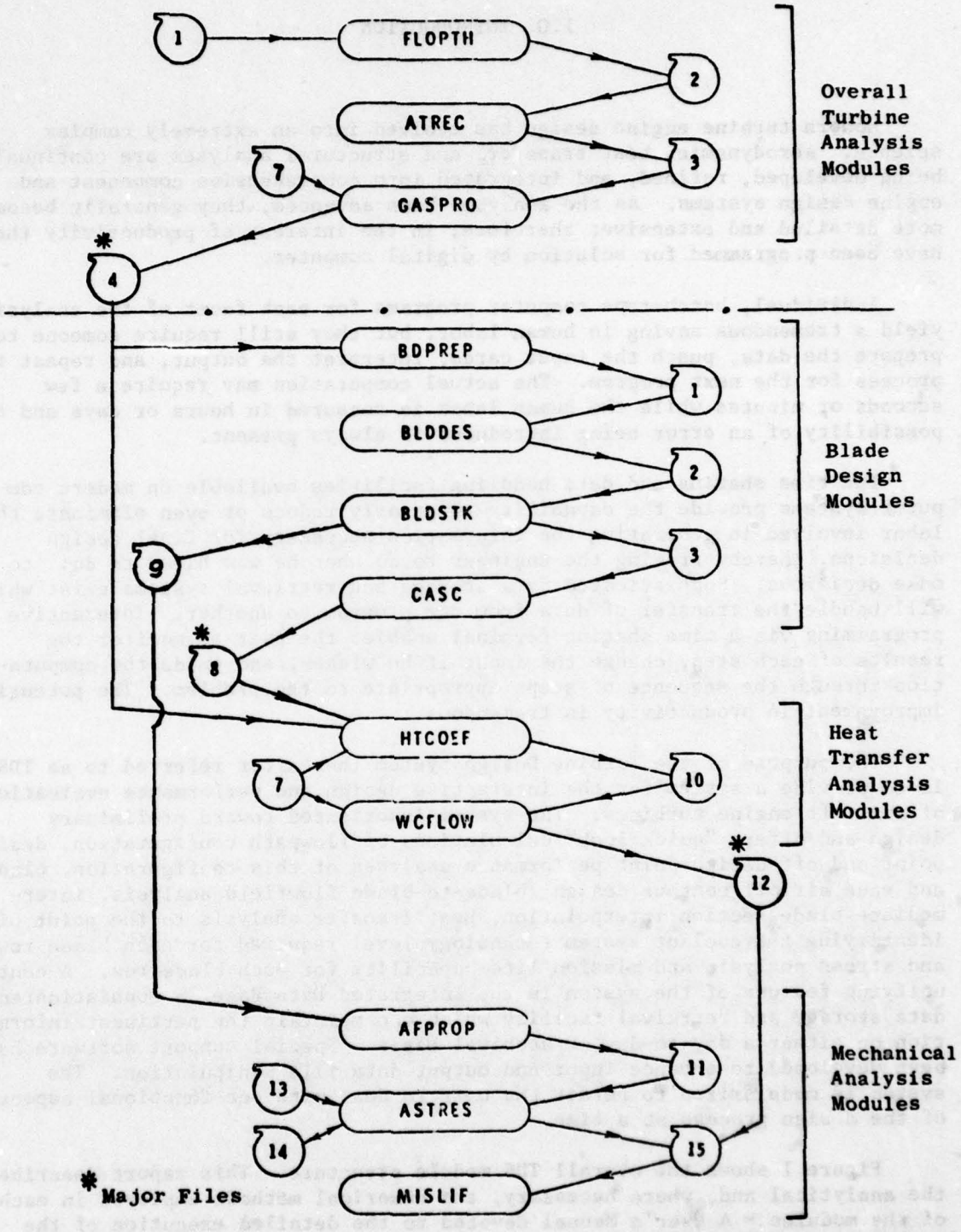

Figure 1. Module and File Structure.

2.0 PRELIMINARY FLOWPATH DESIGN

2.1 INTRODUCTION

The FLOPTH module includes flowpath design, pitchline vector diagram, and solidity calculations. There are three major calculation subroutines: FLPTH provides the means for proportioning and sizing the elementary flowpath of a turbine; TPA calculates pitchline vector diagrams for making a preliminary assessment of the performance characteristics of the flowpath; SOLDTY calculates the number of blades and vanes in each stage based on vector diagram results and input solidity criteria. A function subprogram entitled CPX, working in conjunction with an interpolation routine, provides specific heat data for a broad range of thermodynamic conditions to satisfy the needs of the major routines. Printed and plotted output is available at appropriate points in the program to provide a review of the results. The organization of the module permits user-governed iteration to achieve a favorable configuration. This module is an extension of the methods of Reference 1.

2.2 FLOWPATH DESIGN

The proportioning and sizing of the elementary flowpath is performed by the FLPTH routine. The notion of "elementary" in this context is that the resultant flowpath is simply a "stick" model of a real machine; this is borne out in the plot which is associated with this routine. The endwalls are piecewise networks of cylindrical and conical surfaces; the blade rows appear as line segments at leading and trailing edges. Program capacity accommodates a turbine of up to ten full stages or of nine full stages plus an outlet guide vane row.

Some preliminary calculations are necessary to get the routine started. First, a gas constant for the flowing medium is calculated as

$$RG = \frac{RGA + FAR \cdot RGF}{1 + FAR} \qquad (1)$$

where: RGA = 53.347602 ft lb/lb/°R = gas constant for air

RGF = 55.087694 ft lb/lb/°R = gas constant for JP4 fuel

FAR = fuel/air ratio

FAR = 0 means dry air is the flowing medium.

The work extraction for each stage, in terms of total enthalpy drop per pound of flowing medium, is calculated from total work extraction and energy

split input data. The pitchline reaction for each stage is converted to a fraction using the input percent values. Reaction, as used herein, is defined as

$$RXP = 1 - \frac{1 - \left(\frac{P_1}{P_{T_0}}\right)^{\frac{\gamma-1}{\gamma}}}{1 - \left(\frac{P_2}{P_{T_0}}\right)^{\frac{\gamma-1}{\gamma}}} \qquad (2)$$

where: P_1 = vane exit static pressure
P_{T_0} = vane inlet total pressure
P_2 = blade exit static pressure

The ratio of specific heats, γ, is calculated for the turbine inlet and for each stage exit using total temperatures and work extractions. In each instance, specific heat is first obtained as

$$C_p = f\ (T_T) \qquad (3)$$

where $f(T_T)$ denotes an interpolation process using the CPX routine (discussed in Section 2.5). Then

$$\gamma = \frac{C_p}{C_p - \frac{RG}{788.16}} \qquad (4)$$

where RG is the gas constant of equation (1).

The flowpath calculations begin by calculating the annulus area at the turbine exit plane. First, an exit total temperature is calculated as

$$T_{TVD} = T_{T_0} - \frac{ES}{C_p\ TF} \qquad (5)$$

where: T_{T_0} = total inlet temperature of final stage
ES = desired work extraction of final stage
C_p = average specific heat of the final stage
TF = a test factor
T_{TVD} = vector diagram exit total temperature

The test factor takes cognizance of the fact that a turbine stage designed to a given vector diagram will not yield the full work extraction

implied by that vector diagram. This discrepancy occurs because of losses which occur in the real machine that are unaccountable in the mathematical model. Three-dimensional effects such as secondary flows are the chief culprits. The test factor array is preset internally to unity but can be altered, stage by stage, by user input.

An exit absolute Mach number is calculated from input values of desired exit axial Mach number and swirl, i.e.

$$XMA = \frac{XMF}{\cos \Gamma} \tag{6}$$

where Γ is the absolute value of the swirl angle. Exit total pressure is calculated from turbine inlet total pressure and overall total pressure ratio input data. Exit weight flow is calculated by summing the input values of turbine inlet weight flow and coolant flows injected into the mainstream. A flow function of the form

$$\frac{W\sqrt{T_{TVD}}}{P_{TX}A} = \sqrt{\frac{\gamma g}{RG}} \frac{XMA}{\left[1 + \frac{\gamma-1}{2}(XMA)^2\right]^{\frac{\gamma+1}{2(\gamma-1)}}} \tag{7}$$

is manipulated to yield the area A associated with XMA. Finally, the exit plane annulus area is calculated as

$$A_{AN} = \frac{A}{\cos \Gamma} \tag{8}$$

The outer radius of the exit plane is set by using the input maximum diameter, i.e.

$$R_o = \frac{DTMAX}{2} \tag{9}$$

The inner radius R_I of the exit plane is calculated using R_o and A_{AN}. The pitchline radius R_p is calculated as the average of R_o and R_I.

Exit plane conditions are completed by calculating the exit static temperature

$$T_X = \frac{T_{TVD}}{1 + \frac{\gamma-1}{2}(XMA)^2} \tag{10}$$

the exit axial velocity

$$C_z = XMF \sqrt{\gamma g RG\, T_x^2} \tag{11}$$

and the exit static pressure

$$P_x = P_{TX} \left(\frac{T_X}{T_{TVD}} \right)^{\frac{\gamma}{\gamma-1}} \tag{12}$$

The axial location of the exit plane is arbitrarily set at an initial value of 100 inches.

The calculation of station radii and axial positions now takes place by working forward from the exit plane. The inner, outer, and pitchline radii and axial positions are stored in doubly subscripted arrays. The first subscript denotes stage, and the second subscript denotes station within a stage. Station designation within a stage is as follows:

Station 1 - vane inlet

Station 2 - vane exit

Station 3 - blade inlet

Station 4 - blade exit

Thus, for example, RO (3,2) defines the outer radius of the third stage vane exit station.

In working forward from one station to the next, say from the i^{th} station to the $(i-1)^{th}$ station, the forward axial position is calculated as

$$Z_{i-1} = Z_i - \frac{H_i}{AR} \tag{13}$$

where: H_i = the height of the aft station

AR = an aspect ratio associated with the region being bridged.

The forward endwall radii are calculated using the form

$$R_{i-1} = R_i - \frac{H_i}{AR} \tan WS \tag{14}$$

where WS is a wall slope associated with the region being bridged.

The aspect ratios and inner and outer wall slopes for blades, vanes, intrablade gaps and intrastage spaces are specified by input. Default values are defined in the User's Manual. Figures 2 and 3 show a typical stage and the associated wall slope and aspect ratio relationships.

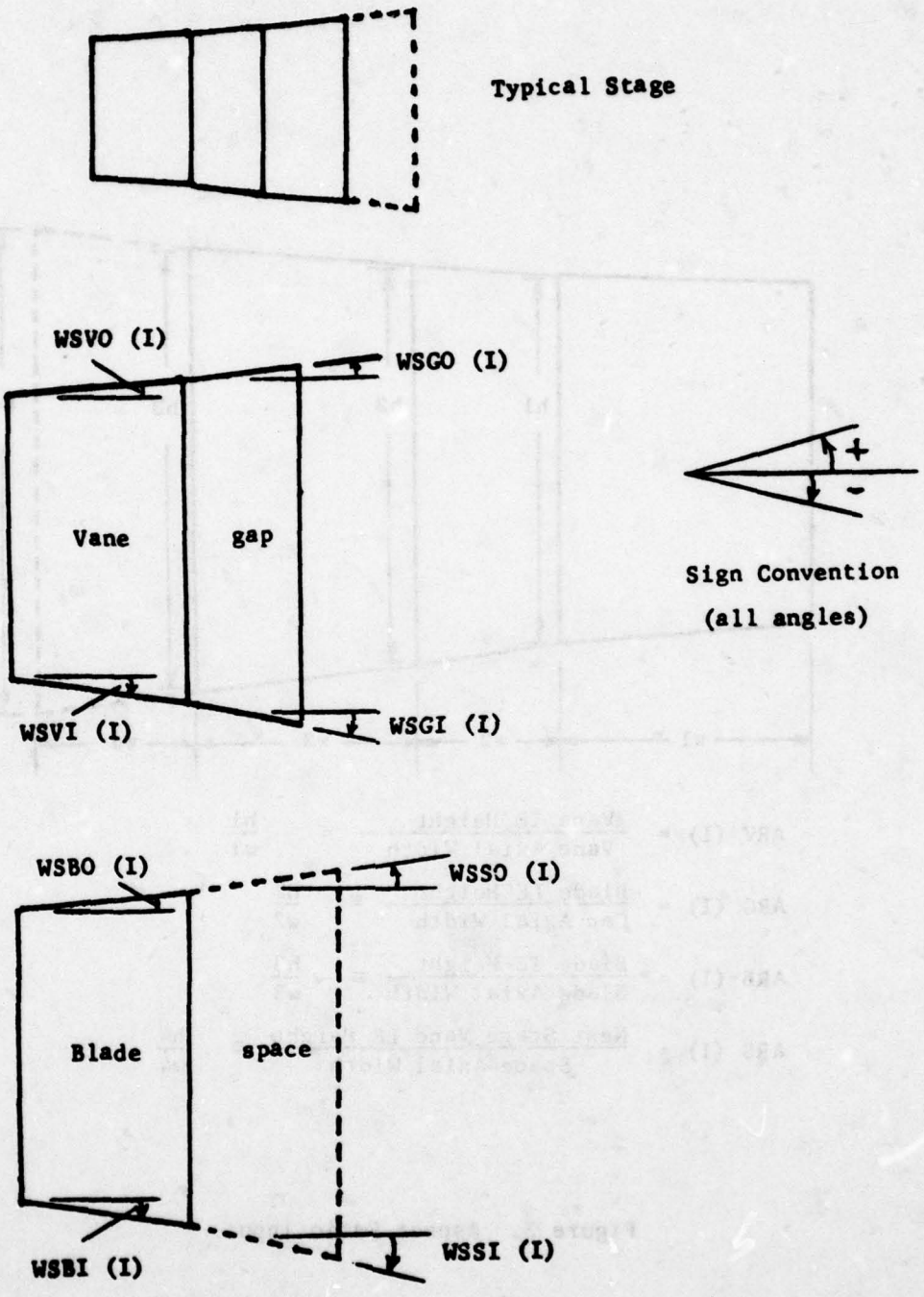

Figure 2. Endwall Slope Input.

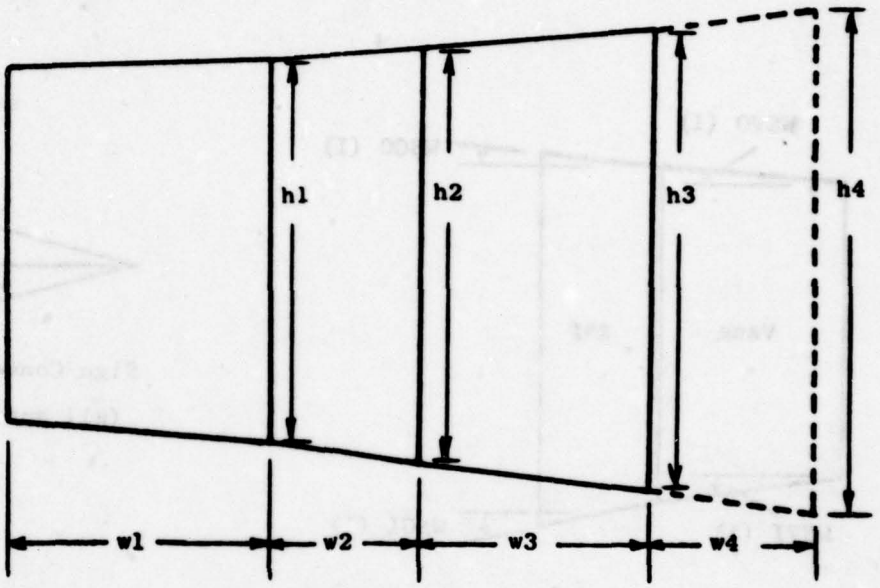

$$ARV\ (I) = \frac{\text{Vane TE Height}}{\text{Vane Axial Width}} \equiv \frac{h1}{w1}$$

$$ARG\ (I) = \frac{\text{Blade LE Height}}{\text{Gap Axial Width}} \equiv \frac{h2}{w2}$$

$$ARB\ (I) = \frac{\text{Blade TE Height}}{\text{Blade Axial Width}} \equiv \frac{h3}{w3}$$

$$ARS\ (I) = \frac{\text{Next Stage Vane LE Height}}{\text{Space Axial Width}} \equiv \frac{h4}{w4}$$

Figure 3. Aspect Ratio Input.

If an outlet guide vane is to be incorporated, the guide vane exit plane becomes the turbine exit. The total temperature for this plane is the same as calculated by equation (5) since no work extraction occurs in the guide vane. The overall total pressure ratio stipulated in the input is assumed to encompass the guide vane. The exit axial Mach number and exit angle from the guide vane are specified by input items OGVEXM and OGVEXA, respectively. Using these data, the exit annulus area is calculated in a similar manner as described above.

The total pressure loss of the outlet guide vane is specified by OGVLOS which is defined as

$$\text{OGVLOS} = \frac{P_T - P_{TX}}{P_T - P} \tag{15}$$

where: P_T = total pressure at exit of the last stage

P = static pressure at exit of the last stage

P_{TX} = total pressure at exit of the guide vane

The exit total pressure is

$$P_{TX} = \frac{P_{TO}}{PRTT} \tag{16}$$

where: PTO = turbine inlet total pressure (input)

PRTT = overall turbine total pressure ratio (input)

The total pressure at exit of the last stage, when an outlet guide vane is present, is

$$P_T = \frac{P_{TX}}{1 - \text{OGVLOS}\left[1 - \left(\frac{T}{T_{TVD}}\right)^{\frac{\gamma}{\gamma-1}}\right]} \tag{17}$$

The outlet guide vane station axial position and endwall radii are calculated as indicated by equations (13) and (14). Input data for wall slopes and aspect ratio are entered with a subscript equal to NSTG+1, where NSTG is the number of full stages.

When all station axial positions and radii have been calculated, attention is given to the inlet plane. First, the annulus area is calculated from inlet plane radii. Then, using input values of inlet weight flow, total temperature, and total pressure, a flow function of the form

$$\frac{W\sqrt{T_{TO}}}{P_{TO}A} = \sqrt{\frac{\gamma g}{RG}} \frac{XMO}{\left[1 + \frac{\gamma-1}{2}(XMO)^2\right]^{\frac{\gamma+1}{2(\gamma-1)}}} \qquad (18)$$

is manipulated and solved by iteration to yield the inlet Mach number, XMO. Inlet static temperature, static pressure, and axial velocity are then calculated by the usual isentropic forms.

The radii and axial positions calculated thus far define the loci of the four stations, 1 thru 4, of each stage. These "stations" are radial lines with constant axial position values and serve to describe the extremities of the blade rows. However, most blades and vanes have tapered axial projections so that leading and trailing edge envelopes do not lie on radial lines. Because of this taper and because the endwalls can be conical, the radii associated with leading and trailing edges are generally different from the "station" radii; hence the annulus areas will differ also. Therefore, the module makes a distinction between "station radii" and "vector diagram radii."

The vector diagram radii are calculated by taking cognizance of the station loci, the endwall slopes, and blade and vane tapers. The taper data are embodied in the input variable BAXWR (blade axial width ratio) and VAXWR (vane axial width ratio). These variables are both defined as the ratio of tip axial width to root axial width. Default values are preset as defined in the User's Manual, but these can be overridden by input entries. The radii thus calculated are used in the vector diagram calculations and are passed on to the ATREC module for its deliberations. Figure 4 depicts a typical situation.

At this point in the program, the entire flowpath is plotted. The stations appear as radial line segments and the blades are shown as axial projections with straight leading and trailing edge envelopes. An option to print a stage-by-stage summary is offered to the user. The diameters shown in this summary are "station diameters." The vector diagram summary which is available later in the program shows the "vector diagram diameters." Following the summary, an option to repeat the flowpath calculation is offered. The user can elect to continue as is, and have the program proceed with vector diagram calculations, or to repeat the flowpath calculation with modified input entered at the terminal.

2.3 VECTOR DIAGRAM CALCULATIONS

The TPA routine is used to calculate pitchline vector diagrams on a stage-by-stage basis. This simplified analysis provides a qualitative assessment of the performance of the flowpath configuration developed in FLPTH.

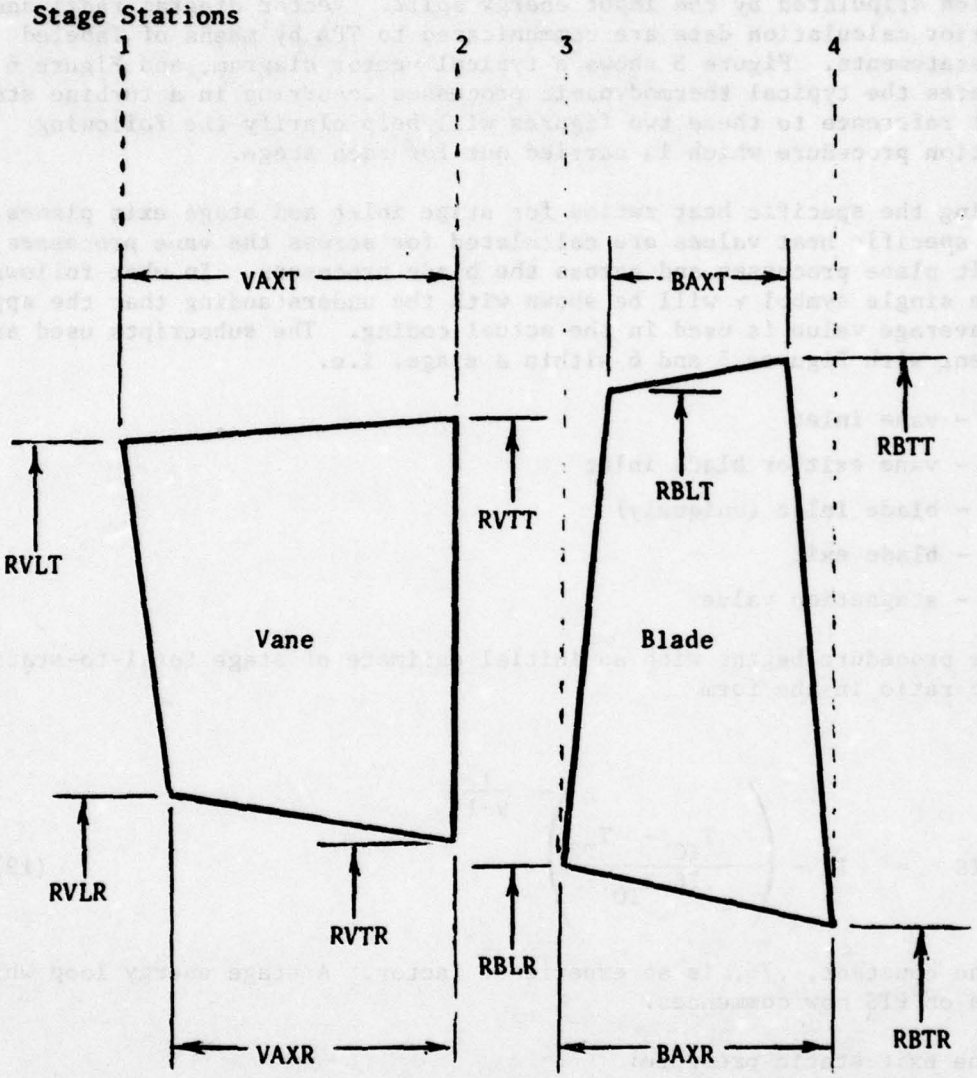

Figure 4. Delineation of "Vector Diagram Radii."

The calculation procedure iterates total to static pressure ratio until the calculated energy extraction is virtually identical to the desired energy extraction stipulated by the input energy split. Vector diagram radii and other prior calculation data are communicated to TPA by means of labeled COMMON statements. Figure 5 shows a typical vector diagram, and Figure 6 illustrates the typical thermodynamic processes occurring in a turbine stage. Frequent reference to these two figures will help clarify the following calculation procedure which is carried out for each stage.

Using the specific heat ratios for stage inlet and stage exit planes, average specific heat values are calculated for across the vane processes, vane exit plane processes and across the blade processes. In what follows, only the single symbol γ will be shown with the understanding that the appropriate average value is used in the actual coding. The subscripts used are consistent with Figures 5 and 6 within a stage, i.e.

0 - vane inlet

1 - vane exit or blade inlet

1A - blade inlet (uniquely)

2 - blade exit

T - stagnation value

The procedure begins with an initial estimate of stage total-to-static pressure ratio in the form

$$PTS = 1 - \left(\frac{T_{TO} - T_{T2}}{.76\ T_{TO}} \right)^{-\frac{\gamma}{\gamma-1}} \tag{19}$$

where the constant, .76, is an experience factor. A stage energy loop which iterates on PTS now commences.

Vane exit static pressure:

$$P_1 = P_{TO} \left\{ 1 - \left[1 - \left(\frac{1}{PTS} \right)^{\frac{\gamma-1}{\gamma}} \right] \left[1 - R_{xp} \right] \right\}^{\frac{\gamma-1}{\gamma}} \tag{20}$$

where R_{xp} is pitchline reaction (input).

Vane exit static temperature:

$$T_1 = T_{TO} \left\{ 1 - \eta_N \left[1 - \left(\frac{P_1}{P_{TO}} \right)^{\frac{\gamma-1}{\gamma}} \right] \right\} \tag{21}$$

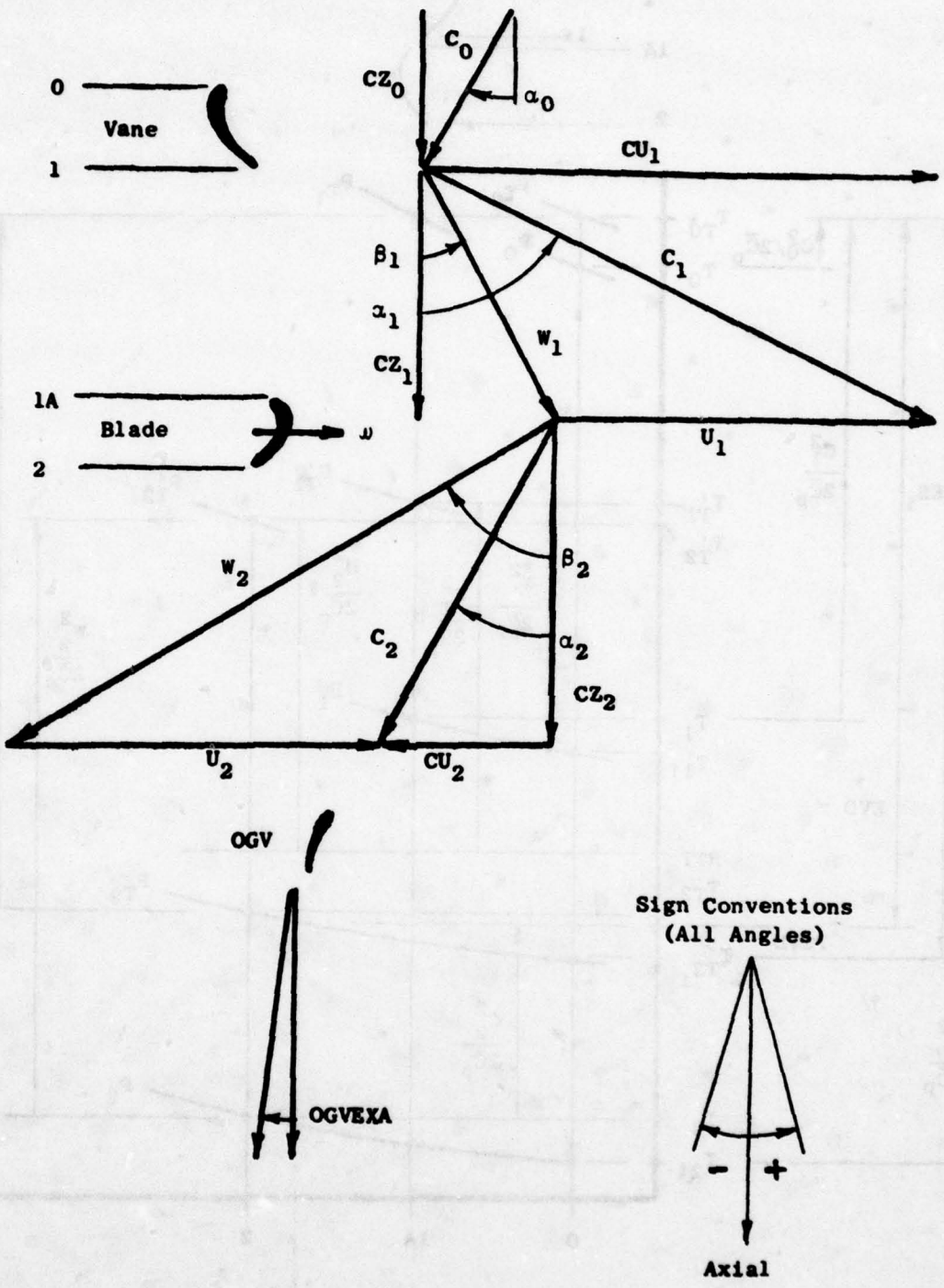

Figure 5. Typical Vector Diagram.

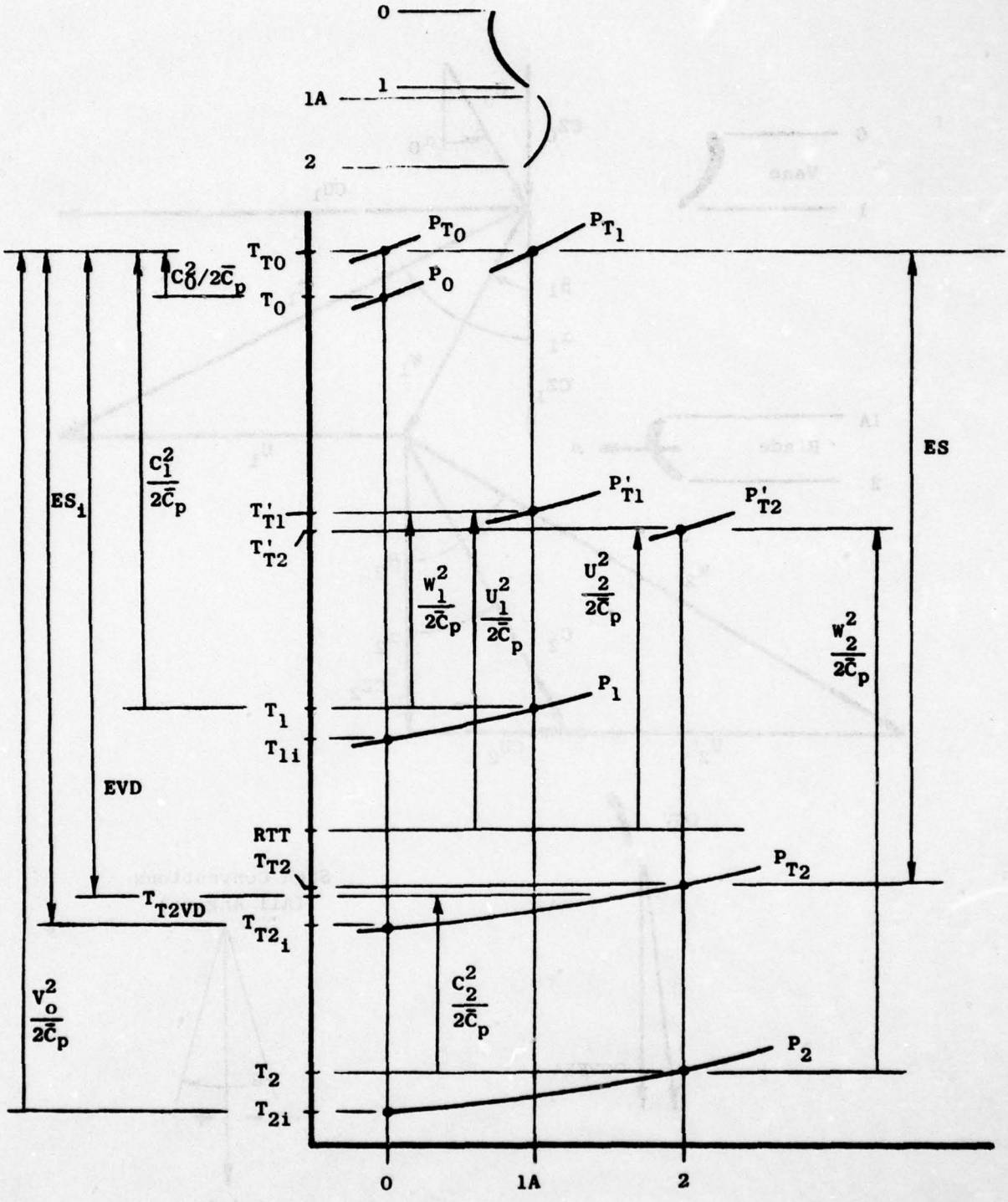

Figure 6. Typical Temperature-Pressure Diagram.

where η_N = vane efficiency (input or 0.97 default).

Vane exit density:

$$\rho = \frac{144\ P_1}{RG \cdot T_1} \tag{22}$$

Vane exit weight flow:

$$WF_1 = WF_o + \frac{WG \cdot DWGV}{100} \tag{23}$$

where: WF_o = current stage inlet flow

WG is turbine inlet flow

DWGV = vane coolant flow added to mainstream in terms of percent WG (input or 0. default)

Blade inlet axial velocity:

$$CZ_{1A} = \frac{WF_1}{\rho_1\ A_{1A}} \tag{24}$$

where A_{1A} = annulus area based on blade inlet radii.

Blade inlet absolute velocity:

$$C_1 = \sqrt{2g\ JC_p\ (T_{TO} - T_1)} \tag{25}$$

Blade inlet absolute flow angle:

$$\alpha_1 = \tan^{-1}\left(\frac{CZ_{1A}}{C_1}\right) \tag{26}$$

Blade inlet absolute tangential velocity:

$$CU_1 = C_1\ \sin\ \alpha_1 \tag{27}$$

Blade inlet RCU:

$$RCU_1 = \frac{R_{P1A}\ CU_1}{12} \tag{28}$$

where R_{P1A} = blade inlet pitchline radius.

Blade inlet wheel speed:

$$U_1 = \frac{R_{P1A}\ \omega}{12} \tag{29}$$

where $\omega = \frac{\pi\ RPM}{30}$ (30)

and RPM = shaft rotational speed (input).

Temperature equivalent of rothalpy:

$$R_{TT} = T_{TO} - \frac{RCU_1\ \omega}{g\ J\ C_p} \tag{31}$$

Blade inlet relative total temperature:

$$T_{T1P} = R_{TT} + \frac{U_1^2}{2g\ J\ C_p} \tag{32}$$

Blade inlet relative total pressure:

$$P_{T1P} = P_1 \left(\frac{T_{T1P}}{T_1}\right)^{\frac{\gamma}{\gamma-1}} \tag{33}$$

Blade inlet relative velocity:

$$W_1 = \sqrt{2g\ J\ C_p\ (T_{T1P} - T_1)} \tag{34}$$

Blade exit static pressure:

$$P_2 = \frac{P_{TO}}{PTS} \tag{35}$$

Blade exit static temperature:

$$T_2 = T_{T1P}\left\{1 - \eta_B\left[1 - \left(\frac{P_2}{P_{T1P}}\right)^{\frac{\gamma-1}{\gamma}}\right]\right\} \tag{36}$$

where η_B is blade efficiency (input or .95 default).

Blade exit vector diagram total temperature:

$$T_{T2VD} = T_{TO} - \frac{ES}{C_p\ TF} \tag{37}$$

where ES = desired stage work extraction (input)

TF = test factor (input or 1.0 default)

Blade exit absolute velocity:

$$C_2 = \sqrt{2g\ J\ C_p\ (T_{T2VD} - T_2)} \tag{38}$$

Blade exit density:

$$\rho_2 = \frac{144\ P_2}{RG \cdot T_2} \tag{39}$$

Blade exit weight flow:

$$WF_2 = WF_1 + \frac{WG \cdot DWGB}{100} \tag{40}$$

where WF_1, comes from equation (23)

DWGB = blade coolant flow added to mainstream in terms of percent WG (input or 0. default)

Blade exit axial velocity:

$$CZ_2 = \frac{WF_2}{\rho_2\ A_2} \tag{41}$$

where A_2 is annulus area based on blade exit radii.

Blade exit absolute angle:

$$\alpha_2 = \tan^{-1}\left(\frac{CZ_2}{C_2}\right) \tag{42}$$

Blade exit wheel speed:

$$U_2 = \frac{R_{P2}\ \omega}{12} \tag{43}$$

where R_{P2} is pitchline radius from FLPTH.

Blade exit relative total temperature:

$$T_{T2P} = R_{TT} + \frac{U_2^2}{2g\ J\ C_p} \tag{44}$$

Blade exit relative total pressure:

$$P_{T2P} = P_2 \left(\frac{T_{T2P}}{T_2} \right)^{\frac{\gamma}{\gamma-1}} \tag{45}$$

Blade inlet relative velocity:

$$W_2 = \sqrt{2g\ J\ C_p\ (T_{T2P} - T_2)} \tag{46}$$

Blade exit relative flow angle:

$$\beta_2 = - \tan^{-1} \left(\frac{CZ_2}{W_2} \right) \tag{47}$$

where the sign suits the convention of Figure 5.

Blade exit relative tangential velocity:

$$WU_2 = W_2 \sin \beta_2 \tag{48}$$

Blade exit absolute tangential velocity

$$CU_2 = WU_2 + U_2 \tag{49}$$

If CU_2 is a negative value, α_2 is set negative to match the convention of Figure 5.

Blade exit RCU:

$$RCU_2 = \frac{R_{P2}\ CU_2}{12} \tag{50}$$

Vector diagram implied energy extraction:

$$EVD = \frac{\omega}{gJ} (RCU_1 - RCU_2) \tag{51}$$

The calculated energy extraction is, therefore:

$$ESC = TF \cdot EVD \tag{52}$$

where TF is the test factor (input or 1.0 default).

The calculated energy extraction, ESC, is compared with the desired energy extraction, ES. If the difference is equal to or less than .00001% of ES, the stage energy loop terminates; otherwise, the loop is repeated with a new value of total to static pressure ratio calculated as

$$PTS\ (new) = PTS\ (old) \cdot \frac{ES}{ESC} \tag{53}$$

which reflects the idea that if calculated energy extraction is too low, the pressure ratio needs to be increased. Experience with the routine for a

variety of cases has shown that the stage energy loop converges in the range of six to eleven iterations.

A variation in this procedure is necessary for the final stage. Having both reaction and exit swirl as input items overspecifies the situation. Therefore, the input reaction for the final stage is treated as a "first guess" for an iteration process. Upon convergence of the stage energy loop with this input reaction, the exit angle α_2 of equation (42) is compared with the specified exit swirl angle, SWRLF. If α_2 is within ±0.1 degree of SWRLF, complete convergence is assumed and summary calculations commence. If α_2 does not meet this criterion, the reaction is adjusted and the stage energy loop is repeated. A coarse reaction adjustment of 1/2 percent is used if α_2 differs from SWRLF by more than 0.3 degree; otherwise, the adjustment is 1/4 percent. The adjustment is positive, i.e., the reaction is increased, if α_2 is more positive than SWRLF. Figure 7 depicts the process. This nested loop convergence scheme involves only simple algebraic calculations and, hence, executes rapidly. SWRLF and RXP are reset to the converged values for summary printout and output file processing.

When the stage energy iteration is complete, inlet conditions to the next stage (if there is one) are calculated and the above procedure is applied to the new stage.

When all stages have been calculated, an option to obtain a detailed vector diagram printout is offered. This printout has three pages per stage plus a final page for an overall summary. In general, only pitchline values appear; there are a few items, however, which show both root and pitch values. These root values are calculated on the basis of free vortex flow, i.e. by assuming that work extraction, axial velocities, and RCU are constant radially. For completeness, some auxiliary parameters are calculated. The more obvious of these, such as Mach numbers and turning angles, will not be shown here. The less obvious are defined for reference.

At vane inlet stations, the variables printed are those used in the vector diagram calculations. At vane exit stations, the variables printed are recalculated to reflect any annulus area differences between vane exit and blade inlet. During vector diagram calculations, blade inlet values were used to assure correct blade energy extraction results. Variables affected are axial velocity, absolute angle, and RCU. Using free vortex assumptions, a reference root reaction is calculated at blade inlet stations in the form

$$RXR = \frac{1 - RXP}{\left(\frac{R_R}{R_p}\right)^2 \sin^2 \alpha_{IR} + \cos^2 \alpha_{IR}} \qquad (54)$$

where: R_R = root radius

R_p = pitch radius

α_{1R} = root exit angle calculated from

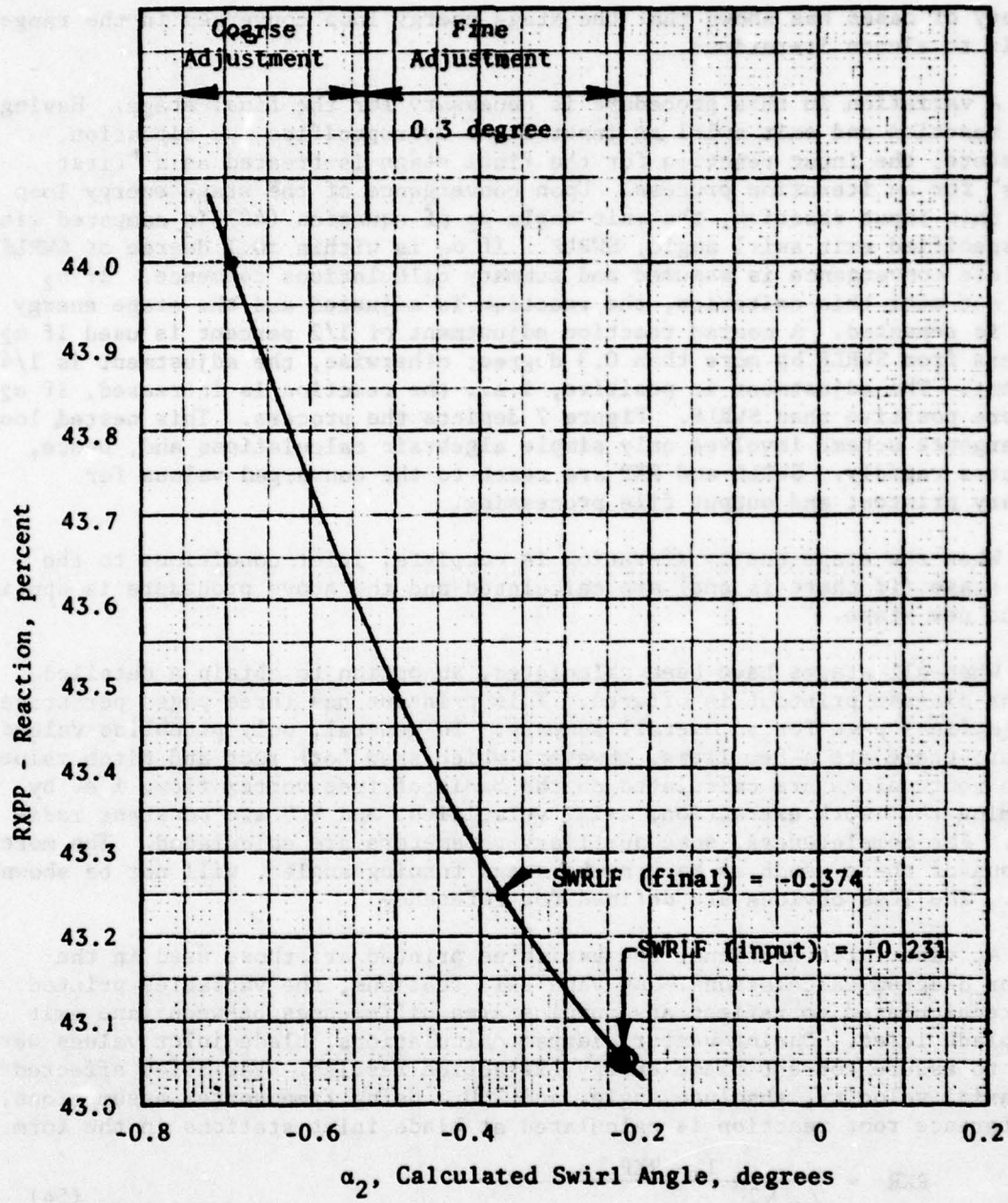

Sample Case:

	Initial	1st Iteration	2nd Iteration
RXRP	44.0	43.5	43.25
α_2	-0.691	-0.501	-0.374

Figure 7. Reaction Iteration for Final Stage.

$$\alpha_{1R} = \tan^{-1}\left[\left(\frac{R_R}{R_p}\right)\tan\alpha_{1P}\right] \tag{55}$$

where α_{1P} is pitchline exit angle.

A variety of stage summary parameters are calculated and printed.

Stage inlet flow function:

$$FF = \frac{WF\sqrt{T_{TO}}}{P_{TO}} \tag{56}$$

Stage speed parameter:

$$RPMT = \frac{R_{PM}}{\sqrt{T_{TO}}} \tag{57}$$

Stage energy parameter:

$$EST = \frac{ES}{T_{TO}} \tag{58}$$

Stage exit flow function:

$$FF_x = \frac{WF_x\sqrt{T_{T2VD}}}{P_{T2}} \tag{59}$$

Stage pitchline loading:

$$PCHLDG = \frac{gJ \cdot ES}{2\bar{U}_p^2} \tag{60}$$

where $\bar{U}_p$ is average pitchline wheel speed.

Stage root loading:

$$HUBLDG = \frac{gJ \cdot ES}{2\bar{U}_R^2} \tag{61}$$

where $\bar{U}_R$ is average root wheel speed.

Stage flow coefficient:

$$CZOU = \frac{CZ_2}{U_2} \tag{62}$$

Stage wheel speed parameter:

$$UVO = \frac{\bar{U}_p}{V_o} \tag{63}$$

where V_o is stage isentropic velocity calculated from

$$V_o = \sqrt{2gJ\ C_p\ T_{TO}\left[1 - \left(\frac{P_2}{P_{TO}}\right)^{\frac{\gamma-1}{\gamma}}\right]} \tag{64}$$

Stage total-total efficiency:

$$\eta_T = \frac{ES}{C_p\ T_{TO}\left[1 - \left(\frac{P_{T2}}{P_{TO}}\right)^{\frac{\gamma-1}{\gamma}}\right]} \tag{65}$$

Stage total-to-static efficiency:

$$\eta_S = \frac{ES}{C_p\ T_{TO}\left[1 - \left(\frac{P_2}{P_{TO}}\right)^{\frac{\gamma-1}{\gamma}}\right]} \tag{66}$$

Stage horsepower:

$$HP = \frac{J \cdot WF \cdot ES}{550} \tag{67}$$

Stage torque:

$$TORQ = \frac{J \cdot WF \cdot ES \cdot \bar{R}_p}{12\ \bar{U}_p} \tag{68}$$

where $\bar{R}_p$ is average blade pitchline radius.

The vector diagram printout concludes with a summary page which includes parameters calculated in a similar fashion as above for overall turbine results. The pitchline vector diagrams are now plotted stage-by-stage. Annotations for these plots are MACH numbers. The wheel speed vectors are annotated with equivalent MACH numbers for consistency's sake.

This concludes the TPA routine. An option to continue as is or to repeat the calculations is offered. If the repeat option is elected, program control returns to the very beginning of the module and terminal input is requested. When the input has been entered and read, the program recalculates the case, starting with the flowpath routine FLPTH. If the continue option is elected, the SOLDTY routine is executed.

2.4 SOLIDITY CALCULATIONS

The SOLDTY routine provides a calculation of the number of vanes and blades to be used in the blade rows of the turbine described by the flowpath. The solidity criteria to be used in establishing these numbers are input by the user in one of two ways. The first way is to specify incompressible Zweifel factors for each vane and blade row. The second way is to enter tables of throat-to-width ratios versus turning angles, where the turning angle data encompass broad enough ranges to permit interpolation at internally calculated values. Blading flow coefficients associated with the tabular input approach may also be input by the user.

These two ways of specifying solidity criteria can be intermixed, i.e., both can appear in the input for a given case. Thus Zweifel parameters can be specified for one or more blade rows, and tabular data can be specified for the other blade rows. The Zweifel number arrays, ZWIV for vanes and ZWIB for blades, are preset internally to an arbitrary large number prior to reading the input file so that user intent can be interpreted properly. The input data of either form are supplemented by angles, radii, and axial station data calculated in the FLPTH and TPA routines.

Where the incompressible Zweifel parameter, ZWIV, is specified, the number of vanes in the row is calculated as

$$N_v = \frac{8\pi R_{p1} \cos \alpha_1 \left[\left(\frac{h_1}{h_o} \right) \cos \alpha_1 \tan \alpha_o - \sin \alpha_1 \right]}{AW \cdot ZWIV \cdot \left(1 + \frac{h_o}{h_1} \right)} \tag{69}$$

where:

R_{p1} = vane exit pitchline radius

α_o = vane inlet angle

α_1 = vane exit angle

AW = vane axial width

h_o = vane inlet annulus height

h_1 = vane exit annulus height

When the incompressible Zweifel parameter, ZWIB, is specified, the number of blades in the row is calculated as

$$N_B = \frac{8\pi R_{p2} \cos \beta_2 \left[\left(\frac{h_2}{h_{1A}} \right) \cos \beta_2 \tan \beta_1 - \sin \beta_2 \right]}{AW \cdot ZWIB \cdot \left(1 + \frac{h_{1A}}{h_2} \right)} \tag{70}$$

where:

R_{p2} = blade exit pitchline radius
β_1 = blade inlet relative angle
β_2 = blade exit relative angle
h_{1A} = blade inlet annulus height
h_2 = blade exit annulus height

Figure 8 shows the sign conventions used for angles in all SOLDTY calculations.

The following derivation shows how the tabular values of throat-to-width ratio and turning angle are used. Throat size is estimated from vector diagram data as

$$THR = \frac{P \cos \alpha \sqrt{\eta}}{CFV} \tag{71}$$

where: P = the tangential spacing (pitch) of the blades
α = the bladerow exit angle
η = the blading efficiency
CFV = the blading flow coefficient

The tangential spacing, or pitch, is

$$P = \frac{\pi D}{N} \tag{72}$$

where: D = diameter
N = number of blades

Dividing equation (71) by axial width AW, combining the result with (72) and rearranging yields a general form for the number of blades as

$$N = \frac{\pi D \cos \alpha \sqrt{\eta}}{CFV \cdot AW \cdot \left(\frac{THR}{AW}\right)} \tag{73}$$

Equation (73) is particularized for vanes and for blades in the program. Pitchline diameter and axial width come from FLPTH results. Exit angles α_1 or β_2 come from TPA results. Blading efficiency and flow coefficient are input items. Turning angles $\Delta\alpha$ or $\Delta\beta$ are calculated from TPA results and used to interpolate the tabular input data, as indicated in Figure 9, to get the throat-to-axial width ratio.

Whenever the number of vanes, N_V, or number of blades, N_B, is an odd number, the program automatically increases the result by one to get an even number. The final step is to calculate the Zweifel parameter for the blade row. Thus, no matter which style of input is used, the printed output has

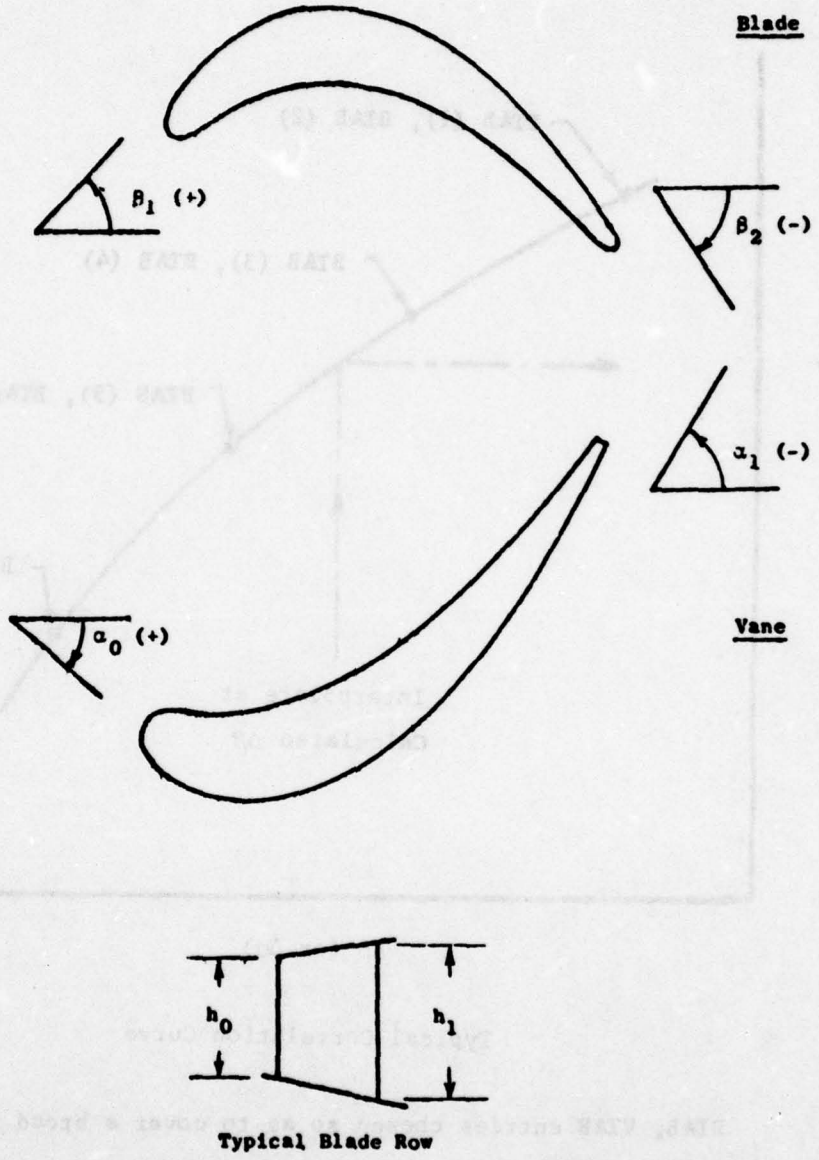

Figure 8. Conventions Used for Zweifel Calculations.

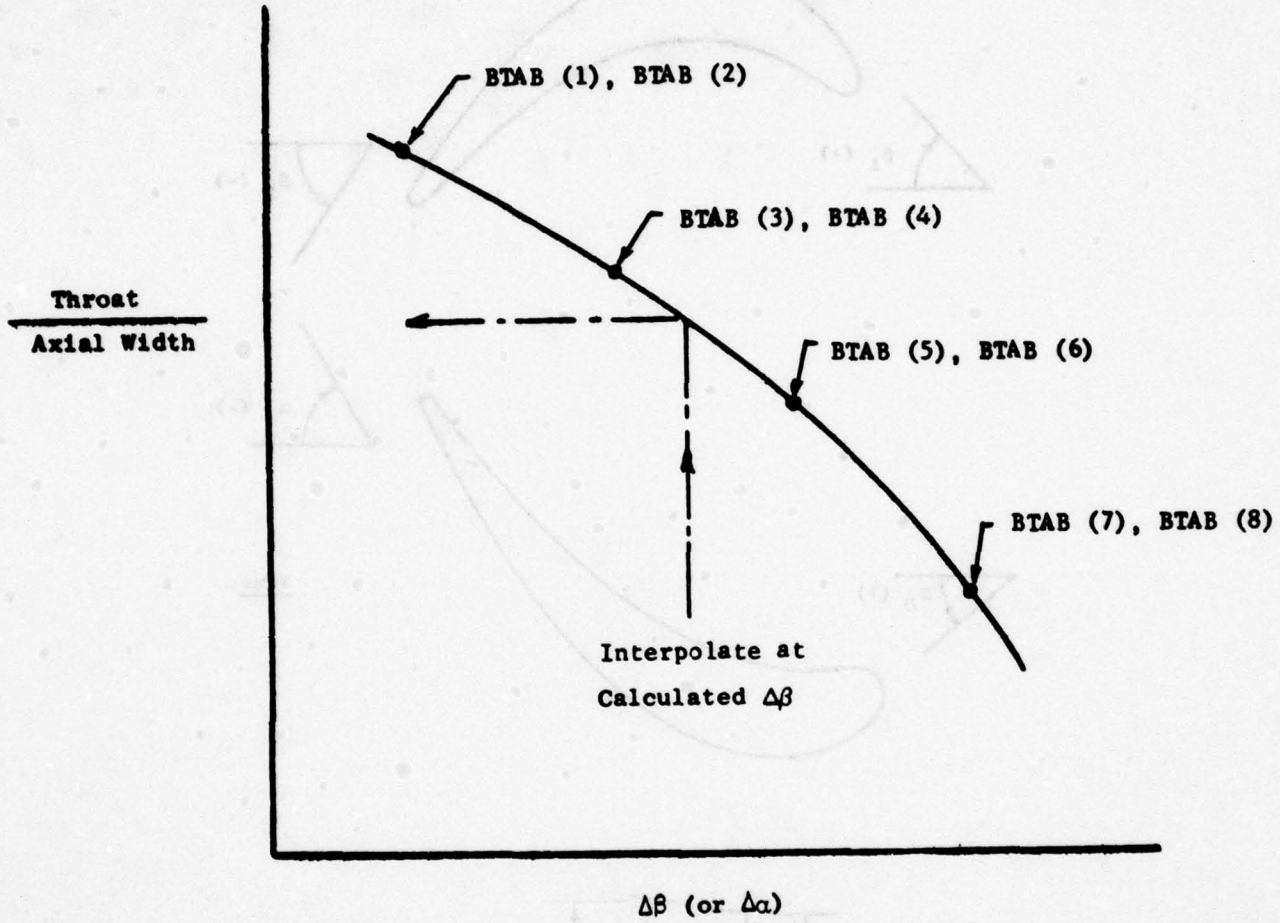

Typical Correlation Curve

BTAB, VTAB entries chosen so as to cover a broad range of turning angle

Figure 9. BTAB, VTAB Input.

Zweifel parameter values which are consistent with the number of blades or vanes shown.

For reference in preparing input or evaluating output, the Zweifel parameter definitions are

$$ZWIV = \frac{4 \cos \alpha_1 \left[\left(\frac{h_1}{h_o} \right) \cos \alpha_1 \tan \alpha_o - \sin \alpha_1 \right]}{1 + \left(\frac{h_o}{h_1} \right)} \cdot \left(\frac{P}{AW} \right) \tag{74}$$

and

$$ZWIB = \frac{4 \cos \beta_2 \left[\left(\frac{h_2}{h_{1A}} \right) \cos \beta_2 \tan \beta_1 - \sin \beta_2 \right]}{1 + \left(\frac{h_{1A}}{h_2} \right)} \cdot \left(\frac{P}{AW} \right) \tag{75}$$

where, again, the sign conventions of Figure 8 are involved.

A brief, stage-by-stage printout summarizes the input and output pertinent to the SOLDTY routine.

2.5 THERMODYNAMIC PROPERTIES

The flowing medium is assumed to be either dry air or the result of combustion involving dry air and JP-4 fuel. The desired fuel/air ratio is represented by an input variable, FAR. FAR is preset internally to zero, thereby implying dry air as the medium. User input overrides this value. The gas constant RG is calculated as shown by equation (1). The equivalence ratio EQR is calculated as

$$EQR = \frac{FAR}{STOICH} \tag{76}$$

where STOICH is the stoichiometric fuel/air ratio.

The flowing medium is treated as a perfect gas whose specific heat is a function of absolute temperature (Rankine scale) and equivalence ratio. A function subroutine CPX is used to provide specific heat tables for dry air and combustion products. The fuel/air ratio and equivalence ratio are communicated to this routine through labeled COMMON since they are held constant throughout the FLOPTH calculations. Thus, temperature is the only argument needed when calling this routine for a specific heat value. Specific heat ratio is then calculated from the gas constant and interpolated specific heat as indicated in equations (1), (3), and (4).

The CPX tables, each having nine entries, are embodied in DATA statements. The temperature table ranges from 300° R to 4000° R. There are five tables of specific heat values corresponding to these temperatures. These

five tables represent equivalence ratios of 0., .25, .5, .75 and 1. When fuel/air ratio is zero, only a single interpolation is required to obtain the desired specific heat. When fuel/air ratio is greater than zero, a double interpolation for temperature and equivalence ratio is required. The CPX routine sets up the appropriate interpolation data; the actual interpolation calculation is performed in a function subprogram entitled RINT. This interpolation procedure is covered in some detail in Section 4.0, the BLDDES module discussion.

The specific heat data tabulated in CPX have been gleaned from the results of a combustion products calculation of JP-4 burned in air having the following constituents:

O_2 - 20.9495%

N_2 - 78.0881%

A - .9324%

CO_2 - .0300%

The gas constants are:

air, RGA = 53.347602 ft lb/lb/°R
JP4, RGF = 55.087694 ft lb/lb/°R

The stoichiometric fuel/air ratio is:

STOICH = .06775149

The background calculations for CPX followed the methods of Reference 2.

3.0 AXISYMMETRIC ANALYSIS

3.1 INTRODUCTION

The quasi two-dimensional fluid dynamic equations for axisymmetric, inviscid steady flow are solved by the ATREC (Axial Turbine Radial Equilibrium and Continuity) module. The assumption is made that the radial velocity components can be neglected in the radial momentum equation. This approximation permits the overall organization of the program to be like that of a one-dimensional calculation, and it permits choking effects to be included. For axial turbines, this method provides a rapid analysis of turbine design and off-design performance with detailed vector diagram information for each blade row as a function of radius.

3.2 NOMENCLATURE

A	One-dimensional flow area
C	Velocity
C_f	Flow coefficient
C_p	Specific heat at constant pressure
F	Blade Force
h	Static enthalpy
H	Total enthalpy
I	Rothalpy
m	Meridional distance
M	Mach number
NDo	Sum of throat dimensions
p	Static pressure
P	Total Pressure
r	Radius
R	Gas constant
s	Entropy
Shth	Station to throat height ratio
T	Temperature
w	Mass flow rate
W	Velocity in coordinate system rotating with blades
β	Flow angle

γ Specific heat ratio

η Efficiency

ρ Density

ψ Reduced stream function

ω Angular velocity

Subscripts

c Due to coolant

e Exit

H Hub

i Isentropic or inlet

j Axial station index

p Polytropic

r Measured in rotating coordinate system

s Station

t Throat

T Tip, or adiabatic based on stagnation conditions

u Tangential (peripheral) component

z Axial component

3.3 THE MOMENTUM EQUATION

The momentum equation will be applied outside blade rows, where the approximations of axisymmetric, inviscid, steady flow without force fields are adequate for engineering purposes. Then

$$\rho\vec{C} \cdot \nabla\vec{C} + \nabla p = 0 \tag{77}$$

where ρ is density, $\vec{C}$ is velocity in the absolute (stationary) reference frame, and p is pressure.

Lamb's form of the momentum equation is obtained by vector identity:

$$\nabla\left[\frac{C^2}{2}\right] = \vec{C} \times (\nabla \times \vec{C}) - \frac{\nabla p}{\rho} \tag{78}$$

Using the thermodynamic relationship

$$dh = Tds + \frac{dp}{\rho} \tag{79}$$

where h is enthalpy, T is temperature, s is entropy, and the definition of the stagnation enthalpy H is

$$H = h + \frac{C^2}{2} \tag{80}$$

the momentum equation (78) is rewritten as

$$\nabla H = \vec{C} \times (\nabla \times \vec{C}) + T\nabla s \tag{81}$$

(this is Crocco's Theorem.)

In view of axisymmetry, the tangential (peripheral) component of equation (81) gives

$$\frac{\partial (r\ C_u)}{\partial m} = 0 \tag{82}$$

in the free spaces between blade rows. In a meridional plane which includes the radial and axial direction, m is the projection of a streamline. The tangential velocity is denoted by C_u and radius by r. In equation (82), radial velocities are not neglected.

By neglecting radial velocities in the radial component of equation (81), the radial equilibrium equation is obtained:

$$\frac{\partial}{\partial r}\left[\frac{C_z^2}{2}\right] + \frac{C_u}{r}\frac{\partial}{\partial r}(r\ C_u) + T\frac{\partial s}{\partial r} - \frac{\partial H}{\partial r} = 0 \tag{83}$$

where C_z is the axial velocity component.

This equation is restricted to axial turbomachines. Generally the error due to omitting radial velocity from equation (83) is negligible when flow-path slopes are less than 10°. Even if the error is significant, it affects only the radial distribution of vector diagrams without invalidating the entire calculation.

Equation (83) is a form which is suitable for solution when the required distribution of C_u is known. This is true when equation (82) can be applied across a free space or in the design mode, where the required distribution of tangential forces is known.

In the off-design mode, equation (83) is rewritten in terms of velocity components relative to the blading. Defining

$$I = H - \omega r C_u \tag{84}$$

$$W_u = C_u - \omega r$$

$$W_z = C_z \tag{85}$$

we obtain

$$\frac{\partial}{\partial r}\left[\frac{W^2}{2}\right] + \frac{(W \sin \beta)^2}{r} + 2 \omega W \sin \beta + T \frac{\partial s}{\partial r} - \frac{\partial I}{\partial r} = 0 \tag{86}$$

Equation (83) or (86) is solved as an ordinary differential equation by trapezoidal integration. $\partial H/\partial r$ or $\partial I/\partial r$ is calculated using streamline positions from the previous iteration. Also, the entropy gradient, $\partial s/\partial r$, and $\sin \beta = W_u/W$ in equation (86) are assumed to be the same as previously calculated.

An iteration loop including the momentum, continuity, and energy equations is repeated until continuity is satisfied.

The axial component of the momentum equation is not solved directly. It is used to analyze the results to find the axial blade force components. The blade force for free spaces should turn out to be zero, and may be used as a check on the accuracy of the calculation.

3.4 THE ENERGY EQUATION

The Euler turbine equation, which follows from Newton's law and the definition of power, states that for adiabatic flow along a streamline past blading moving with angular velocity ω,

$$\frac{\partial H}{\partial m} = \omega \frac{\partial (r C_u)}{\partial m} \tag{87}$$

or, using equations (82) and (84),

$$\frac{\partial I}{\partial m} = 0 \tag{88}$$

Equation (88) is employed by taking the current value of stream function (calculated by continuity) and finding the value of I at the same stream function at the previous radial line of calculation. This value is modified by the introduction of coolant.

Static enthalpy is determined by

$$h = I + \frac{\omega^2 r^2 - W^2}{2} \tag{89}$$

which follows from definitions (80), (84), and (85).

Enthalpy and temperature are related by

$$C_p \frac{\partial T}{\partial m} = \frac{\partial h}{\partial m} \tag{90}$$

and specific heat at constant pressure C_p is given by

$$C_p = \frac{\gamma}{\gamma - 1} R \tag{91}$$

where γ is the ratio of specific heats and R is the gas "constant" of the fluid (universal gas constant divided by molecular weight).

In order to evaluate density ρ, we assume a semiperfect gas

$$\rho = \frac{p}{RT} \tag{92}$$

From equations (79) and (90) through (92), the density derivative satisfies

$$\frac{\partial}{\partial m} \ln (\rho R) = \frac{1}{\gamma - 1} \frac{\partial}{\partial m} \ln T - \frac{1}{R} \frac{\partial s}{\partial m} \tag{93}$$

Equation (93) can be integrated exactly in the case of a perfect gas. The integration is a satisfactory approximation for a semiperfect gas. Integrating along a streamline from station j-1 to station j,

$$\rho_j = \rho_{j-1} \frac{R_{j-1}}{R_j} \left(\frac{T_j}{T_{j-1}} \right)^{\frac{1}{\gamma_j - 1}} e^{\frac{s_{j-1} - s_j}{R_j}} \tag{94}$$

The gas constant R can change only by the introduction of coolant. If γ_j were evaluated at the log mean of T_{j-1} and T_j, equation (94) would conform to the trapezoidal integration rule. In practice this requirement is relaxed so that γ_j is evaluated at a temperature between T_{j-1} and T_j or is given a priori. The evaluation of s_j will be discussed in the section on loss assessment. Temperature T_{j-1} is reduced and density ρ_{j-1} increased by the ratio of stagnation enthalpies when coolant is added.

Perfect gas relationships are used only to relate density, enthalpy, and entropy to inlet total temperature and pressure and to display local total pressure and temperature. These local total temperatures and pressures are not strictly correct, except in the case of a perfect gas, and are not employed in the internal analysis, which is accurate for a semiperfect gas.

3.5 LOSS ASSESSMENT

Defining relative total enthalpy as

$$H_r = I + \frac{\omega^2 r^2}{2} \tag{95}$$

in accordance with usual turbine analysis practice, a calculation station efficiency is defined as

$$\eta_s = \frac{1 - \frac{h}{H_r}}{1 - \left[\frac{p}{P_{ri}} \right]^{\frac{\gamma - 1}{\gamma}}} \tag{96}$$

where P_{ri} is the effective total pressure which would exist in the rotating frame of reference if the flow were isentropic from the previous calculation station. Using, for this purpose only, the approximation $h = C_p T$ and equations (79), (91), and (92)

$$\frac{s_j - s_{j-1}}{R} = -\frac{\gamma}{\gamma - 1} \ln \left[\frac{H_r}{h} + \frac{1 - \frac{H_r}{h}}{\eta_s} \right] \tag{97}$$

with all quantities evaluated at j where not otherwise specified. Since the entropy change associated with coolant introduction is determined by a more detailed analysis than is possible in the present situation, an additional term is provided to specify total pressure loss for coolant introduction:

$$\frac{s_j - s_{j-1}}{R} = -\frac{\gamma}{\gamma-1}\left[\ln \frac{H_r}{h} + \frac{1 - \frac{H_r}{h}}{\eta_s}\right] - \ln\left[1 - \frac{\Delta P}{P}\right]_c \qquad (98)$$

Two options are provided to determine the station (blade row) efficiency η_s. The first alternative gives the designer more control over the results but does not attempt to predict the effect of design variables on efficiency. The second alternative is intended to predict the effect of vector diagram variations on efficiency.

User specification of η_s, the first alternative, gives a moderately reasonable trend of loss against Mach number. Typical values of η_s are 0.99, 0.97, and 0.95 for blade inlet, stator exit, and rotor exit stations, respectively.

In order to predict efficiency, the second alternative, the dependence of η_s on blade row flow coefficient and deflection must be correlated. A correlation which predicts efficiency of most turbine stages within ±1% follows:

η_s = 1 *ETAS (J); at blade row inlet

$$\eta_s = \frac{1}{C_\eta \left| \frac{\Delta(rC_u)}{\overline{Wr}} \sqrt{1 + \left(\frac{\overline{W}_u}{\overline{C}_z}\right)^2} \right| + 1} \text{ *ETAS (J)} \qquad (99)$$

at blade row exit with $\Delta(rC_u)$ being the change in rC_u across the blade row and $\overline{W}_u$ being the average of inlet and exit relative tangential velocity. C_η is an adjustable coefficient for which the value .054 is suitable if the only losses to be assessed are of the form (99).

Under the assumption of symmetrical blading, the correlation (99) is equivalent to a correlation of the stage efficiency against stage work loading $\Delta H/(2\omega^2 r^2)$ and stage flow coefficient $C_z/(\omega r)$. For modern stages of high flow, (99) predicts significantly better efficiency than older published correlations. No consistent Mach number effect is evident for stages designed for the appropriate operating conditions, and this simple correlation is effective over the full range of Mach number for which suitable data were available.

Some caution is required when employing the correlation for unusual operating conditions. Under extreme conditions the predicted blade row efficiency may be low enough to prevent the calculation from continuing. This is most likely to happen when an unexpected or unusual vector diagram is required.

At blade row inlets, an off-incidence loss may be assessed in the off-design mode by calculating the cosine of the difference between design and actual inlet angles raised to a power. This fraction of the relative kinetic energy is passed on to the next calculation station. The remainder is converted into entropy; thus, static temperature will increase while static pressure remains constant. A power of 0 assesses no additional loss, while a power of 2 is most widely accepted and corresponds to a loss of the kinetic energy associated with the component of velocity normal to the design inlet velocity vector. The off-incidence correlation is unrealistic if it predicts a station efficiency less than 0.5, in which case an effective efficiency of 0.5 is used. In the design mode, the design inlet angle is, by definition, the actual incidence angle, so there is no off-incidence loss. The design angle is saved for possible later use.

At the rotor exit, a test factor may be applied which is the ratio of effective work output to vector diagram work output. Enthalpy, temperature, and entropy are adjusted accordingly. When a nonunity test factor is employed, the Euler turbine equation and the continuity equation are not satisfied, so that it is preferable to account for as much of the loss as possible in η_s instead of test factor.

3.6 CONTINUITY

The total flow across a calculation station must be the known sum of the flow across the previous station and the added cooling flow:

$$2\pi \int_{r_T}^{r_H} \rho \, C_z \, r \, dr = w \qquad (100)$$

integrating from tip radius to hub radius, with w being the required mass flow. Density ρ is determined by equation (94). In the design mode and at free stations, axial velocity C_z is found directly from equation (83).

In the off-design mode at blade row exit stations, relative velocity W is found by equation (86). The relative flow angle β must be found by a continuity analysis between the given throat flow area and the exit station. A flow model is assumed in which flow is isentropic from the previous station to the throat. Throat pressure is assumed equal to the pressure at sonic velocity or the exit pressure, whichever is higher. The loss assessed according to equation (98) occurs between the throat and exit.

While this model is too simple to give fully satisfactory results in all cases, it has proved better than other known practical models. It works well when the exit to throat height ratio is close to unity.

According to equation (79), with dp = 0 according to the model, using equation (90), the temperature increases from the throat to the exit by a ratio

$$e^{\frac{s_i - s_{i-1}}{C_p}} = \frac{1}{\frac{H_r}{h} + \frac{1 - \frac{H_r}{h}}{\eta_s}}$$

by equation (97), where the additional loss for coolant flow injection in (98) is applied ahead of the throat. Relative velocity W decreases between throat and exit by the factor $\eta_s^{1/2}$. By continuity, for subsonic flow the model requires an increase in one-dimensional flow area between throat and exit:

$$\frac{A_e}{A_t} = \frac{1}{\sqrt{\eta_s}\left[\frac{H_r}{h} + \frac{1 - \frac{H_r}{h}}{\eta_s}\right]} \tag{101}$$

When the exit pressure is less than isentropic sonic pressure, an additional area increase is required to pass the flow set in the throat. Defining an isentropic or ideal Mach number:

$$M_i^2 = \frac{2}{\gamma - 1}\left(\frac{1}{\frac{\frac{h}{H_r} - 1}{\eta_s} + 1} - 1\right) \tag{102}$$

when $M_i > 1$, instead of equation (101), we use

$$\frac{A_e}{A_t} = \frac{\left[\frac{2 + (\gamma-1) M_i^2}{\gamma+1}\right]^{\left(\frac{1}{\gamma-1} + \frac{1}{2}\right)}}{\eta_s^{1/2} M_i \left[\frac{H_r}{h} + \frac{1 - \frac{H_r}{h}}{\eta_s}\right]} \tag{103}$$

If γ does not change, use of equation (103) holds the flow rate constant as pressure drops below sonic pressure. Use of the one-dimensional supersonic area function is an approximation valid only for low supersonic Mach numbers since it ignores shocks. Thus the use of a perfect gas relationship is adequate for this purpose.

The effective flow area at the throat is the sum of the individual passage throat dimension NDo times a flow coefficient C_f times the stream tube height. At the exit, an area $2\pi r$ times stream tube height is available. Assuming that the stream tube height ratio is the same as the station to throat height ratio Shth, the flow angle is

$$\cos \beta = \frac{C_f \, ND_o}{2\pi r \, Shth} \, \frac{A_e}{A_t} \tag{104}$$

with the sign of β given a priori. In the off-design mode, this permits the calculation

$$C_z = W \cos \beta \tag{105}$$

$$W_u = W \sin \beta$$

In the design mode, the calculation is inverted to obtain ND_o (assuming C_f=1) which is a required result of the design calculation.

The calculated vector diagram will not satisfy equation (100) in the unchoked case until the proper tip velocity has been found. The internal stream function which must be found to permit calculation along streamlines (ψ = constant) is calculated:

$$\psi(r) = \frac{\int_{r_t}^{r} \rho \, C_z \, r \, dr}{\int_{r_t}^{r_H} \rho \, C_z \, r \, dr} \tag{106}$$

C_z is required to be positive, so that

$$0 \leq \psi \, (r) \leq 1$$

is always true regardless of the error in the temporary solution. This definition prevents difficulty with streamwise interpolation. A reasonable estimate of streamline position is obtained even when the velocities are far from correct.

When using equation (83) with subsonic axial velocity or equation (86) with $M_i < 1$ at at least one radius, the error in equation (100) is taken to be a function of the tip velocity. This is termed the unchoked case. The secant method is used to find the tip velocity for the next iteration. This estimate is required to be positive (large enough to avoid numeric underflow) and no larger than may be required to detect choke. Also, the first two iterations must be different. Iterations are performed until the relative error in equation (100) is less than 10^{-5}. Fewer than 20 iterations are required.

In the choked case, using equation (86) with $M_i > 1$ at all radii, equation (103) is relied upon to give the proper flow. Since some of the information required to solve equation (86) is taken from the previous iteration, the calculation must be repeated until the relative change in flow is below 10^{-5}. Continuity may not be satisfied to this accuracy, but application of the tight tolerance is required to insure repeatability of results. This may require four iterations.

Stations are assumed initially to be unchoked. If, while trying to solve equation (100), it is found that $M_i \geq 1$ at all radii but not enough flow is passed, a choke-finding iteration is initiated. The tip velocity is adjusted so that the smallest value of M_i is 1. This is done exactly if the smallest M_i should turn out to occur at the tip, which is the reason for starting at the tip and integrating inwards. The absolute Mach number is usually smallest at the tip. The station calculation is iterated as in the choked case, but the error in equation (100) now is taken to be a function of the tip velocity at the upstream controlling station. The controlling station is the last choked station or the first calculation station. A secant calculation is performed to find the new tip velocity at the controlling station, and the calculations at all stations from controlling to choking station are repeated. This is by far the most time-consuming function of the ATREC program, as it involves an additional level of iteration.

When a choke point has been found, the calculation must proceed through the last station before the decision can be made to make the new choked station become the new controlling station. If a downstream station is choked or a required operating point has been passed, the work just completed to find a choke point must be discarded, and the station reverts to the unchoked mode.

This completes the analysis of the basic function of the ATREC program. The general scheme is that the radial momentum equation ties the field variables together in a cross-stream direction. The energy equation supplies the streamwise relationships. Continuity is satisfied at each station in turn by a one-parameter iteration. Each iteration gives an improved estimate of streamline positions required in the momentum and energy equations, so that when the continuity equation is satisfied, all relationships are satisfied.

3.7 EFFICIENCY

Calculation of efficiency for a fluid flow system with varying gas properties and injection of a somewhat dissimilar fluid is a controversial subject. In the following analysis the view is taken that an efficiency calculation must be based on all the fluid which is involved in the system. This implies that effective inlet enthalpy and pressure must be calculated for a hypothetical combination of the mainstream flow and the cooling flow which will be added before the exit station at which efficiency is calculated. Stage efficiency is based on the flow which passes through the stage exit station. Overall stage efficiency is based on mass averaged properties. Likewise, overall turbine efficiency is based on mass average properties for all the flow which is involved.

Polytropic efficiency is defined as

$$\eta_p = \frac{dH}{dH_i} \tag{107}$$

where dH_i is the total enthalpy change which would be obtained in an isentropic process with the same total pressures. Using equations (79) and (92),

$$\eta_p = 1 + \frac{P\, ds}{R\, dP} \tag{108}$$

where P is total pressure, which is found by the perfect gas equations (92) and

$$\frac{P}{p} = \left(\frac{H}{h}\right)^{\frac{\gamma}{\gamma-1}} \tag{109}$$

In order to use finite differences, equation (108) is approximated by

$$\eta_p = 1 + \frac{s_e - s_i}{R \ln \frac{P_e}{P_i}} \tag{110}$$

where i and e refer to inlet and exit conditions. This formula is exact in the case of constant total temperature and R or for a perfet gas. When flow is added, entropy which has been generated between the inlet station and the dilution station must be corrected so that the prior losses are not charged to the cooling flow.

Strictly speaking, overall efficiency should be derived by using mass average total enthalpy in equation (102). This requires some form of total temperature weighting as well as mass averaging to determine the overall entropies and pressures to be used in equation (110). In practice, some simplification is justified since η_p is usually about 0.9, in which case the error in η_p is only 0.1 times the error in the calculation of Pds/RdP. Since the properties of the calculated flow are not affected by the calculation of η_p, the most critical requirement is that η_p must be calculated in a way sufficiently consistent to permit evaluation of design variations.

We chose to use mass-averaged entropy in equation (110). This requires a consistent method for averaging pressure. The appropriate averaged pressure must be higher than a mixed pressure, since entropy must increase in a mixing process.

Clearly, the mass-averaged total enthalpy is

$$\bar{H} = \int_0^1 H \, d\psi \tag{111}$$

It is consistent with the other approximations which have been made to use constant specific heat in the averaging.

Consider a hypothetical process in which the local thermodynamic variables are changed to the average values. There is an entropy change by equation (79).

$$\frac{\Delta s}{R} = \frac{\gamma}{\gamma-1} \ln \frac{\bar{H}}{H} - \ln \frac{\bar{P}}{P} \tag{112}$$

As a mass averaged entropy is to be used in equation (110), the mass average of Δs must be zero, giving

$$\ln \bar{P} = \int_0^1 \ln P \, d\psi + \frac{\gamma}{\gamma-1} \left[\ln \bar{H} - \int_0^1 \ln H \, d\psi \right] \tag{113}$$

The somewhat surprising inequality $\ln \bar{P} \geq \int_0^1 \ln P \, d\psi$ holds.

This must be taken as a reminder that $\bar{P}$ is intended to reflect available energy of the unmixed streams of the flow, not the pressure which would be the result of mixing the streams together. It should be noted that the "mixing" calculations employed in some published programs of a similar nature can easily violate the second law of thermodynamics, giving erroneous efficiencies.

Equation (113) is applied to the mainstream flow. Before efficiency is calculated, the appropriate cooling flow source pressures must be included in the average. Since this is treated as a mixing process, the terms based on enthalpy difference can be omitted.

Adiabatic efficiency based on stagnation inlet and exit conditions is calculated from polytropic efficiency using perfect gas relationships:

$$\eta_T = \frac{1 - \left[\frac{P_e}{P_i}\right]^{\frac{\gamma-1}{\gamma}\eta_p}}{1 - \left[\frac{P_e}{P_i}\right]^{\frac{\gamma-1}{\gamma}}} \qquad (114)$$

It is most appropriate to use the γ evaluated at exit conditions since it refers to the properties of all the streams of flow mixed together. The perfect gas definition of η_T based on total temperature would be much less accurate than the present method of calculation in the case of varying specific heats. If $s_e = s_i$, η_p and η_T will be unity, while other methods will satisfy this requirement only for perfect gas.

3.8 COOLANT FLOW INJECTION

Cooling flow is introduced on surfaces where it is subject to mixing in secondary flows. Its influence cannot be restricted in terms of two-dimensional streamline analysis. Since the ATREC program is most concerned with correct prediction of the one-dimensional performance of the turbine, one source of coolant for each axial calculation station is sufficient. The coolant is assumed to mix uniformly by mass with the main flow.

Since calculation of entropy associated with cooling flow mixing depends on knowledge of local flow conditions, it is outside the scope of a quick-look calculation. If the effect of coolant on the total pressure is known, the program will accept this efficiency as input. The most important effects of coolant addition are the effects on enthalpy and flow rate, which can be handled correctly. The points where the influence of coolant addition is considered are indicated in the analysis.

3.9 BLADE FORCES

Blade forces are not usually considered part of the aerodynamic design requirements, but are needed for mechanical design. The tangential forces or torque are directly related to the work output and can be calculated

accurately. Axial forces can be calculated adequately by applying the axial component of the momentum equation, which was not required in the aerodynamic analysis. Little of the information required to calculate radial aerodynamic force is available in this analysis, but these forces may not be significant in an axial turbine. Viscous forces are neglected as they are an order of magnitude less than the total force.

Blade forces are determined from the momentum integral equation. A control volume is drawn bounded by station j-1 and j and the hub and tip flow paths. Applying Green's theorem to equation (77), with $\nabla\cdot(\rho\vec{C}) = 0$, attributing unbalanced forces to the force exerted on the blading,

$$\vec{F} = -\oiint_S (p + \rho\vec{C}\,\vec{C}\cdot)\, d\vec{S} \tag{115}$$

Equation (115) is differentiated with respect to radius on the station j face in order to obtain an approximate distribution of force. The differential force is viewed as the force on a slice of blade between conical surfaces extending from station j-1 to station j. The slice thickness is chosen to vary in an appropriate way. For tangential force, the flows on the upstream and downstream faces are made equal. If cooling flow addition is significant, this could be inaccurate. For axial force, the slice thickness is proportional to blade height.

Tangential force per unit blade height is given by

$$\frac{dF_u}{dr} = -2\pi\rho\, C_z \left[(r\, C_u)_j - (r\, C_u)_{j-1}\right] \tag{116}$$

Torque is obtained by multiplying equation (116) by r and power by multiplying again by ω. In view of equation (87), rotor torque can be calculated equally well from total enthalpy H.

Calculation of axial blade force is somewhat controversial. There is not much uncertainty in the calculation of total axial force, which is more important than the detailed distribution of force. When the flowpath is not cylindrical, pressure on the hub and tip walls contributes to the momentum balance. To be strictly correct, the force calculation should follow stream tubes through the blade row, but the questionable additional accuracy to be obtained does not justify the effort.

On the upstream face, both fluid momentum and pressure enter the control volume:

$$F_{zj-1} = \int_{r_{Tj-1}}^{r_{Hj-1}} (p + \rho C_z^2)\, 2\pi r dr \qquad (117)$$

Similarly, on the downstream face:

$$F_{zj} = -\int_{r_{Tj}}^{r_{Hj}} (p + \rho C_z^2)\, 2\pi r dr \qquad (118)$$

On the tip flow path a trapezoidal integration gives

$$F_{zT} = \frac{\pi}{2} (r_{Tj}^2 - r_{Tj-1}^2)\ (p_{Tj} + p_{Tj-1}) \qquad (119)$$

and on the hub flowpath

$$F_{zH} = \frac{\pi}{2} (r_{Hj}^2{}_{-1} - r_{Hj}^2)\ (p_{Hj} + p_{Hj-1}) \qquad (120)$$

The unbalanced resultant is ascribed to blade force:

$$F_z = F_{zj-1} + F_{zj} + F_{zT} + F_{zH} \qquad (121)$$

An approximation to the axial force distribution is obtained by differentiating equations (117) and (118), and dividing (119) and (120) proportionately:

$$\frac{dF_z}{dr} = \frac{F_{zT} + F_{zH}}{r_{Tj} - r_{Hj}}$$

$$+2 \frac{r_{Tj-1} - r_{Hj-1}}{r_{Tj} - r_{Hj}} (p + \rho C_z^2)_{j-1} r_{j-1} \qquad (122$$

$$-2\pi (p + \rho C_z^2)_j r_j$$

where the calculation is done on segments of equal proportional height, not on true stream tubes. The total axial force comes out the same as if stream tubes were used. The local and, to a smaller extent, the total axial force are affected by the neglect of radial velocity in equation (83), so that the result of equation (122) is not fully consistent. On the other hand, the numerical accuracy of the axial force prediction is well within the capability of experimental verification. This prediction is for the force on the blading only. The forces on disc, shrouds, seals, etc. must be accounted for separately.

3.10 UNITS

The ATREC program is written to permit change of systems of units by changing the conversion factors, which can be done in the input data set. The following discussion refers to the customary engineering units for which preset conversion factors are contained in the program. The units for input and output are given in the description of input and output variables. Equivalent internal variables may have different units and will be discussed in the order in which they appear in the analysis.

Internal enthalpy, equation (80), is in units consistent with the external units of velocity, which are feet per second. To obtain external enthalpy, divide by the constant, GJ = 25036 lb ft^2/Btu sec^2. Internal temperature is GJ times external temperature, with external temperature in degrees Rankine. Thus entropy, which is an internal variable, is in Btu/lbm° R.

Angular velocity ω is true angular velocity divided by the constant FT = 12 inches/foot. Thus ω is in ft/in.-sec, so that r C_u can be kept in the external units in.-ft/sec.

Internal gas constant R, equation (91), is in the same units as entropy (Btu/lbm ° R). Multiplying by the factor GC/GJ gives external RG in ft/° R. Density ρ, equation (92), is in pound mass per cubit foot, and pressure p is in pound force per square inch, requiring the conversion factor GC*FT**2, where GC = 32.17405 ft/sec^2.

In equation (100), flow rate w is in pound mass per second, requiring a conversion factor FT^{-2}.

Metric (SI) units can be used by setting the constants GJ, FT, and GC to 1.

3.11 CORRECTION TO STANDARD CONDITIONS

The parameters EQN, WEQ, and DHEQ are intended to indicate the speed (rev/min), weight flow, and work output (Btu/lb) which would be required to give equivalent performance at NACA standard inlet conditions. These are

14.696 psia, 518.7° R, molecular weight 29.0, and specific heat ratio 1.4. The definitions are:

$$WEQ = w \varepsilon \sqrt{\frac{\theta}{\delta}}$$

$$DHEQ = \frac{DHS}{\theta}$$

$$EQN = \frac{RPM}{\sqrt{\theta}}$$

$$\varepsilon = \frac{ENS}{\gamma \left(\frac{2}{\gamma+1}\right)^{\frac{\gamma}{\gamma-1}}}$$

$$ENS = 0.7395945 \text{ for } \gamma = 1.4$$

$$\theta = \frac{V_{cr}^2}{VCRS}$$

Standard sonic velocity squared VCRS = 1,038,600 ft^2/sec^2

$$\delta = \frac{P}{PSTD}$$

$$PSTD = 14.696 \text{ psia}$$

4.0 INTERSTAGE GAS TEMPERATURE PROFILES

4.1 INTRODUCTION

The GASPRO module calculates turbine interstage gas temperature profiles. From inputs of combustor exit fuel/air ratios or stage exit gas temperature profiles, successive downstream radial temperature profiles are calculated at each vane row and blade row inlet. An energy balance is performed on the gas stream to account for coolant air addition and rotor work extraction. Cooling air is uniformly distributed radially. Maximum peak profiles are diluted using airfoil (vane and blade) cooling flows only. Dilution of the average profiles is accomplished by using all input cooling flows.

Calculations are usually initiated at the combustor exit with fuel/air ratio profiles as input. The calculation methodology allows for additional burning through the first-stage vane, thus it is possible (though not likely) that the first-stage blade inlet temperatures may be higher than vane inlet temperatures. Calculations may begin at any stage inlet by inputing temperature profiles in the place of fuel/air ratio profiles. There is a maximum of 11 radial calculation stations. There is also a maximum of 10 stages.

4.2 TECHNICAL BACKGROUND

To conduct a detailed heat transfer analysis of a complete turbine, it is necessary that the local gas temperatures throughout the turbine be known. An underestimate of the gas temperatures will result in reduced lives of the components; an overestimate of the gas temperature will result in over-designing the components. A design that is too conservative will result in an increased life cycle cost because of increased development and hardware cost along with increased fuel consumption. The fuel consumption will increase since the pressure losses associated with introduction and mixing of the cooling air with the gas stream will be higher. Thus, it becomes necessary that the gas temperatures throughout the turbine be predicted as closely as possible. To accomplish this, the GASPRO module was developed.

4.3 PROGRAM OUTLINE

The program starts with an input of the cycle average first-stage rotor inlet average temperature. To this temperature is added the design turbine inlet temperature margin, DTDM. This represents any variation in the design point turbine inlet temperature due to engine deterioration, engine-to-engine variation, and tolerance stackup. With the combustor inlet temperature and combustion efficiency, the turbine inlet average fuel/air ratio can be defined. This fuel/air ratio is then used to define the vane inlet fuel/air ratio by taking the vane cooling air out of the hot gas mixture.

With this increased fuel/air ratio, an average vane inlet temperature is defined. The vane inlet average fuel/air ratio is also used, along with the combustor exit fuel/air ratio normalized profile, to define the starting radial temperature profile. Two profiles are used -- the maximum peak and the average profiles. The maximum peak profile represents the profile of the highest possible fuel/air ratios that might be expected to be seen in the engine. This profile is generally used for the design of stationary components. The average profile represents the locus of all possible circumferentially averaged profiles. This profile is generally used for rotating turbine components. The reason for using the circumferentially averaged profile is that the rotor in essence experiences such a profile as it rotates.

The program conducts both a mass and energy balance at each calculation station. Cooling air dilution is accounted for along with rotor work extraction. It is assumed that band and shroud cooling air along with any leakage never penetrates to the vane midspan. Thus, none of this cooling air is used in the dilution of the maximum peak temperature profile.

At the exit of each turbine stage, the average profile can be flattened out to reflect a radial mixing due to secondary flow associated with the blade row.

The major work done by the GASPRO program is accomplished in three subroutines. HPVANE calculates fuel/air ratios and the resultant temperature rises. The fuel/air ratios are diluted with vane cooling air and new temperatures are calculated. Subroutine BLADE, using an energy balance on the gas stream, accounts for rotor work extraction and dilution by blade cooling air. Subroutine VANE, also using an energy balance, accounts for dilution of the gas stream by vane cooling air.

Enthalpy is calculated by interpolation of tabular data generated using the methods of Reference 3. Interpolations are made for fuel/air ratio and temperature. Function HGAS was developed to accomplish this and is explained in Section 4.8. Combustor temperature rise is calculated by tabular data obtained from Reference 4. Interpolations are made for fuel/air ratio and combustor inlet temperature. Variations due to pressure are neglected, and data is used for a pressure of ten atmospheres. Function COMBTR was developed to accomplish this and is explained in detail in Section 4.7.

4.4 SUBROUTINE HPVANE

The first computations performed in subroutine HPVANE determine the fuel/air ratio required to produce the desired design average turbine inlet temperature. This is accomplished using the "false position" method of zero finding with function COMBTR (combustor temperature rise interpolating routine) providing the temperature rise for an estimated fuel/air ratio. The method of false position obtains a new estimate of the independent variable by linear interpolation of two previous estimates.

The input to function COMBTR is FA, T, and ETAC, where:

FA = fuel/air ratio for which combustion temperature rise is desired

T = combustor inlet temperature, ° F

ETAC = combustion efficiency.

From the average rotor inlet fuel/air ratio, the average vane inlet (combustor exit) fuel/air ratio is calculated by removing the first-stage nozzle cooling and leakage air dilution. At the nozzle inlet, the fuel/air ratio is

$$FAAV = \frac{FA41AV\ (1-WCT)}{(1 - WCT \cdot FA41AV)} \qquad (123)$$

where:

FAAV = average vane inlet fuel/air ratio at the first-stage nozzle

FA41AV = stage-one rotor inlet fuel/air ratio

WCT = WCV(1) + WCBND(1) (124)

WCV(1) = first-stage vane airfoil coolant airflow expressed as fraction of vane inlet gas flow

WCBND(1) = first-stage band and leakage airflow expressed as fraction of vane inlet gas flow

Function COMBTR is used at this point to calculate the average vane inlet temperature from the calculated average fuel/air ratio and combustor inlet temperature, T3.

With the input maximum peak fuel/air ratio profile, as normalized by the overall fuel/air ratio, the radial maximum peak fuel/air ratio distribution can be defined:

$$FA4OPK(I) = FAPK(I) \cdot FAAV \qquad (125)$$

where:

FAPK(I) = ratio of the local maximum peak fuel/air ratio to the average fuel/air ratio at nozzle inlet

FA4OPK(I) = local maximum peak fuel/air ratio at each radial calculation point at nozzle inlet

The maximum peak fuel/air ratio represents the locus of the maximum fuel/air ratios that might be encountered by any location.

With the input of the ratio of the locus of circumferentially averaged profiles to the average fuel/air ratio, then the radial average fuel/air ratio profile can be defined as

$$FA40LOP(I) = FALOP(I) \cdot FAAV \tag{126}$$

where:

FALOP(I) = ratio of the locus of circumferentially averaged fuel/air ratio profiles to the average fuel/air ratio at nozzle inlet

FA40LOP(I) = fuel/air ratio profile at nozzle inlet that represents the locus of all possible circumferentially integrated radial profiles.

The gas stream maximum peak total temperature profile, T40PK(I), and the average total temperature profile, T40LOP(I), are then calculated by means of the function COMBTR with inputs of combustor inlet temperature, combustor efficiency, and the respective fuel/air ratios.

The vane cooling air is divided up among the stream tubes that are consistent with the calculation stations. The cooling air is added to the gas stream, and the diluted fuel/air ratio at the nozzle exit is evaluated:

$$FA41PK(I) = \frac{FA40PK(I)}{[1 + WCV(1) \cdot \{1 - FA40PK(I)\}]} \tag{127}$$

which yields the maximum peak fuel/air ratio profile downstream of the first-stage nozzle. Similarly, the average fuel/air ratio downstream of the first-stage nozzle is calculated:

$$FA41LOP(I) = \frac{FA40LOP(I)}{[1 + WCV(1) \cdot \{1 + FA40LOP(I)\}]} \tag{128}$$

Once again, these profiles are input with the combustor inlet temperature and combustion efficiency into function COMBTR to produce the blade inlet maximum peak temperatures, T41PK(I), and average absolute total temperature, T41LOP(I), profiles.

Finally, the blade inlet total temperature profile as "seen" by the rotor (referred to as relative) is calculated:

$$TTB(I) = T41LOP(I) \cdot TTB41(I) \tag{129}$$

where:

TTB41(I) = ratio of relative to absolute gas temperatures supplied from the ATREC module

4.5 SUBROUTINE BLADE

From user-supplied blade coolant temperatures and design average blade inlet temperature, the corresponding enthalpies are calculated using function HGAS. Function HGAS interpolates enthalpy data from Reference 3 for temperature and fuel/air ratio. The average blade exit enthalpy is calculated by first removing rotor work extraction, then accounting for cooling air dilution. The rotor work extraction profile is specified by first normalizing the enthalpy drop profile, DH (I), by the rotor inlet absolute gas temperature, TTS, both supplied by the ATREC module:

$$DHOT(I) = DH(I)/TTS \tag{130}$$

This ratio is then multiplied by the radial temperature profile at the blade row inlet to give the radial work extraction distribution. This work extraction is then subtracted from the rotor inlet enthalpy before being diluted with the coolant air. The maximum peak profile is diluted with only the blade cooling air while the average profile is diluted with all the chargable coolant air. For the maximum peak temperature profile the rotor exit enthalpy is:

$$HOUTPK = \frac{HINPK - DHOT(I) \cdot TINPK(I) + WCBLD \cdot HCBLD}{1 + WCBLD} \tag{131}$$

where:

HINPK = local profile value of rotor inlet enthalpy, based on rotor inlet maximum peak gas temperature (Btu/lb)

TINPK(I) = rotor inlet maximum peak radial gas temperature profile (R°)

WCBLD = rotor blade cooling air flow expressed as a fraction of rotor inlet gas flow

HCBLD = enthalpy of the rotor cooling air (Btu/lb).

The average temperature profile at the rotor exit is similarly evaluated except for handling the cooling air. All the cooling air is added into the gas stream. The rotor exit average enthalpy equation is

$$HOUTLOP = \frac{HINLOP - DHOT(I) \cdot TINLOP(I) + WCT \cdot HCT}{(1 + WCT)} \tag{132}$$

where:

HINLOP = local profile value of rotor inlet enthalpy based on the rotor inlet average profile (Btu/lb)

TINLOP(I) = rotor inlet average profile gas temperature, (° R)

WCT = total of the vane band, WCBND, the rotor shroud and leakage cooling air, WCSHL, and the blade cooling air, WCBLD all of which are expressed as a fraction of rotor inlet gas flow

HCT = Weighted average enthalpy of the individual enthalpies of WCBND, WCSHL, and WCBLD which thus makes it consistent with WCT (Btu/lb).

The rotor exit maximum peak temperature profile, TOUTPK(I), and the average temperature profile, TOUTLOP(I), are now evaluated by means of the function TGAS. Function TGAS is a zero-finding routine (false position method) which uses function HGAS to recursively estimate the temperature corresponding to the input enthalpy HOUTPK or HOUTLOP (see Section 4.9):

$$\text{TOUTPK(I)} = \text{TGAS(F, HOUTPK)} \tag{133}$$

$$\text{TOUTLOP(I)} = \text{TGAS(F, HOUTLOP)} \tag{134}$$

A correction factor on the average temperature profile is introduced at this point. This correction factor is designed to allow the average profile to be flattened out so as to reflect radial mixing of the hot midspan gases with the cooler endwall gases:

$$\text{BETA} = \frac{\text{TOUTLOP(I)}_{corr} - \text{TAV}}{\text{TOUTLOP(I)}_{uncor} - \text{TAV}} \tag{135}$$

where $0 \leq \text{BETA} \leq 1$

A typical example of this correction is presented in Figure 10. A BETA value of 0 results in a flat radial temperature profile and a temperature equal to the average blade exit temperature. A BETA value of 1.0 leaves the profiles unaltered. If modifying the average temperature profile results in a maximum peak temperature less than the average temperature, at any particular radial location, the maximum peak temperature is set equal to the average temperature. This would most likely occur near the end wall.

The final phase of this subroutine consists of defining the rotor exit fuel/air ratio. This is accomplished by simply mixing in the blade and shroud cooling air:

$$\text{FAAV}_{out} = \frac{\text{FAAV}_{in}}{1 + \text{WCB} \cdot (1 + \text{FAAV}_{in})} \tag{136}$$

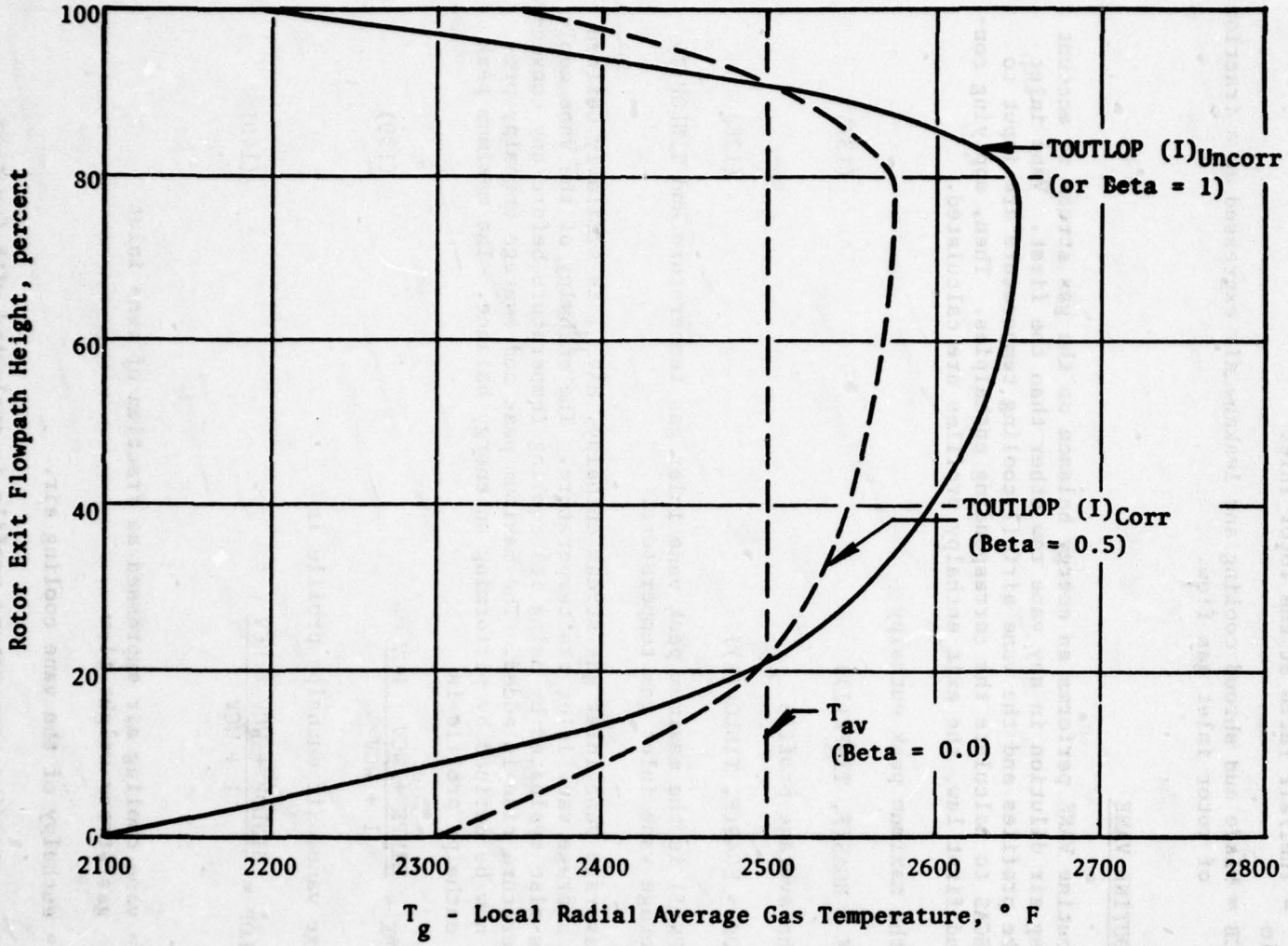

Figure 10. Rotor Exit Average Profile Radial Mixing Parameter.

where:

$FAAV_{in}$ = fuel/air ratio at the rotor inlet

WCB = blade and shroud cooling and leakage air expressed as a fraction of rotor inlet gas flow.

4.6 SUBROUTINE VANE

Subroutine VANE performs an energy balance on the gas stream to account for cooling air dilution in any vane row other than the first. Vane inlet temperature profiles and the vane airfoil cooling temperature are input to function HGAS to calculate the corresponding enthalpies. Then, applying continuity and first law, the exit enthalpy profiles are calculated.

For the maximum peak enthalpy

$$HINPK = HGAS(F, TINPK(I)) \tag{137}$$

and for the average profile

$$HINLOP = HGAS(F, TINLOP(I)) \tag{138}$$

where TINPK(I) is the maximum peak vane inlet gas temperature and TINLOP(I) is the average vane inlet gas temperature.

The average vane inlet gas stream enthalpy, HAV_{IN}, is similarly defined using the average vane inlet gas temperature. The enthalpy of the vane cooling air is also evaluated by using its cooling temperature before any convection temperature rise is added. The maximum peak and average enthalpy profiles can now be defined by performing an energy balance. The maximum peak vane exit enthalpy profile is

$$HOUTPK = \frac{HINPK + WCV \cdot HCV}{1 + WCV} \tag{139}$$

and average vane exit enthalpy profile is

$$HOUTLOP = \frac{HINLOP + WCV \cdot HCV}{1 + WCV} \tag{140}$$

where:

WCV = vane cooling air expressed as fraction of vane inlet gas stream weight flow

HCV = enthalpy of the vane cooling air.

The corresponding temperature profile is evaluated with function

TGAS. The average vane exit temperature is defined by using the average inlet enthalpy and diluting it with both the vane and band cooling air.

where:

$$HAV_{out} = \frac{(HAV_{in} + WCT \cdot HCT)}{1 + WCT} \tag{141}$$

WCT = sum of vane, band, and leakage airflow expressed as a fraction of vane inlet gas flow

HCT = weighted average enthalpy of the vane, band, and leakage airflow (Btu/lb)

The average vane exit fuel/air ratio is diluted using the vane, band, and leakage airflows

$$FAAV_{out} = \frac{FAAV_{in}}{1 + WCT\ (1 + FAAV_{in})} \tag{142}$$

where $FAAV_{in}$ = average fuel/air ratio at vane inlet.

The average gas stream temperature is defined with the average vane exit enthalpy level, HAV_{out}, and function TGAS.

The rotor blade inlet relative gas temperature is defined from the ratio of the blade inlet relative gas temperature to the corresponding absolute gas temperature. The product of this ratio and the rotor inlet average absolute temperature profile, TOUTLOP(I), will then yield the relative gas temperature profile.

4.7 FUNCTION COMBTR

This function interpolates adiabatic combustor temperature rise data from Reference 4 for fuel/air ratio and combustor inlet temperature. Tabular data is used for combustor inlet temperatures of 540° F, 1040° F, and 1540° F, and for fuel/air ratios from 0 to 0.135 (twice stoichiometric) in increments of 0.005. Interpolation is made first for fuel/air ratio at the three tabular inlet temperatures. This interpolation uses a five-point Lagrangian interpolating polynomial:

$$\begin{aligned}\Delta T[f/a_o + P(\Delta f/a)] = {} & \frac{(P^2-1)P(P-2)}{24}\Delta T_{-2} - \frac{(P-1)(P)(P^2-4)}{6}\Delta T_{-1} \\ & + \frac{(P^2-1)(P^2-4)}{4}\Delta T_o - \frac{(P+1)P(P^2-4)}{6}\Delta T_1 \\ & + \frac{(P^2-1)P(P+2)}{24}\Delta T_2\end{aligned} \tag{143}$$

where: P is the fraction of the interpolated value between tabular points.

This results in three values of adiabatic temperature rise corresponding to the tabular inlet temperature points. These three values are then used in a three-point Lagrangian interpolating polynomial to interpolate for combustor inlet temperature:

$$\Delta T[T_{3_o} + PT(\Delta T_3)] = \frac{PT(PT-1)}{2} \Delta T_{-1} + (1-PT^2)\Delta T_o + \frac{PT(PT+1)}{2} \Delta T_1 \quad (144)$$

The combustor exit temperature is calculated using the interpolated value of adiabatic temperature rise, and input values for inlet temperature and combustor efficiency:

$$T_4 = T_3 + \eta_c \Delta T \quad (145)$$

4.8 FUNCTION HGAS

Function HGAS interpolates tabular enthalpy data generated from Reference 3 for temperature and fuel/air ratio. Tabular data is used for fuel/air ratios from zero to stoichiometric in increments of 0.01, and for temperatures from 640° F to 4040° F in increments of 100° F. Interpolation is first made for temperature at the three nearest tabular fuel/air ratios using a five-point Lagrangian interpolating polynomial. Then interpolation is made between these three points for fuel/air ratio using a three-point Lagrangian polynomial.

4.9 FUNCTION TGAS

TGAS calculates the temperature which corresponds to an input enthalpy. This is accomplished using the method of false position. Two initial estimates are made for the temperature (1000° R, 5000° R), then a third estimate is calculated by linear interpolation of the enthalpies corresponding to these temperatures. The input enthalpy is "trapped" between the new estimate and one of the previous estimates and the third estimate is discarded. A new estimate is obtained by linear interpolation of the enthalpies. This process continues until the enthalpy corresponding to the current temperature estimate is within 0.01% of the input enthalpy.

5.0 BLADE DESIGN

5.1 GENERAL

The Blade Design module, BLDDES, provides the means for designing the basic root, pitch, and tip sections of each blade row. These three sections form the major geometric definition of the external airfoil contours for each blade row. The output from this module is used as input to the intermediate section interpolation module, BLDSTK, and the blade-to-blade flow field analysis module, CASC. These basic sections can lie on either cylindrical or conical meridional stream surfaces. The airfoil shape can be derived analytically through specification of parametric input variables or can be described directly by inputing digitized coordinate data.

The following sections describe the analytical methods employed in the blade design procedure. The routines discussed in Sections 5.2 and 5.3 are adaptations of methods found in Reference 5.

5.2 INTERPOLATION

The interpolation technique employed herein is that due to Lagrange, who first published the method in 1795. The basic formulation arises from the fact that, for a polynomial $f(\bar{X})$ of degree "n," the divided differences of order (n + 1) are zero, i.e.

$$f(X_o, X_1, X_2, \ldots\ldots\ldots X_n, \bar{X}) = 0 \qquad (146)$$

To expand (146), one recalls that the arguments X_o, X_I.....X_n represent points at which functional values $f(X_o)$, $f(F_1)$.....$f(X_n)$ are known, and $\bar{X}$ represents the point at which interpolation is desired. Then equation (146) can be manipulated to the useful form

$$f(\bar{X}) = \frac{(\bar{X} - X_1)\ (\bar{X} - X_2)\ \ldots\ldots\ \ (\bar{X} - X_m)}{(X_o - X_1)\ (X_o - X_2)\ \ldots\ldots\ (X_o - X_m)}\ f(X_o)$$

$$+ \frac{(\bar{X} - X_o)\ (\bar{X} - X_2)\ \ldots\ldots\ (\bar{X} - X_m)}{(X_1 - X_o)\ (X_1 - X_2)\ \ldots\ldots(X_1 - X_m)}\ f(X_1)$$

$$+ \frac{(\bar{X} - X_o)\ (\bar{X} - X_1)\ \ldots\ldots\ (\bar{X} - X_{m-1})}{(X_m - X_o)\ (X_m - X_1)\ \ldots\ldots\ (X_m - X_{m-1})}\ f(X_m) \qquad (147)$$

Two observations are in order. First, note that in the coefficient for a given argument (e.g. X_1), the numerator is devoid of a factor $(\bar{X} - X_1)$, etc. Second, note that the denominator for a given argument (e.g. X_1) never has a factor $(X_1 - X_1)$ which would be tantamount to dividing by zero.

A function subprogram entitled RINT (Routine for Interpolation) has been written to perform the calculation indicated by equation 147. The form which is coded in RINT is

$$f(\bar{X}) = \sum_{I=1}^{N} \left[\frac{\prod_{\substack{J=1 \\ J \neq I}}^{N} (\bar{X} - X_J)/(\bar{X} - X_I)}{\prod_{\substack{J=1 \\ J \neq I}}^{N} (X_I - X_J)} f(X_I) \right] \tag{148}$$

The associated FORTRAN statement needed to get an interpolated value is

$$\bar{Y} = \text{RINT } (X, Y, \bar{X}, N) \tag{149}$$

where N is the number of X, Y pairs being supplied, $\bar{X}$ is the X-value at which interpolation is desired, and $\bar{Y}$ is the interpolated value. Subscripts I and J start at 1 since FORTRAN abhors zero subscripts. The numerator of equation 148 consists of a product of all differences divided by the difference which must be excluded in keeping with the first observation stated above. The denominator consists of a product of all differences except the one where I = J, in keeping with the second observation. In the event that $\bar{X}$ is equal to one of the supplied X values, the corresponding Y value is returned as $\bar{Y}$. When N = 2, the formulation yields a linear interpolation. The routine RINT is used in other modules besides BLDDES.

5.3 SIMULTANEOUS EQUATIONS

There are several instances in BLDDES where sets of up to five linear simultaneous equations require solution. Rather than use a commonly available library routine which is generalized for a large set of equations and thereby incurs an unnecessarily large program storage requirement, a small subroutine entitled SIMEQN has been provided. The technique used is a Gauss-Jordan reduction with maximum pivot strategy. In this method, each pass at reduction is made with the pivot element of largest absolute magnitude which is not in a row or column of a previously used pivot element. Input to the routine consists of an augmented matrix, i.e., the original coefficient matrix with right-hand side appended. The routine COEFB sets up the augmented matrix. Communication from the calling routine through COEFB to SIMEQN is handled by labeled common, viz:

```
COMMON /SOLN/ A (6,6), COF (5)                    (150)
```

where A is the augmented matrix and COF is the solution vector. The calling statement has the form

```
CALL COEFB (X, Y, EPS)                                    (151)
```

where X, Y is a set of five coordinate pairs and EPS is the minimum magnitude allowable for a pivot element. EPS is set at 1.0 E - 10. If a pivot element is found to be smaller than this, the matrix is assumed to be singular or nearly singular, and a zero value is returned for the determinant.

5.4 SIMULTANEOUS FUNCTION SOLUTION

There are several instances in BLDDES where two homogeneous functions must be solved simultaneously to yield an X, Y pair which is common to the two functions. The technique employed is that accorded to Newton and Raphson.

Assuming that one has two functions, F1 (X, Y) = 0 and F2 (X, Y) = 0 and that the objective is to find an X, Y pair that satisfies both functions simultaneously, the procedure is as follows. A set of "starting values" is identified, i.e., (X_i', Y_i'), and checked for possible satisfaction by the inequality

$$SUM = [F1^2 (X_i', Y_i') + F2^2 (X_i', Y_i')] \leq TOLERANCE \qquad (152)$$

where the tolerance is a small number. If the starting values do not satisfy the criterion of equation (152), successive corrections are calculated iteratively as

$$X_i^{n+1} = X_i^n - DX$$

$$Y_i^{n+1} = Y_i^n - DY \qquad (153)$$

where "n" denotes the nth iteration and

$$DX = \frac{F1 \frac{\partial F2}{\partial Y} - F2 \frac{\partial F1}{\partial Y}}{D} \qquad (154)$$

and

$$DY = \frac{F2 \frac{\partial F1}{\partial X} - F1 \frac{\partial F2}{\partial X}}{D} \qquad (155)$$

In equations (154) and (155), the denominator D is the determinant of the Jacobian of the partial derivatives, i.e.,

$$D = \frac{\partial F1}{\partial X}\frac{\partial F2}{\partial Y} - \frac{\partial F1}{\partial Y}\frac{\partial F2}{\partial X} \tag{156}$$

Experience with the functions used in BLDDES has shown that convergence is achieved with four or five iterations at most. Note that all of the special functions discussed in the following sections are defined in homogeneous form, i.e., with right-hand side equal to zero, for use in the Newton-Raphson solution.

5.5 GENERAL CONIC FUNCTION

One of the special functions used in BLDDES is the general conic defined as

$$F(X, Y) \equiv X^2 + f_1X + f_2Y^2 + f_3Y + f_4\,XY + f_5 = 0 \tag{157}$$

The slope of the tangent at any point is

$$m_T \equiv -\frac{\frac{\partial F}{\partial X}}{\frac{\partial F}{\partial Y}} = -\frac{-2X - f_1 - f_4Y}{2f_2Y + f_3 + f_4X} \tag{158}$$

The slope of the normal at any point is

$$m_N \equiv \frac{\frac{\partial F}{\partial Y}}{\frac{\partial F}{\partial X}} = \frac{2\,f_2Y + f_3 + f_4Y}{2X + f_1 + f_4Y} \tag{159}$$

Given a set of five X, Y pairs, the coefficients F_1 through F_5 are obtained through use of the COEFB and SIMEQN routines to solve five simultaneous equations of the form:

$$\begin{aligned} &f_1X_1 + f_2Y_1^2 + f_3Y_1 + f_4\,X_1Y_1 + f_5 = -X_1^2 \\ &\cdots\cdots \\ &f_1X_5 + f_2Y_5^2 + f_3Y_5 + f_4\,X_5Y_5 + f_5 = -X_5^2 \end{aligned} \tag{160}$$

The discussion thus far has been general in nature. The following sections cover the specific applications of these ideas in the BLDDES module.

5.6 TRAILING EDGE ATTACHMENT

The STE link of BLDDES establishes the precise tangent points to which the trailing edge configuration is fitted. The suction surface coordinate arrays, (XS, YS), and the pressure surface coordinate arrays, (XP, YP), are used as is the trailing edge thickness, TE. Figure 11 should help to clarify the procedure.

The final point of the suction surface, XS(NS), YS(NS), is used as the suction side tangent point. Angle DSPR is calculated as perpendicular to the final suction side segment extending from point NS-1 to NS. A distance equal to one-half of the trailing edge thickness is stepped off along angle DSPR to locate the trailing edge center point, XC, YC. Angle DSPC is calculated as perpendicular to the final pressure side segment extending from point NP-1 to NP. A distance of one-half of the trailing edge thickness is stepped off from point XC, YC along angle DSPC. The terminus of this step is defined as the calculated pressure side tangent point.

The last five points of the input pressure surface, NP-4 through NP, are used in a general conic function curve fit to yield coefficients C_{11} through C_{15}. Associated with these coefficients is a function PTF which, having the form shown in equation (157), represents the fitted portion of the surface. Points NP-4 through NP-1 also become the first four points in a set of auxiliary arrays, XPF, YPF. The fifth point of these auxiliary arrays is the calculated pressure side tangent point. DSPA is the mean orientation angle for the trailing edge wedge.

The calculated pressure side tangent point is tested for how well it fits the pressure side by substituting it into the function PTF. The result of this substitution is called PCHK. A perfect fit would yield a zero value for PCHK; in general, the result is small but non-zero. If the trailing edge thickness, TE, is not compatible with the surface coordinate data, the PCHK value is large. The absolute magnitude of PCHK is compared against a preset tolerance, TOLER (1). If PCHK exceeds this tolerance, the third and fourth points of the auxiliary arrays, XPF, YPF, are adjusted by interpolation in an attempt to get a smooth curve through all five points. If PCHK is equal to or less than this tolerance, XPF and YPF are used as is.

The throat calculation is now performed as described in the next section. Then a diagnostic plot is presented showing the suction side points NS-4 through NS and the auxiliary arrays, XPF, YPF. Figure 12 shows a typical STE plot which serves as a visual guide to whether or not the edge thickness and contour are acceptable. An optional diagnostic printout lists the pertinent variables associated with the tangent point and throat calculations. A repeat option provides an opportunity to rerun the STE calculations with a different trailing edge thickness. When the user is satisfied with the results and elects to continue as is, the input pressure side points NP-4 through NP are replaced by the auxiliary XPF, YPF arrays.

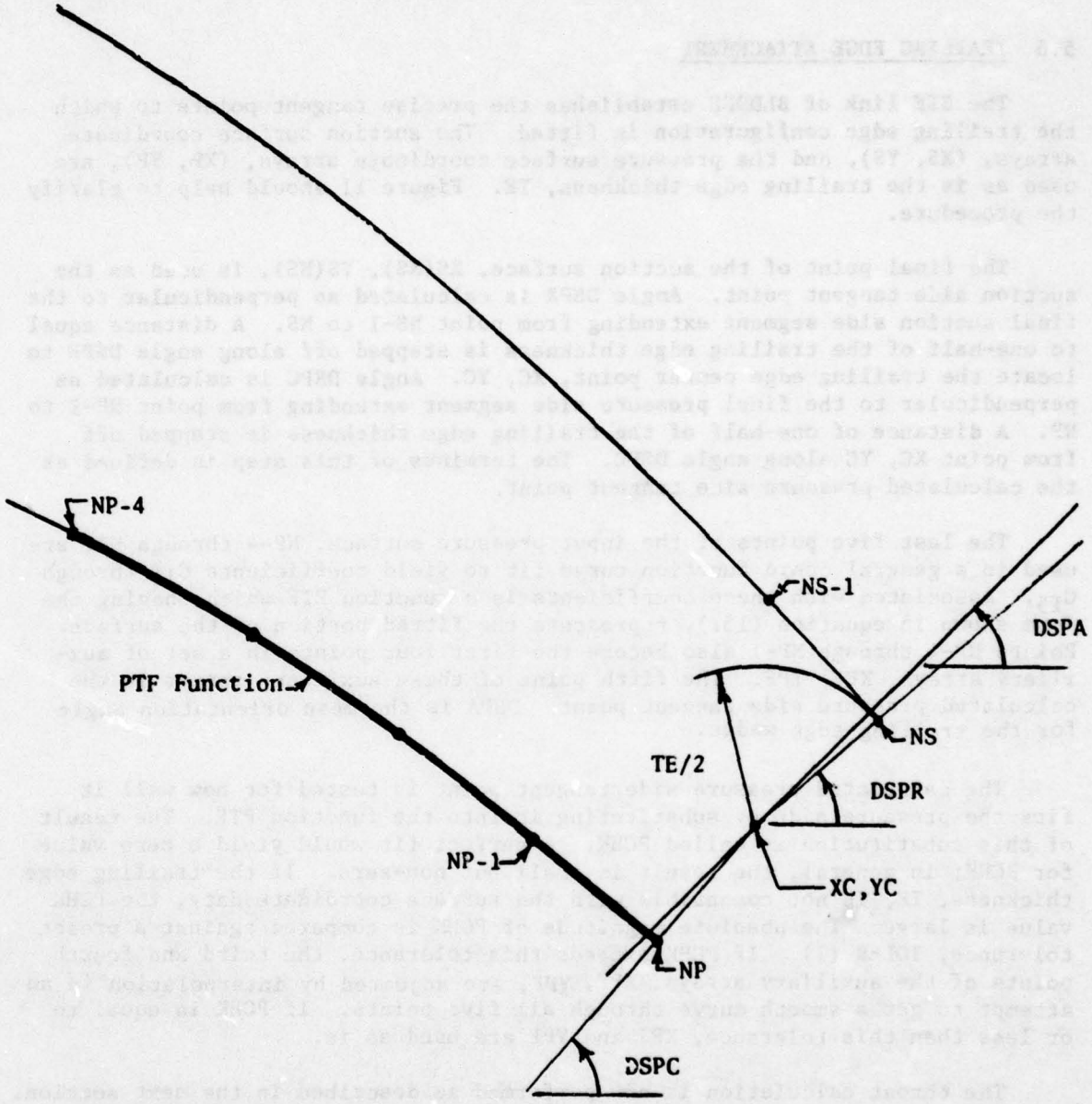

Figure 11. Trailing Edge Attachment Calculations (STE).

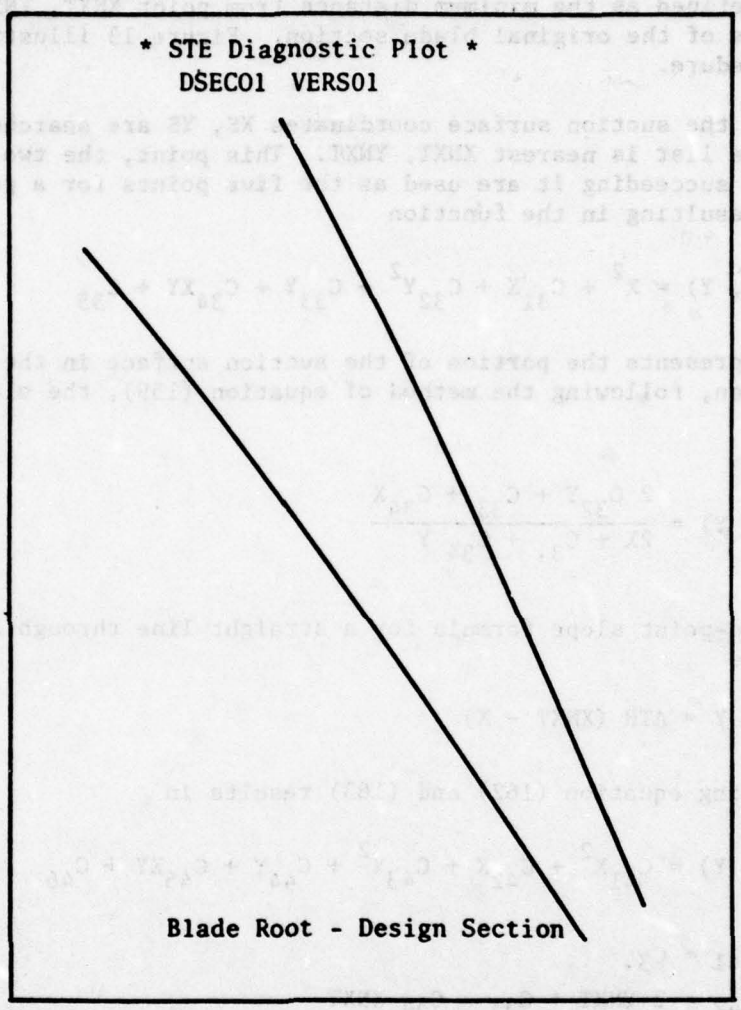

Figure 12. Typical STE Diagnostic Plot.

5.7 THROAT CALCULATION

The calculated pressure side tangent point and the blade spacing variable, PSPACE, are used to calculate the corresponding point on an adjacent blade section. This corresponding point is identified as XNXT, YNXT. The throat is defined as the minimum distance from point XNXT, YNXT to the suction surface of the original blade section. Figure 13 illustrates the calculation procedure.

First, the suction surface coordinates XS, YS are searched to find which point in the list is nearest XNXT, YNXT. This point, the two preceding it, and the two succeeding it are used as the five points for a general conic curve fit resulting in the function

$$\text{THS}(X, Y) = X^2 + C_{31}X + C_{32}Y^2 + C_{33}Y + C_{34}XY + C_{35} \tag{161}$$

THS represents the portion of the suction surface in the vicinity of the throat. Then, following the method of equation (159), the slope of a normal to THS is

$$\text{ATH}(X, Y) = \frac{2\,C_{32}Y + C_{33} + C_{34}X}{2X + C_{31} + C_{34}\,Y} \tag{162}$$

The two-point slope formula for a straight line through XNXT, YNXT with slope ATH is

$$\text{YNXT} - Y = \text{ATH}\,(\text{XNXT} - X) \tag{163}$$

Combining equation (162) and (163) results in

$$\text{THF}(X, Y) = C_{41}X^2 + C_{42}X + C_{43}Y^2 + C_{44}Y + C_{45}XY + C_{46} \tag{164}$$

where:

$C_{41} = C_{34}$

$C_{42} = 2\ \text{YNXT} + C_{33} - C_{34}\ \text{XNXT}$

$C_{43} = -C_{34}$

$C_{44} = C_{34}\ \text{YNXT} - C_{31} - 2C_{32}\ \text{XNXT}$

$C_{45} = 2C_{32} - 2$

$C_{46} = C_{31}\ \text{YNXT} - C_{33}\ \text{XNXT}$

Functions THS and THF are solved simultaneously, using the Newton-Raphson procedure, giving the point XTH, YTH as the suction surface throat locus. Finally, the throat is calculated as the distance between XTH, YTH and XNXT, YNXT.

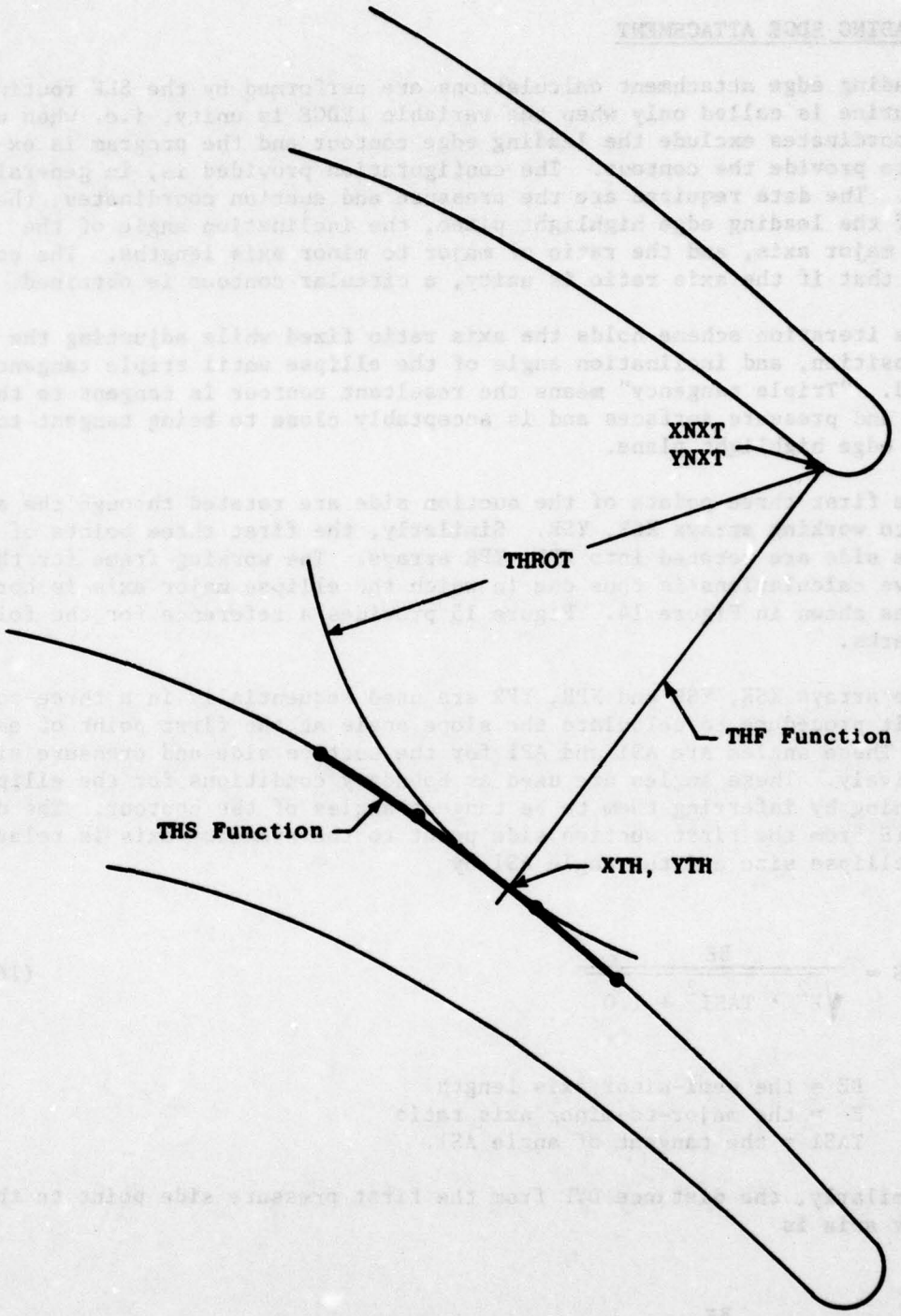

Figure 13. Throat Calculation (STE).

5.3 LEADING EDGE ATTACHMENT

Leading edge attachment calculations are performed by the SLE routine. This routine is called only when the variable LEDGE is unity, i.e. when user input coordinates exclude the leading edge contour and the program is expected to provide the contour. The configuration provided is, in general, an ellipse. The data required are the pressure and suction coordinates, the locus of the leading edge highlight plane, the inclination angle of the ellipse major axis, and the ratio of major to minor axis lengths. The coding is such that if the axis ratio is unity, a circular contour is obtained.

The iteration scheme holds the axis ratio fixed while adjusting the size, position, and inclination angle of the ellipse until triple tangency is achieved. "Triple tangency" means the resultant contour is tangent to the suction and pressure surfaces and is acceptably close to being tangent to the leading edge highlight plane.

The first three points of the suction side are rotated through the angle EPSI into working arrays XSR, YSR. Similarly, the first three points of the pressure side are rotated into XPR, YPR arrays. The working frame for the iterative calculations is thus one in which the ellipse major axis is horizontal as shown in Figure 14. Figure 15 provides a reference for the following remarks.

The arrays XSR, YSR and XPR, YPR are used sequentially in a three-point curve fit procedure to calculate the slope angle at the first point of each array. These angles are AS1 and AP1 for the suction side and pressure side, respectively. These angles are used as boundary conditions for the ellipse positioning by inferring them to be tangent angles of the contour. The distance DYS from the first suction side point to the symmetry axis is related to the ellipse size and the angle AS1 by

$$DYS = \frac{BE}{\sqrt{E^2 \cdot TASI^2 + 1.0}} \tag{165}$$

where: BE = the semi-minor axis length
E = the major-to-minor axis ratio
TAS1 = the tangent of angle AS1.

Similarly, the distance DYP from the first pressure side point to the symmetry axis is

$$DYP = \frac{BE}{\sqrt{E^2 \cdot TAPI^2 + 1.0}} \tag{166}$$

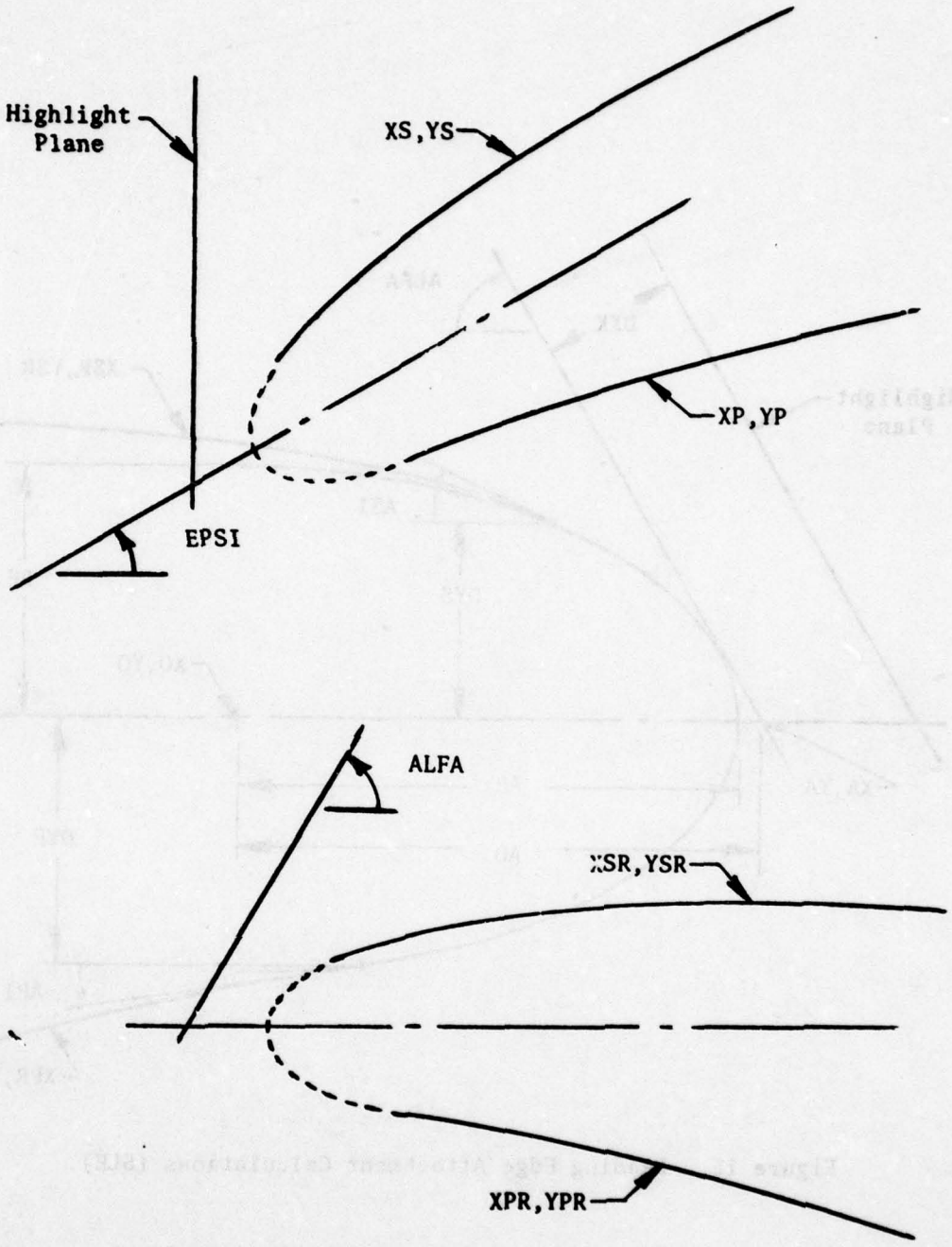

Figure 14. Leading Edge Rotation to Working Frame (SLE).

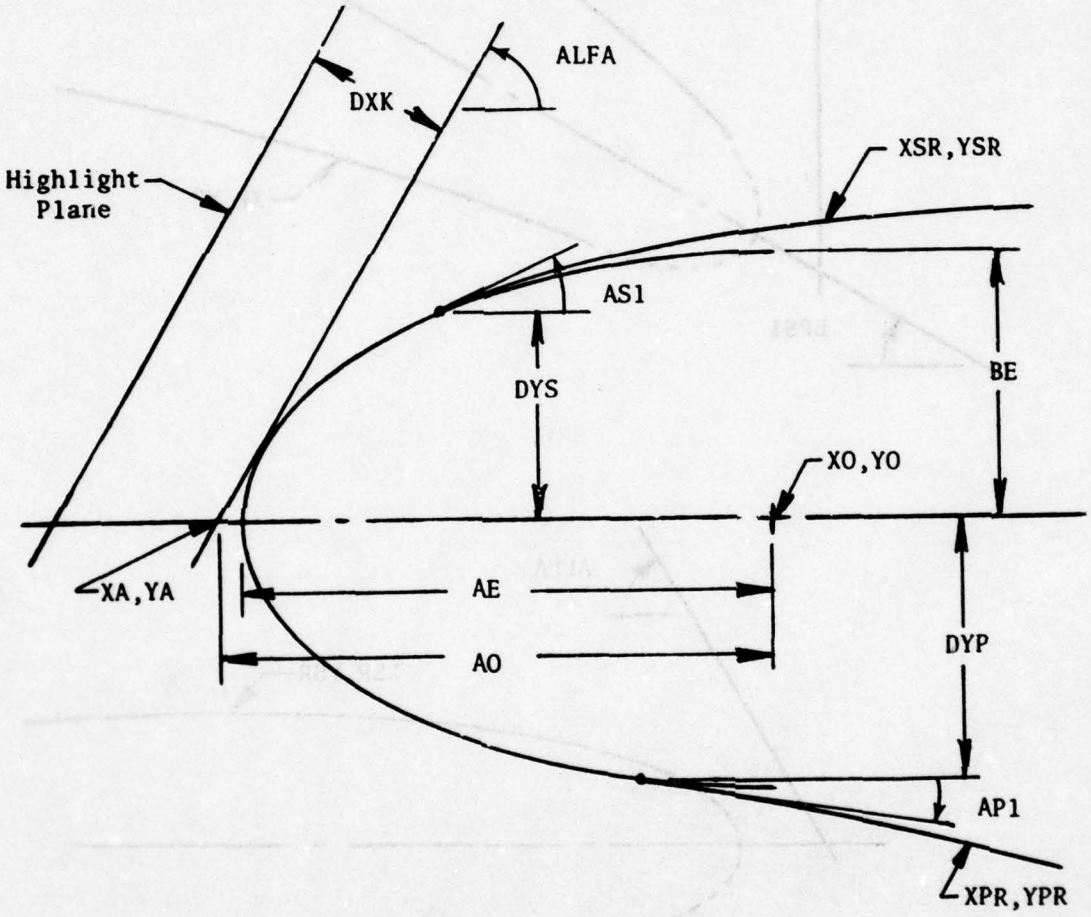

Figure 15. Leading Edge Attachment Calculations (SLE).

where TAP1 is the tangent of angle AP1.

The sum of the distances DYS and DYP is

$$DYS + DYP = YSR(1) - YPR(1) \tag{167}$$

The semi-minor axis length BE is calculated by manipulating equations (165) through (167). Then the semi-major axis length AE is calculated by

$$AE = E \cdot BE \tag{168}$$

The location of the ellipse center point XO, YO is calculated as follows:

$$XO = XSR(1) + E^2 \cdot TAS1 \cdot DYS \tag{169}$$

$$YO = YSR(1) - DYS \tag{170}$$

The angle ALFA is the complement of EPSI, i.e.

$$ALFA = 90 - EPSI \tag{171}$$

and represents the inclination of the leading edge highlight plane in the rotated working frame. Assume that there is an auxiliary line parallel to the highlight plane, i.e. inclined at angle ALFA, and that this line is tangent to the ellipse contour. The symmetry axis intersects this line at point XA, YA. This point lies at a distance AO to the left of the ellipse center point, XO, YO. If EPSI is zero, AO is equal to AE and point XA, YA is then the point where the symmetry axis pierces the contour. For the general case where EPSI is not zero, the distance AO is calculated as

$$AO = \frac{BE \cdot \sqrt{E^2 \cdot TALF^2 + 1.0}}{TALF} \tag{172}$$

where TALF is the tangent of angle ALFA.

Then XA, YA are

$$XA = XO - AO \tag{173}$$

$$YA = YO$$

Point XA, YA is rotated back to the input frame of reference as point XKA, YKA. Then

$$DXK = XKA - XK \tag{174}$$

where XK is the locus of the highlight plane.

Thus, DXK is the measure of how near the contour is to being tangent to the highlight plane. If the magnitude of DXK is less than, or equal to, the preset tolerance TOLER (2), the iteration ends. The default value for the tolerance is 5.0×10^{-7} and may be overridden by user input. If the tolerance is not met, the XSR, YSR and XPR, YPR arrays are adjusted and the procedure is repeated, starting with the calculations of AS1 and AP1.

The iteration ends where the DXK tolerance check is satisfied. Experience to date has shown convergence occurring in three to five iterations. The simple algebraic relationships execute rapidly.

The next step is to calculate six points on both the suction side and pressure side of the ellipse contour. In both cases, the first point is where the symmetry axis pierces the ellipse contour. If EPSI is zero, the first point is also the highlight point. Otherwise, the points are distributed so that the first four points are symmetric about the major axis. The fourth point is the highlight point. The routine is coded to accommodate the fact that the highlight point is on the suction side when EPSI is positive and is on the pressure side when EPSI is negative. Points five and six are not symmetrical: they lie between point four and the first points of the XSR, YSR and XPR, YPR arrays.

A diagnostic plot is now presented for user review. The plot arrays have twelve points for both suction and pressure sides and lie in the input frame of reference. These arrays include the ellipse contour points, the iteratively adjusted XSR, YSR and XPR, YPR arrays, and additional points for the original input coordinate data. Hash marks show the resultant tangent point locations, and a vertical line shows the highlight plane location. An optional diagnostic printout is available. A repeat option is also available and, if taken, affords the user an opportunity to alter the E, EPSI, or TOLER (2) values. Figure 16 shows a sample SLE diagnostic plot.

5.9 BLADE SECTION GENERATOR

The foregoing discussions have inferred the availability of coordinate arrays which describe the suction and pressure surfaces of a blade section. It was seen that this description extends from leading edge tangent point to trailing edge tangent point for each surface, leaving the edge configurations to be supplied by module calculations. There are two ways in which these arrays can be established. The first way is by direct user input when the data are acquired by digitizing an available engineering drawing of the section. The second way is to engage the services of a BLDDES link called BSGEN, which provides the means for automatically generating these arrays

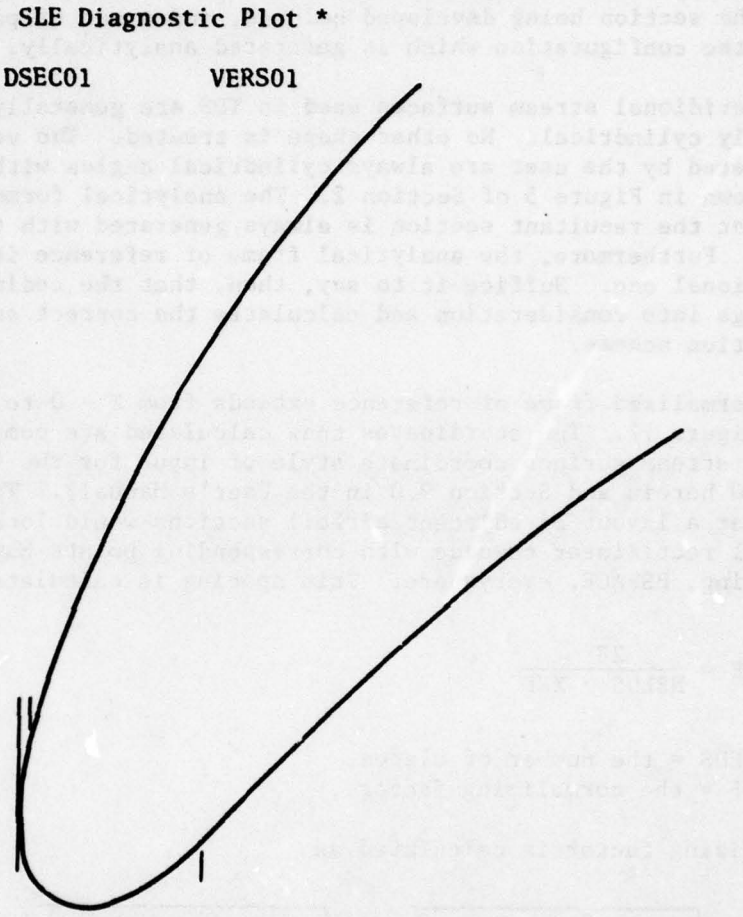

Figure 16. Typical SLE Diagnostic Plot.

using parametric input supplied by the user in lieu of the digitzed data. The techniques used in BSGEN are the subject of this section.

The input items utilized by BSGEN include a stream surface definition in terms of leading and trailing edge axial positions and radii, the vector diagram gas angles, an incidence angle, the number of blades in the blade row to which the section being developed belongs, and a set of parameters which influence the configuration which is generated analytically.

The meridional stream surfaces used in TDS are generally conical and occasionally cylindrical. No other shape is treated. The vector diagram angles entered by the user are always cylindrical angles with a sign convention as shown in Figure 5 of Section 2. The analytical formulation of BSGEN is such that the resultant section is always generated with the pressure side uppermost. Furthermore, the analytical frame of reference is a normalized, two-dimensional one. Suffice it to say, then, that the coding takes all of these things into consideration and calculates the correct angles for use in the generation scheme.

The normalized frame of reference extends from X = 0 to X = 1.0, as shown in Figure 17. The coordinates thus calculated are compatible with the normalized stream surface coordinate style of input for the CASC module (see Section 7.0 herein and Section 9.0 in the User's Manual). The normalization is such that a layout of adjacent airfoil sections would look like a two-dimensional rectilinear cascade with corresponding points having a constant pitch spacing, PSPACE, everywhere. This spacing is calculated as

$$\text{PSPACE} = \frac{2\pi}{\text{NBLDS} \cdot \text{XNF}} \tag{175}$$

where: NBLDS = the number of blades
XNF = the normalizing factor.

The normalizing factor is calculated as

$$\text{XNF} = \frac{\sqrt{(\text{ZM}-\text{ZL})^2 + (\text{RM}-\text{RL})^2}}{1/2\ (\text{RM} + \text{RL})} + \frac{\sqrt{(\text{ZT}-\text{ZM})^2 + (\text{RT}-\text{RM})^2}}{1/2\ (\text{RM} + \text{RT})} \tag{176}$$

where: ZL = the leading edge axial position
ZT = the trailing edge axial position
ZM = the arithmetic average of ZL and ZT
RL = the leading edge radius
RT = the trailing edge radius
RM = the arithmetic average of RL and RT.

As mentioned previously, the β_1 and β_2 angles of Figure 17 are either cylindrical or meridional angles with proper algebraic signs as required. The dimensional input variables, TE and TMAXX, are appropriately normalized.

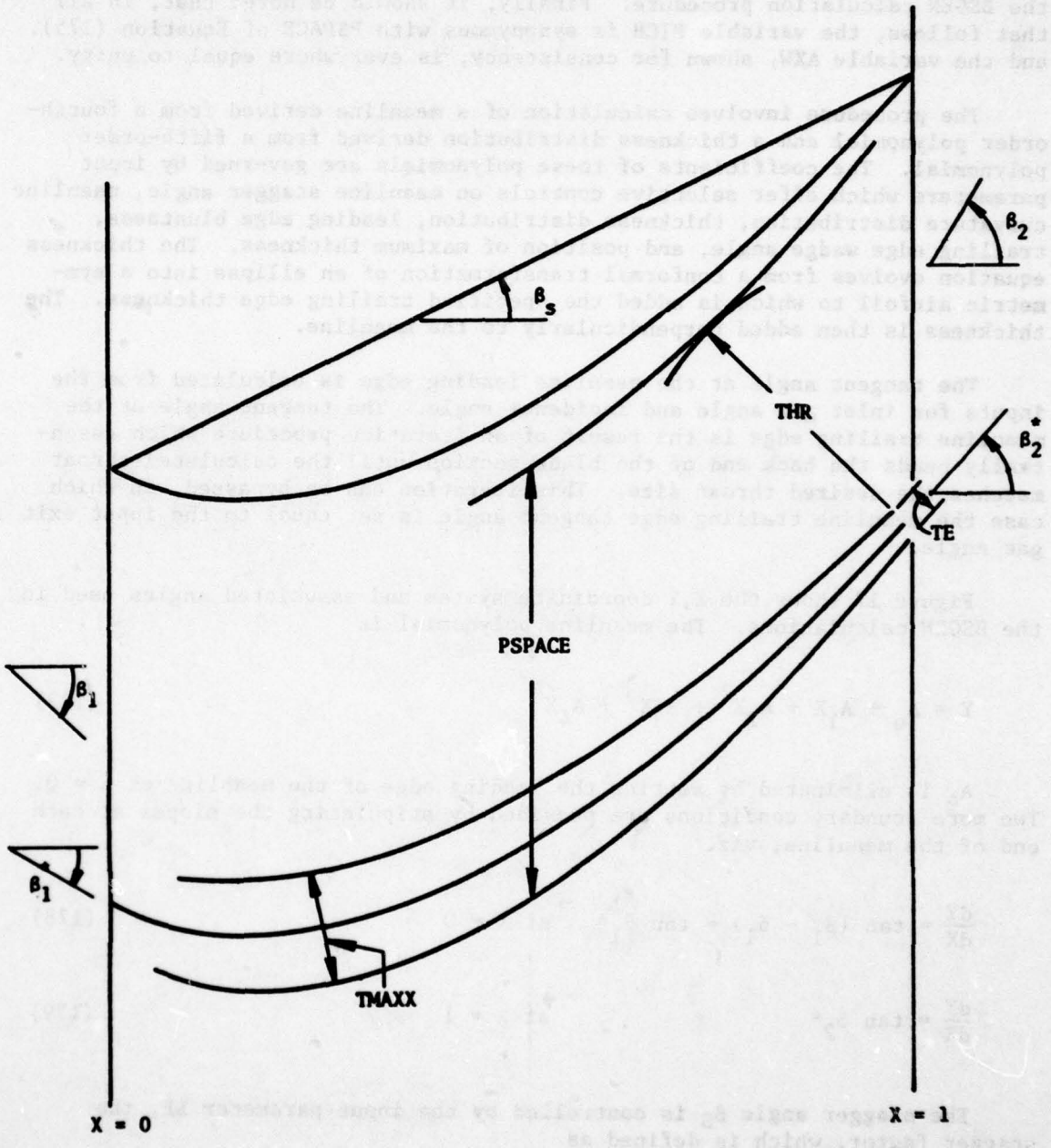

Figure 17. Blade Generator Coordinate System (BSGEN).

To reemphasize these points, it is noted that the user inputs dimensional quantities for TE and TMAXX, and cylindrical gas angles with vector diagram sign conventions, and the program takes care of reformulating the data for the BSGEN calculation procedure. Finally, it should be noted that, in all that follows, the variable PICH is synonymous with PSPACE of Equation (175), and the variable AXW, shown for consistency, is everywhere equal to unity.

The procedure involves calculation of a meanline derived from a fourth-order polynomial and a thickness distribution derived from a fifth-order polynomial. The coefficients of these polynomials are governed by input parameters which offer selective controls on meanline stagger angle, meanline curvature distribution, thickness distribution, leading edge bluntness, trailing edge wedge angle, and position of maximum thickness. The thickness equation evolves from a conformal transformation of an ellipse into a symmetric airfoil to which is added the specified trailing edge thickness. The thickness is then added perpendicularly to the meanline.

The tangent angle at the meanline leading edge is calculated from the inputs for inlet gas angle and incidence angle. The tangent angle at the meanline trailing edge is the result of an iteration procedure which essentially bends the back end of the blade section until the calculated throat matches the desired throat size. This iteration can be bypassed, in which case the meanline trailing edge tangent angle is set equal to the input exit gas angle.

Figure 17 shows the X,Y coordinate system and associated angles used in the BSGEN calculations. The meanline polynomial is

$$Y = A_o + A_1X + A_2X^2 + A_3X^3 + A_4X^4 \tag{177}$$

A_o is eliminated by setting the leading edge of the meanline at X = 0. Two more boundary conditions are provided by stipulating the slopes at each end of the meanline, viz.

$$\frac{dY}{dX} = \tan(\beta_1 - \delta_1) = \tan \beta_1^* \quad \text{at } X = 0 \tag{178}$$

$$\frac{dY}{dX} = \tan \beta_2^* \quad \text{at } X = 1 \tag{179}$$

The stagger angle β_S is controlled by the input parameter SF, the stagger factor, which is defined as

$$SF = \frac{\tan \beta_2^* - \tan \beta_S}{\tan \beta_S - \tan \beta_1^*} \tag{180}$$

SF has the effect of controlling the distribution of "curvature", d^2Y/dX^2; smaller SF increases curvature at the leading edge and decreases curvature at the trailing edge. In order to control the relationship of leading and trailing edge curvatures to midchord curvature, one more condition is introduced:

$$\frac{d^2Y}{dX^2} = C_3 \, f \, (\beta_1^*, \, \beta_2^*, \, SF) \qquad \text{at } X = 1 \tag{181}$$

where $f(\beta_1^*, \beta_2^*, SF)$ is determined from the special case

$$\frac{d^3Y}{dX^3} = 0 \qquad \text{at } X = 1 \; (C_3 = 1 \text{ implied}) \tag{182}$$

The reason for the choice of C_3 and f in Equation (181) is that the meanline is nearly parabolic (exactly parabolic when $C_3 = 1$, SF = 1). Thus, normal trailing edge curvature is obtained when the meanline is parabolic at the trailing edge as specified by (182).

For convenience, new coefficients are defined as:

$$B_1 = \frac{(1 + SF) \, A_2}{\tan \beta_1^* - \tan \beta_2^*} \tag{183}$$

$$B_2 = \frac{(1 + SF) \, A_3}{\tan \beta_1^* - \tan \beta_2^*}$$

and

$$B_3 = \frac{(1 + SF) \, A_4}{\tan \beta_1^* - \tan \beta_2^*} \tag{185}$$

With these definitions and boundary conditions, the meanline coefficients become

$$B_1 = \frac{C_3}{2} \, (1 - 3SF) + 3SF - 3 \tag{186}$$

$$B_2 = C_3 \, (3SF - 1) - 5SF + 3 \tag{187}$$

$$B_3 = \frac{C_3}{2} \, (1 - 3SF) + 2SF - 1 \tag{188}$$

The thickness distribution is developed from a circular cylinder which gives a continuous slope around the leading edge. The factors which must be controlled are:

1. Maximum thickness, TMAXX
2. Trailing edge thickness, TE
3. Leading edge bluntness, TI
4. Location of maximum thickness, C_1
5. Trailing edge included angle, δ_2

Expanding the thickness distribution of the cylinder linearly and separating the resulting elliptical shape about the major axis is accomplished by the following equation:

$$TH = \frac{TMAXX - TE}{AXW} \sqrt{\zeta\ (1 - \zeta)} + \frac{TE}{2\ AXW} \qquad 0 \leq \zeta \leq 1 \tag{189}$$

This half-thickness relationship provides control on the first two items of the list. Let $\zeta(X)$ be a fifth-order polynomial whose coefficients are evaluated using the last three control factors and two additional constraints. Thus

$$\zeta\ (X) = 2X\ (TI + A_1X + A_2X^2 + A_3X^3 + A_4X^4) \tag{190}$$

where TI, the bluntness factor, is related to leading edge radius of curvature. Figure 18 shows how the elliptical half-thickness distribution is applied using the ζ function. The boundary condition on ζ are:

$$\zeta = 0 \quad \text{at } X = 0 \tag{191}$$

$$\zeta = 1 \quad \text{at } X = 1 \text{ since } Th = \frac{TE}{2\ AXW} \text{ at } X = 1 \tag{192}$$

$$\zeta = 1/2 \quad \text{at } X = C_1, \text{ the point of maximum thickness} \tag{193}$$

The derivative of the half-thickness with respect to X is

$$\frac{dTH}{dX} = \frac{TMAXX-TE}{AXW} \frac{1 - 2\zeta}{2\sqrt{\zeta\ (1 - \zeta)}} \frac{d\zeta}{dX} \tag{194}$$

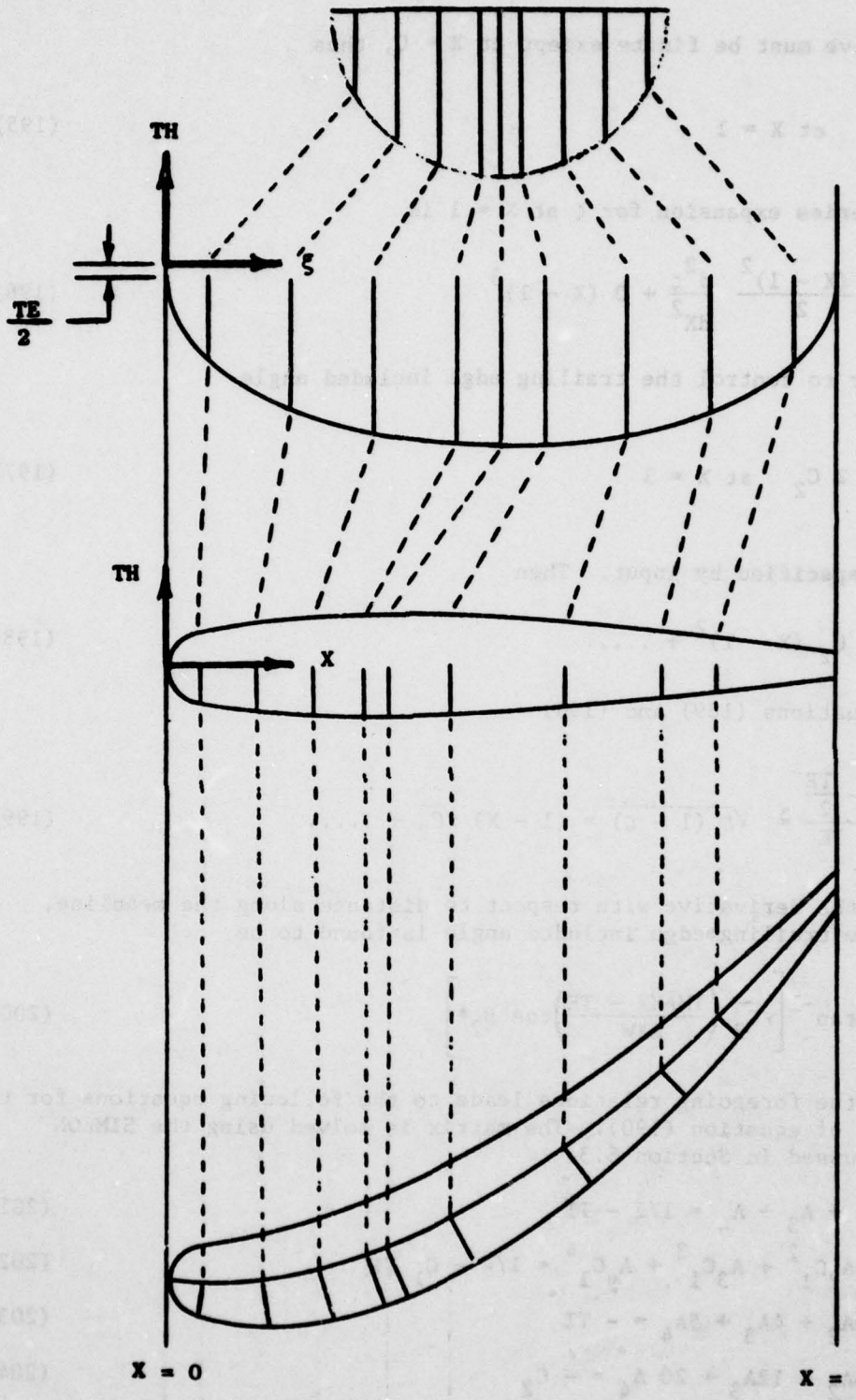

Figure 18. Blade Generator Half-Thickness Transformation (BSGEN).

This derivative must be finite except at X = 0, thus

$$\frac{d\zeta}{dX} = 0 \quad \text{at } X = 1 \tag{195}$$

The Taylor Series expansion for ζ at X = 1 is

$$\zeta = 1 + \frac{(X-1)^2}{2}\frac{d^2\zeta}{dX^2} + 0\,(X-1)^3 \tag{196}$$

In order to control the trailing edge included angle

$$\frac{d^2\zeta}{dX^2} = -2\,C_2 \quad \text{at } X = 1 \tag{197}$$

where C_2 is specified by input. Then

$$\zeta = 1 - C_2\,(X-1)^2 + \ldots\ldots \tag{198}$$

From equations (189) and (198)

$$\frac{AXW \cdot TH - \frac{TE}{2}}{TMAXX - TE} = \sqrt{\zeta\,(1-\zeta)} = (1-X)\sqrt{C_2} + \ldots\ldots \tag{199}$$

Taking the derivative with respect to distance along the meanline, $X/\cos\beta_2^*$, the trailing edge included angle is found to be

$$\delta_T = 2\tan^{-1}\left[\sqrt{C_2}\left(\frac{TMAXX - TE}{AXW}\right)\cos\beta_2^*\right] \tag{200}$$

Use of the foregoing relations leads to the following equations for the coefficients of equation (190). The matrix is solved using the SIMEON routine discussed in Section 5.3.

$$A_1 + A_2 + A_3 + A_4 = 1/2 - TI \tag{201}$$

$$A_1C_1 + A_2C_1^2 + A_3C_1^3 + A_4C_1^4 = 1/4 - C_1\,TI \tag{202}$$

$$2A_1 + 3A_2 + 4A_3 + 5A_4 = -TI \tag{203}$$

$$2A_1 + 6A_2 + 12A_3 + 20\,A_4 = -C_2 \tag{204}$$

The meanline trailing edge angle β_2^* is initially set equal to the exit gas angle β_2. If CF is entered as zero, this angle is preserved but no throat calculation is performed. If CF is greater than zero, an iteration procedure is used to find the minimum distance from the trailing edge pressure side coordinate to the suction side of the next blade, resulting in the throat, THR, as

$$THR = CF \cdot PICH \cdot \cos \beta_2 \tag{205}$$

A diagnostic plot of the pressure side and suction side coordinate is presented at the conclusion of the calculations. In this plot, the pressure side is uppermost for vane sections while the suction side is uppermost for rotor blade sections. An optional diagnostic printout is available, and an option to repeat the BSGEN calculations with revised input is available. The conventions defined for input apply to terminal entries. Electing to continue as-is causes program control to return to the main link for the next step.

5.10 UPPER/LOWER SURFACE ORGANIZATION

Surface coordinates come about in one of two ways: as input data digitized from a drawing of the section or as output from the blade section generator. Furthermore, the digitized input data may describe only the surface proper from leading edge tangent point to trailing edge tangent point (LEDGE = 1 mode), or they may include the leading edte configuration (LEDGE = 2 mode). In the LEDGE = 1 mode, the program supplies the leading edge configuration via the SLE link. Use of the blade generator is automatically a LEDGE = 1 mode of operation. SLE provides the precise tangent points and ellipse size and orientation data for defining the leading edge. In all cases, the precise tangent points for attaching the trailing edge shape are calculated in the STE link. Finally, no matter what scale size and blade orientation are used in the input, all internal calculations are carried out in normalized form and, beyond the blade generator step, the suction surface is uppermost.

Whatever mode is used, the ULSRF routine organizes the data into two sets of coordinates. The "upper" or suction side extends from the leading edge point (where the meanline pierces the leading edge contour) to the trailing edge point (where the meanline pierces the trailing edge contour). The "lower" or pressure side is defined by arrays having the same initial and final points as the upper arrays. A diagnostic printout lists these arrays, and a diagnostic plot of the section thus organized is available. Figure 19 indicates the results of this organization. Internal counters are employed to keep track of which pairs are the tangent points.

The diagnostic plot of ULSRF is the first opportunity the user has of seeing the completely assemoled blade section. Therefore, an option is offered to restart the case from the very beginning with terminal input or to terminate the case with no output file so as to have additional time to consider what possible changes might be made. Electing to continue as is commits the blade section to the final calculation steps.

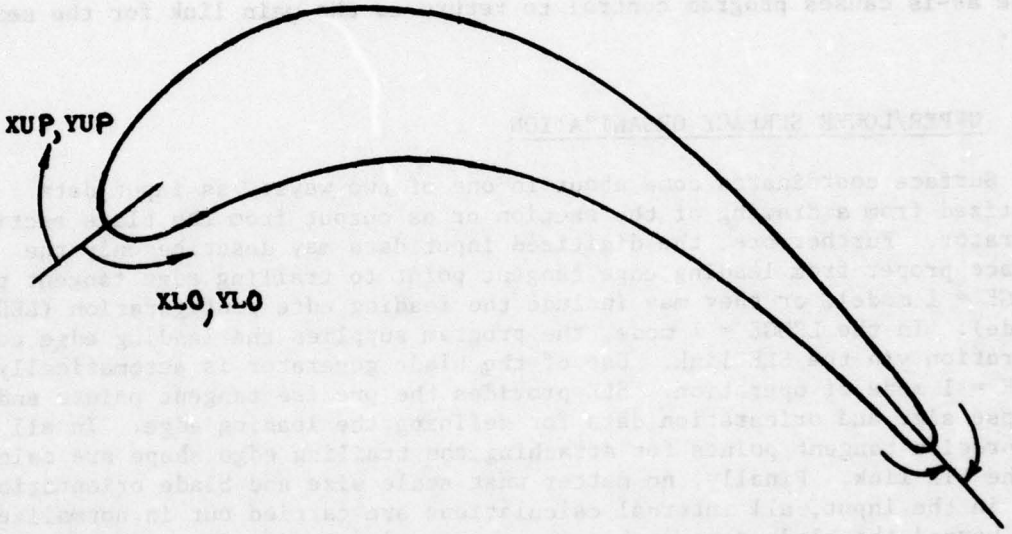

Figure 19. Upper-Lower Surface Delineation (ULSRF).

5.11 CASC INPUT

The CSCIN routine utilizes the upper/lower coordinate arrays from ULSRF and meridional stream surface data to develop specially formulated arrays which can be written on the BLDDES output file for subsequent input to the CASC module.

The coordinate arrays are normalized stream surface values with the suction side uppermost. CASC is always run with this orientation for both blade and vane sections because, for the highly cambered airfoil sections which are common in turbine blading, a more favorable calculation grid is achieved. Furthermore, CASC input requires that the trailing edge be left open. Therefore, the CASC coordinate arrays are merely subsets of the ULSRF array and extend from the leading edge point where the meanline pierces the contour to the trailing edge tangent points of each surface. There are at most 31 coordinate pairs for each surface. Surface tangent angles at each coordinate point are calculated by a flexible beam analogy routine. Figure 20 illustrates the results. Note that the origin has been shifted to the leading edge highlight plane.

The next order of business is to calculate the meridional stream surface description tables. There are three tables containing 13 corresponding entries. The first table, ZM, is axial position; the second table, RM, is radius; the third table, HM, is stream tube thickness. The ZM and RM values are best described by simply referring to Figure 21, which shows the arrangement for a typical conical section. The surface is composed of a cylindrical segment, a parabolic curve into the leading edge point, a segment through the blade proper, a parabolic trailer curve, and a terminating cylindrical segment. Points 5 and 6 are repeated to delineate the leading edge point; points 8 and 9 are repeated to delineate the trailing edge point.

The stream tube thickness at the leading edge point, HMLE, is set to unity. The stream tube thickness at the trailing edge, HMTE, is an input item obtained from the ATREC module results. ATREC provides an HMR array which represents the ratio of stream function values for each streamline calculated therein. The blade preprocessor module, BDPREP, selects the appropriate value for HMTE from this array when setting up the input file for BLDDES. Using these leading and trailing edge values and the RM values, the HM table is calculated so as to give a smooth stream tube area distribution. The progression is as follows.

$$ZM(1) = ZLE - 2 \cdot (ZTE - ZLE) \qquad (206)$$

where: ZLE = the leading edge axial position (input or 0 default)
ZTE = the trailing edge axial position (input).

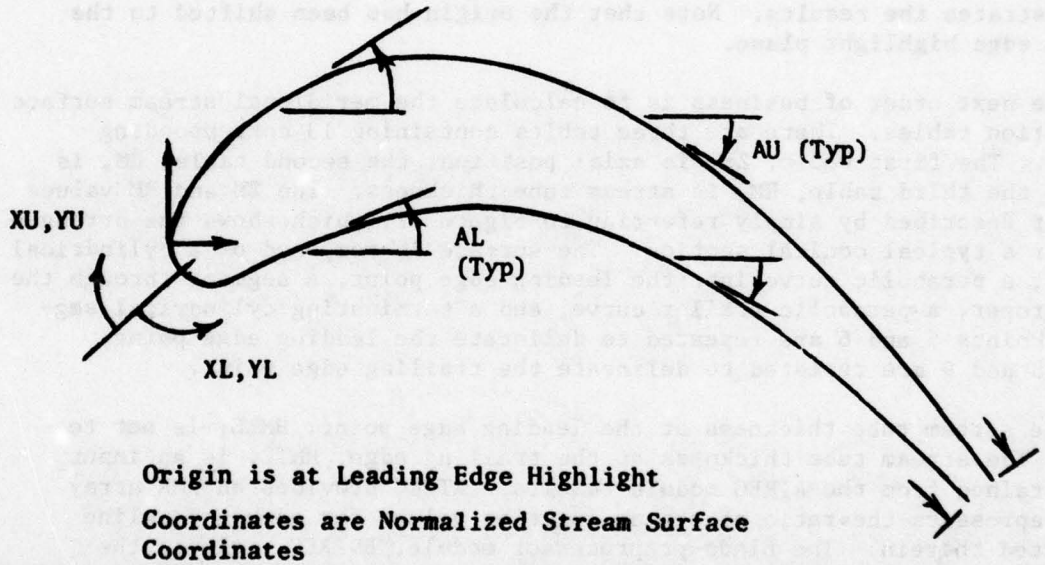

Origin is at Leading Edge Highlight

Coordinates are Normalized Stream Surface Coordinates

Surface Angles Measured as Shown

Figure 20. Output Coordinates for CASC (CSCIN).

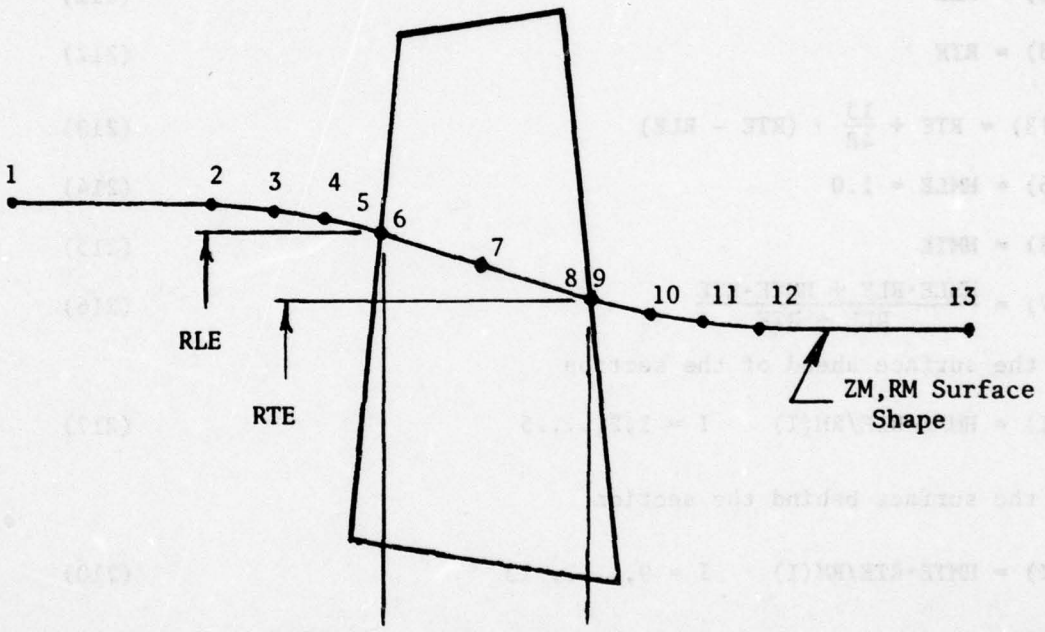

The stream tube thickness, HM, is calculated for each of the above points.

Figure 21. Output Stream Surface for CASC (CSCIN).

$$ZM(6) = ZLE \tag{207}$$

$$ZM(8) = ZTE \tag{208}$$

$$ZM(13 = ZTE + 2 \cdot (ZTE - ZLE) \tag{209}$$

$$RM(1) = RLE - \frac{13}{48} \cdot (RTE - RLE) \tag{210}$$

where: RLE = the leading edge radius (input)
RTE = the trailing edge radius (input).

$$RM(6) = RLE \tag{211}$$

$$RM(8) = RTE \tag{212}$$

$$RM(13) = RTE + \frac{13}{48} \cdot (RTE - RLE) \tag{213}$$

$$HM(6) = HMLE = 1.0 \tag{214}$$

$$HM(8) = HMTE \tag{215}$$

$$HM(7) = \frac{HMLE \cdot RLE + HMTE \cdot RTE}{RLE + RTE} \tag{216}$$

For the surface ahead of the section

$$HM(I) = HMLE \cdot RLE/RM(I) \qquad I = 1,2,....5 \tag{217}$$

For the surface behind the section

$$HM(I) = HMTE \cdot RTE/RM(I) \qquad I = 9,...., 13 \tag{218}$$

There are several individual variables required by CASC whose values are set from the ZM table. These are ZUP, Z1, Z2, and ZDOWN which are set to ZM (1), ZM (6), ZM (8), and ZM (15), respectively. Values of ZM and RM which have not been mentioned specifically in the foregoing equations are calculated with appropriate constants to yield the cylindrical-parabolic shape desired.

The final function of the CSCIN routine is to convert the non-CASC data to dimensional form for the remaining portion of the BLDDES module. The conversion is a straightforward interpolation procedure which changes the normalized X,Y data to Z,Rθ coordinates. There are no diagnostic plots or printouts in the CSCIN routine.

AD-A066 092 GENERAL ELECTRIC CO CINCINNATI OHIO AIRCRAFT ENGINE GROUP F/G 21/5
TURBINE DESIGN SYSTEM.(U)
NOV 78 R R WYSONG, T C PRINCE, D T LENAHAN F33615-75-C-2073
UNCLASSIFIED R78AEG XXX AFAPL-TR-78-92 NL

2 OF 3
ADA
066092

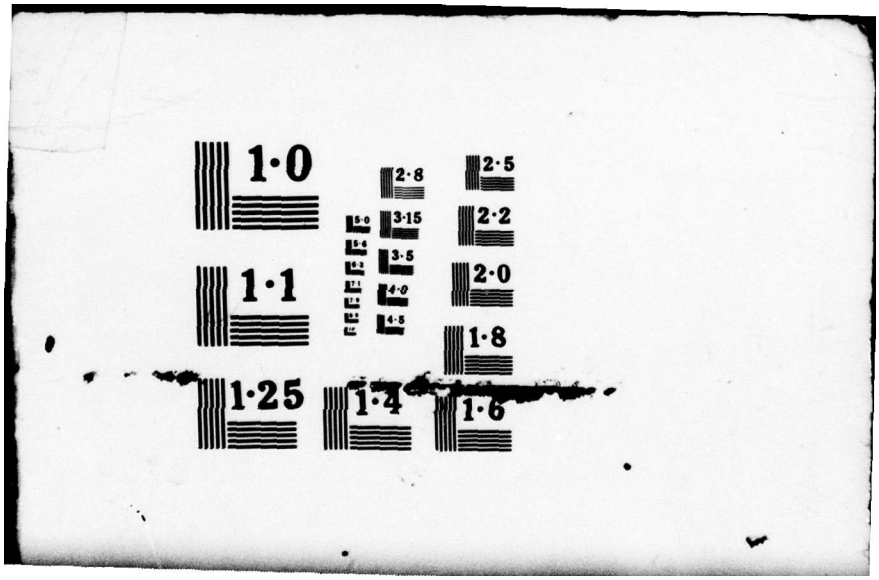
1·0
1·1
1·25
1·4
1·6
1·8
2·0
2·2
2·5
2·8
3·15
3·5
4·0
4·5
5·0

5.12 SECTION PROPERTIES

The section properties routine, SECPRO, calculates the cross-sectional area and center of gravity location for the solid blade section. If the user has requested a rotation of the section by including the variable ROTATE in the input, the rotation calculations are performed herein. SECPRO utilizes the upper and lower surface coordinate arrays which have been established by the ULSRF routine and which have been converted to dimensional form by the CSCIN routine. These data are used to partition the section into 54 subdivisions as shown in Figure 22. The area and center of gravity are calculated for each subdivision. These results are then summed to determine these characteristics for the entire section.

Thus

$$\text{AREA} = \sum_{1}^{54} A_i \tag{219}$$

$$\text{XCGI} = \frac{\sum_{1}^{54} A_i \bar{X}_i}{\text{AREA}} \tag{220}$$

$$\text{YCGI} = \frac{\sum_{1}^{54} A_i \bar{Y}_i}{\text{AREA}} \tag{221}$$

where: A_i = area of a subdivision

$\bar{X}_i$ = X-location of the CG of a subdivision

$\bar{Y}_i$ = Y-location of the CG of a subdivision

AREA = total cross-section area

XCGI, YCGI = location of the CG of the total cross section with respect to the origin of the input data.

A diagnostic plot is available which shows the cross section, the CG location, and the throat location (as calculated in STE).

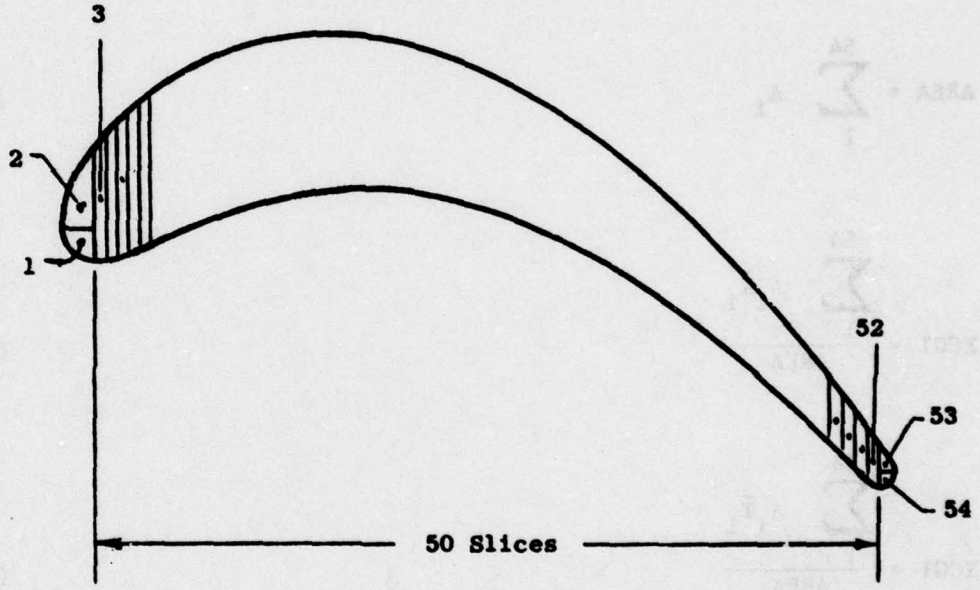

Figure 22. Subdivision for Section Property Calculations (SECPRO).

5.13 STANDARDIZED NUMBERING

The STNDPT link is used to calculate the final output coordinates which serve as the standardized definition of the section. The blade sections processed through the BLDDES module become the basic defining sections which are subsequently used by the BLDSTK module in interpolating for additional, intermediate blade sections for more complete definition of a blade row. Hence, this standardization provides a logical and orderly arrangement for eventual point-to-point interpolation.

The standardized numbering scheme is shown in Figure 23. There are 64 unique coordinate locations plus a 65th which repeats point 1 for complete closure. These coordinates are oriented with respect to the stacking point selected by the user via ISTK and STKPT input variables. Numbering begins at the leading edge point and proceeds around the suction surface to the trailing edge and then along the pressure surface. This sequence holds for both vane and blade sections. Special points are as follows:

1	Leading edge point where meanline pierces the contour
7	Suction side leading edge tangent point
11	Suction side point at 12% of axial width
25	Suction side point at 96% of axial width
28	Suction side trailing edge tangent point
33	Trailing edge point where meanline pierces the contour
38	Pressure side trailing edge tangent point
41	Pressure side point at 96% of axial width
55	Pressure side point at 12% of axial width
59	Pressure side leading edge tangent point

The points from 12% axial width to 96% axial width are equally distributed and lie directly opposite each other in the tangential direction. The 12% and 96% values quoted above are nominal. The program will adjust these as necessary to avoid overlapping the edge contour regions.

The routine makes use of the upper and lower surface lists and special coordinate point counters generated in the ULSRF routine. Leading edge points are redistributed so that the leading edge highlight point is:

Point 4 if EPSI is greater than zero
Point 1 if EPSI is equal to zero
Point 62 if EPSI is less than zero

where EPSI, the leading edge inclination angle, is as measured in the current suction-side-up orientation. The surface points are redistributed using the Lagrange interpolation routine RINT, discussed in Section 5.2. The trailing edge points are the same as those calculated in ULSRF; they are merely renumbered to suit the STNDPT scheme. The final calculation involves a translation of coordinates such that the origin for the output data is the user-selected stacking point. The location of the center of gravity with respect to this origin is also calculated and identified as XCG, YCG.

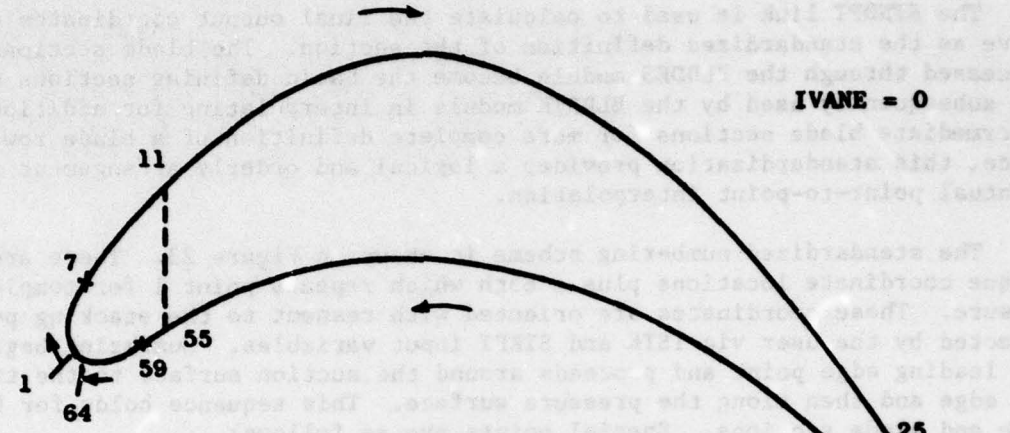

Output coordinates are WRT stack point

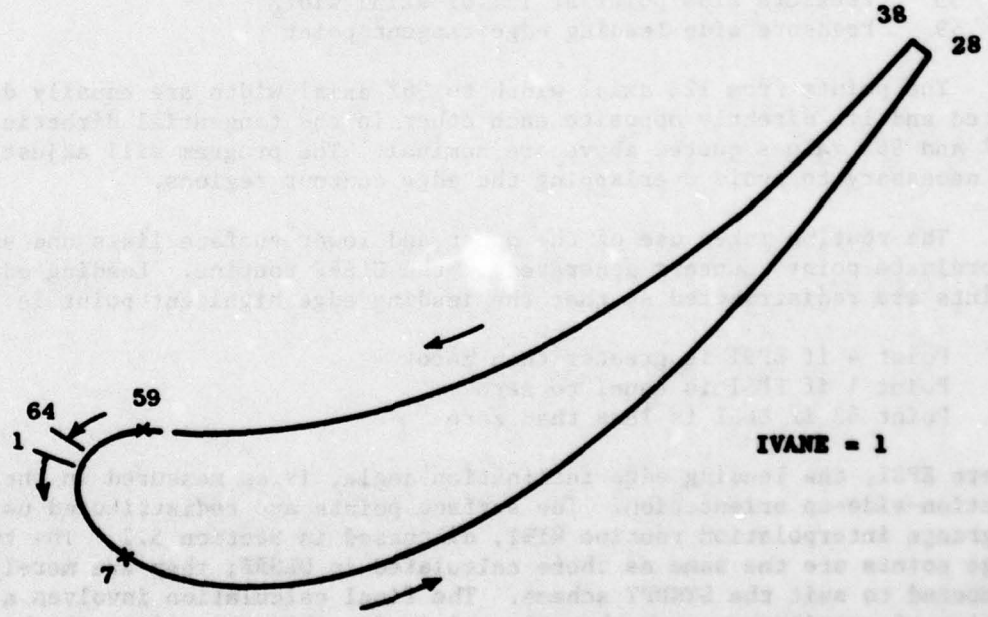

Figure 23. Standard Numbering - Output Coordinates (STNDPT).

The final coordinates which are written on the output file are identified as ZF, RF, and TF arrays of 65 values each. These constitute a three-dimensional Z, R, θ representation of the blade section and serve as input to the BLDSTK module. The origin of the data is where the stacking axis intersects the turbine centerline Z-axis. ZF and RF are specified in inches; TF is in radians. Furthermore, the TF values are specified with respect to the stacking axis, which is arbitrarily assumed to be at 90 degrees ($\pi/2$ radians). The reason for this arbitrary reference is that the resulting TF values are all positive numbers and present a neat tabular appearance when the output file is listed. The usual X,Y forms can be obtained from

$$X = ZF \tag{222}$$

$$Y = RF \cdot \left(\frac{\pi}{2} - TF\right) \tag{223}$$

A diagnostic plot is presented showing three adjacent sections in cascade orientation. A cross is plotted on the middle section to show the location of the stacking point. If the section is cylindrical, the pitch spacing of the plot is correct. If the section is conical, the spacing is correct at the trailing edge only. There is no diagnostic printout.

5.14 THICKNESS AND BLOCKAGE

The BLOKG link provides calculations of thickness, blockage, blockage derivative, and meanline slope for up to 20 user-selected positions on the blade section. These kinds of data are, in general, necessary as inputs for an axisymmetric flow field analysis which utilizes calculation stations inside blade rows. This link is optional and is only executed when the user includes the variables SLICE and NSLICE or NSLPCT in the input list.

Using the standardized coordinate arrays developed in STNDPT, a group of interpolation tables is established. Each table has 20 values and covers the blade section from leading edge highlight point to trailing edge highlight point. These tables include axial position measured from leading edge highlight, tangential thickness, upper and lower surface coordinates, meanline coordinates, and tangential blockage. Blockage is defined as

$$BLKG = TKI/PICH \tag{224}$$

where: TKI = tangential thickness
PICH = tangential blade spacing.

A table of blockage derivative, DLAM, which represents the rate of change of BLKG with respect to axial distance, is calculated using the general conic and tangent slope formulations discussed in Section 5.5. The tangential thickness table is scanned for the maximum thickness and its location.

After these preliminaries, the user input is interpreted as the fraction of axial width at which interpolated data is desired. The interpolations are made using RINT routine discussed in Section 5.2. The interpolated data are stored in COMMON for eventual printing as page three of the five-page summary printed at the conclusion of the module.

A diagnostic printout is available to list the tables used for interpolation, and a diagnostic plot is available to show the blade section surface and meanline inferred by these tables.

5.15 SUMMARY PRINTOUT

PRINTR is the final link called in BLDDES and provides a summary printout of results associated with the current blade section. If BLOKG data have been calculated, there are five pages of summary; otherwise, there are four pages.

As mentioned earlier, the internal calculations of BLDDES are carried out with the data scaled to 1X size and with the blade section oriented with the suction side up. For this final printout, the input data are rescaled to their original SCALIN size and, if appropriate, revamped to pressure-side-up orientation.

Page 1 of the summary gives leading and trailing edge configuration data, general items such as axial width, chord, etc., and stacking point data.

Page 2 contains the input coordinates along with a note on scale size. These are either the digitized input data or the output from the blade generator, depending on how the module has been run.

Page 3 shows the thickness and blockage data at the user-selected slices.

Page 4 lists the standardized output coordinates with respect to the stacking point along with a note on scale size and stack point option used.

Page 5 lists the CASC input data as generated by the CSCIN link.

6.0 BLADE STACKING

6.1 INTRODUCTION

The BLDSTK module performs several tasks associated with a complete spanwise definition of the blade row which is currently being processed. The first task is to provide a set of eleven sections via an interpolation of the basic design sections created by the BLDDES module. The second task is to provide, on an optional basis, plots of the individual interpolated sections and/or a stack plot of all eleven sections. The third task is to assemble an optional summary printout of the major geometric characteristics of the interpolated sections. The fourth task is to offer an optional three-view display of the blade oriented at user-selected angles. The final task is to write two output files to be used as input for subsequent modules.

6.2 THE INTERPOLATION PROCEDURE

The output file from BLDDES used as input to the BLDSTK module is presumed to have at least one version each of root, pitch, and tip design sections. On-line terminal queries permit the user to specify a case identifier of up to 40 characters and the level of interpolation desired. A level of 2 means that only root and tip sections will be used and the resultant interpolation is linear. A level of 3 means root, pitch, and tip sections will be used in a parabolic interpolation. A third on-line query then permits the user to specify which versions of design sections are to be used. BLDSTK reads the appropriate data sets and stores this input in readiness for the interpolation calculations.

The input design sections may be all conical, all cylindrical, or a mix of these. The coordinate data are embodied in three arrays identified as RF, ZF, and TF, each having 65 values. The first 64 are unique points: the 65th point is a repeat of point 1. These data are measured with respect to the stacking axis as established by the user when executing the BLDDES module. Additional input items include the bladerow type, the number of blades, and two reference radii, RREF, which identify the radial extremities of the bladerow. The smaller of these reference radii defines the zero percent span height while the larger defines the 100 percent span height. Using these radii, an internal table of eleven values of radial position is calculated. These eleven values, extending from zero to 100% span height in increments of 10%, are the positions at which interpolated sections are calculated. Hence, all interpolated sections are cylindrical with the following exceptions. If the root section is conical, the first interpolated section will also be conical. Similarly, if the tip section is conical, the eleventh interpolated section will be conical (see Figure 24).

The interpolation is point-to-point for 65 locations on each section, utilizing the standardized numbering system of BLDDES. The interpolation routine is the Lagrange method discussed in Section 5.2. The coordinate

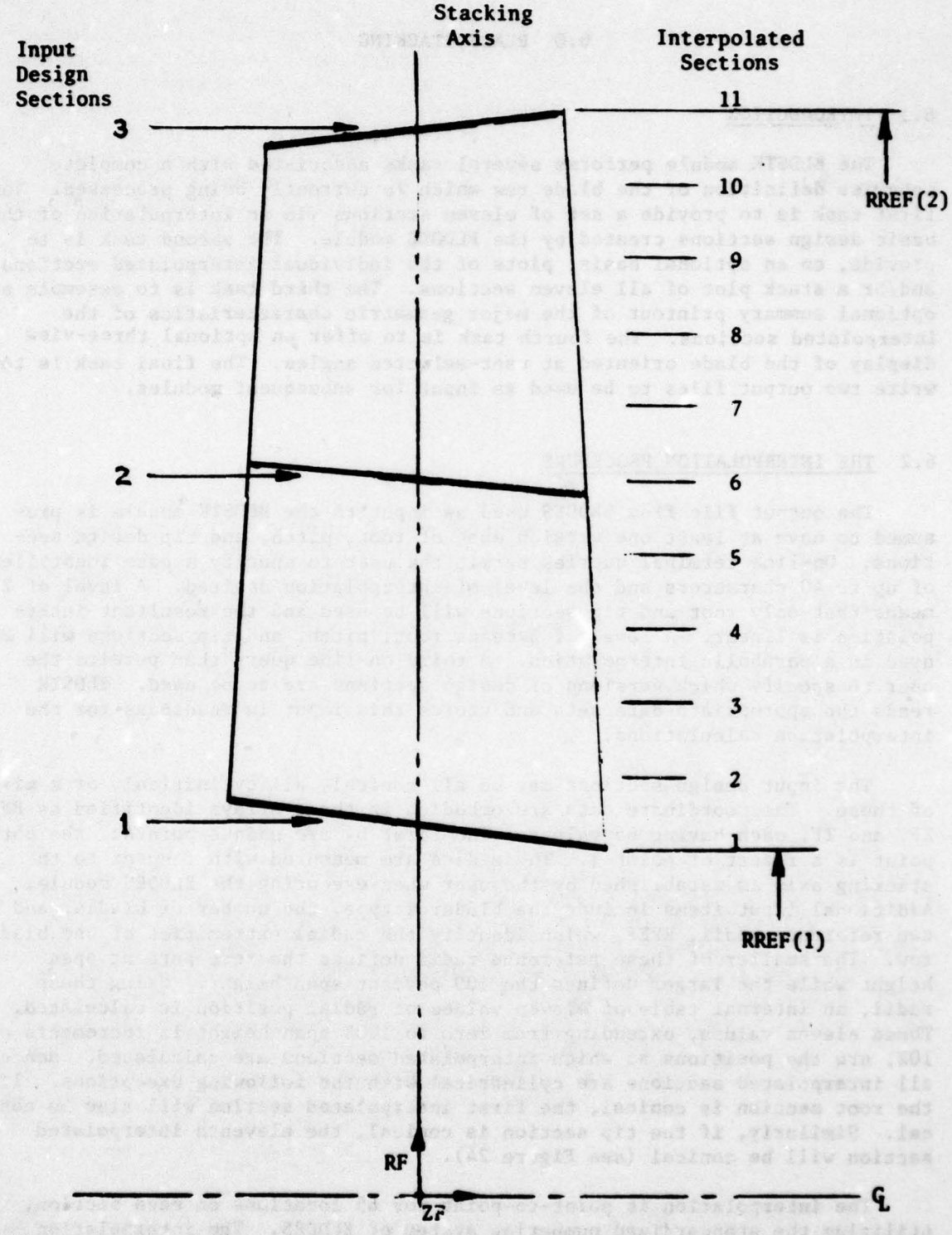

Figure 24. Interpolated Section Arrangement (BLDSTK).

output for each interpolated section consists of three arrays of 65 values each. These are: RF, radius; ZF, axial position; TF, angle in radians. The data are measured with respect to a stacking axis which is arbitrarily assumed to be oriented at 90° ($\pi/2$ radians). To render these coordinates into X,Y-type coordinates, use the following relationships:

$$X(I) = ZF(I) \tag{225}$$

$$Y(I) = RF(I) \cdot [\pi/2 - TF(I)] \tag{226}$$

where I extends from 1 through 65. The resultant airfoil would have its pressure side uppermost for a vane section and its suction side uppermost for a blade section. This orientation is borne out in the plots.

There are additional items calculated for each section for inclusion in the summary printout and on the output file. These include radius at the stacking point, cross-sectional area, chord, axial width, stagger angle, and maximum tangential thickness.

Two output files are written. One contains a copy of all of the design section input data sets obtained from the BLDDES module plus a separate data set for each of the eleven interpolated sections. This file becomes the input file to the CASC module. The second file contains a single data set of items extracted in appropriate fashion for input to the airfoil properties module, AFPROP, discussed in Section 10.

6.3 BLADE DISPLAY

At the conclusion of the blade stacking functions, an on-line query offers the user an option to utilize the DISPLA portion of this module in obtaining spanwise views (plots) of the stacked blade or vane at arbitrary, user-defined orientations. A given set of input results in three plots, each of which has a fixed viewpoint as shown in Figure 25. This input consists of three angles which serve to reorient the blade within the viewing space. The first plot is a view of the blade when looking radially inward along the original stacking axis. The second plot is the view when looking from the left along a line normal to the original stacking axis. The third plot is the view when looking along a line parallel to the centerline of the machine. The default option on this third view is from forward of the blade looking aft. A fourth item of input, SGN, can be entered as +1.0 to obtain the third view as from aft looking forward. The "viewing space" encompasses only the blade; the axes are remote.

When the option to run the DISPLA portion is invoked, an initial set of three views is plotted with all angles zero and SGN equal to -1.0. The

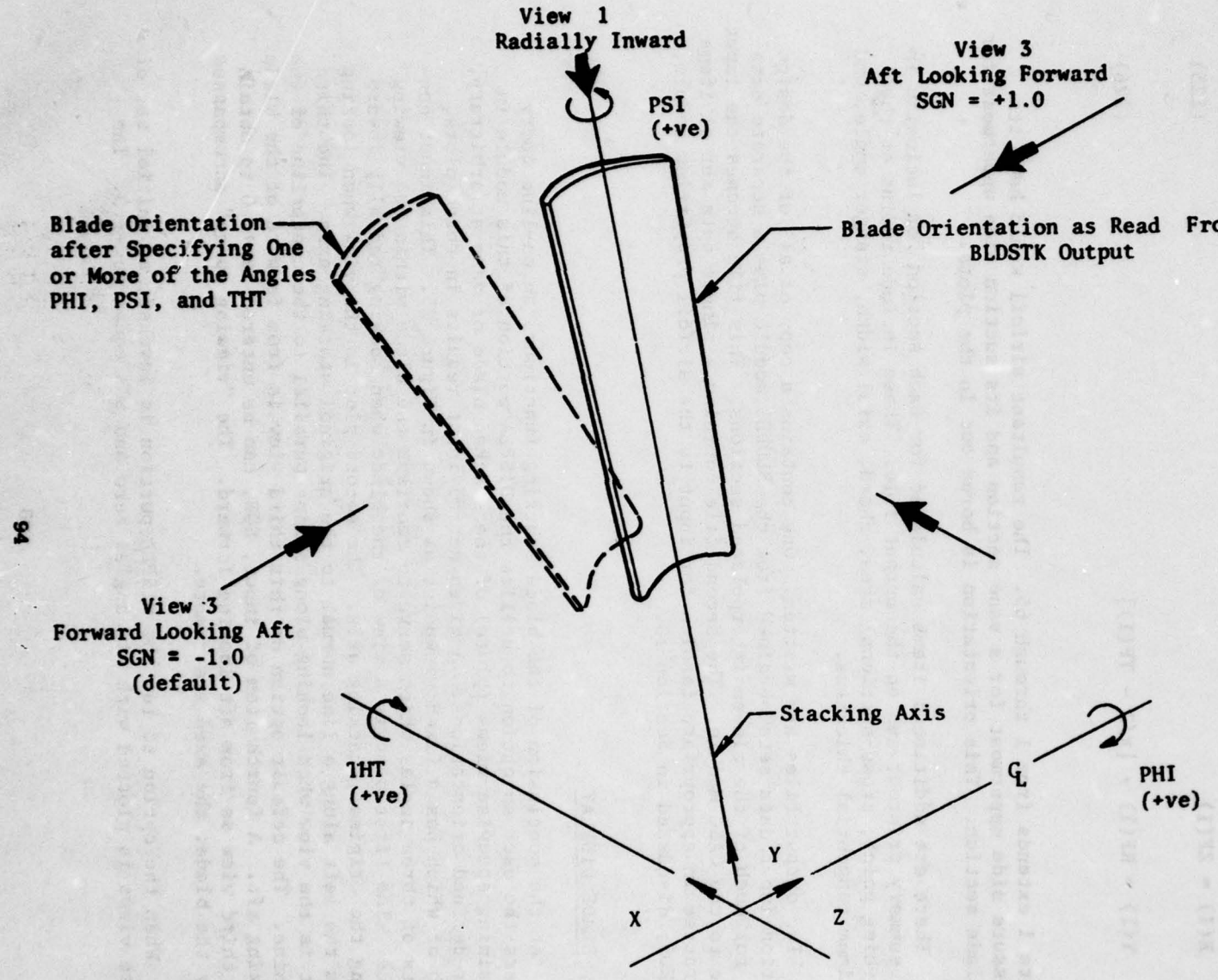

Figure 25. Viewing Definitions for DISPLA Plots.

program pauses after each view is plotted to afford an opportunity for making a hard copy. The screen is cleared automatically at continuation. At the conclusion of a set, all angles are reset to zero and SGN is set to -1.0; then a terminal query offers the user an option to repeat the new input or to stop. Each plot is labeled to show what input was used.

The internal input data are the RF, ZF, TF arrays for the eleven sections. When all angles PHI, PSI, and THT are zero, the blade is viewed in its stacked position. Any angle not specified in the request for input is zero. The transformation used to reorient the data for viewing is adapted from Reference 6 and consists of a 3 × 3 matrix whose elements are as follows:

$$A(1,1) = \cos(THT) \cdot \cos(PSI)$$

$$A(1,2) = \cos(PSI) \cdot \sin(THT) \cdot \sin(PSI)\ \ \sin(PSI) \cdot \cos(PHI)$$

$$A(1,3) = \sin(THT) \cdot \cos(PHI) \cdot \cos(PSI) + \sin(PHI \cdot \sin(PSI)$$

$$A(2,1) = \sin(PSI) \cdot \cos(THT)$$

$$A(2,2) = \sin(THT) \cdot \sin(PHI) \cdot \sin(PSI) + \cos(PHI) \cdot \cos(PSI)$$

$$A(2,3) = \sin(THT) \cdot \cos(PHI) \cdot \sin(PSI) - \sin(PHI) \cdot \cos(PSI)$$

$$A(3,1) = -\sin(THT)$$

$$A(3,2) = \cos(THT) \cdot \sin(PHI)$$

$$A(3,3) = \cos(THT) \cdot \cos(PHI)$$

Then, through selective use of these elements, each "view" consists of 65 X, Y plot coordinates for each of the eleven sections. Thus, View 1 (radially inward) is calculated as

$$\begin{bmatrix} X_o \\ Y_o \end{bmatrix} = \begin{bmatrix} A(1,1) & A(1,2) & A(1,3) \\ A(2,1) & A(2,2) & A(2,3) \end{bmatrix} \begin{bmatrix} X_I \\ Y_I \\ Z_I \end{bmatrix} \qquad (227)$$

where: X_o, Y_o = plot coordinates

X_I = ZF

$$Y_I = RF \cdot (\frac{\pi}{2} - TF)$$

$$Z_I = RF$$

View 2 (from left side) is calculated as

$$\begin{bmatrix} X_o \\ Z_o \end{bmatrix} = \begin{bmatrix} A(1,1) & A(1,2) & A(1,3) \\ A(3,1) & A(3,2) & A(3,3) \end{bmatrix} \begin{bmatrix} X_I \\ Y_I \\ Z_I \end{bmatrix} \quad (228)$$

where: X_o, Z_o = plot coordinates

X_I, Y_I, Z_I are as in equation (227)

View 3 is calculated as

$$\begin{bmatrix} Y_o \\ Z_o \end{bmatrix} = \begin{bmatrix} A(2,1) & A(2,2) & A(2,3) \\ A(3,1) & A(3,2) & A(3,3) \end{bmatrix} \begin{bmatrix} X_I \\ Y_I \\ Z_I \end{bmatrix} \quad (229)$$

where: Y_o, Z_o = plot coordinates

X_I, Y_I, Z_I are as before.

The Y_o coordinates are multiplied by the variable SGN. SGN is -1.0 by default to yield a view which is "forward looking aft." If SGN is entered as +1.0, the view is "aft looking forward."

7.0 AIRFOIL PRESSURE DISTRIBUTION

7.1 INTRODUCTION

The distribution of pressure (or Mach number) on the surface of the airfoil is the basic ingredient in the evaluation of the blade section performance and in the prediction of the blade heat transfer rates.

The CASC method (Cascade Analysis by Streamline Curvature), described herein, provides a relatively accurate prediction of these pressure distributions, with few grid points (less than 200) for quick-look evaluations.

The streamline curvature (SLC) method employed in CASC has not been discussed significantly in the literature. Nevertheless, the method is a very natural one. For example, engineers rely on one-dimensional compressible flow relationships for first-order solutions of ducted flows. The SLC approach is similar except that a number of confluent streamtubes with somewhat different properties are added together to obtain the total flow in the passage. Each streamtube is handled in much the same way as is the one streamtube in the one-dimensional problem.

As described in the following sections, the CASC method includes "type-dependent differencing" to account for subsonic and supersonic flow regimes, enforcement of "repeating" boundary conditions outside of the "covered" blade-to-blade passage, and a direct matrix solution for reliable convergence. The governing equations of motion include centrifugal and Coriolis force terms, and, hence, they apply to radial or mixed axial and radial impellers as well as to purely axial cascades.

The blade-to-blade solution is very much dependent upon the radius and lamina thickness variation through the blade row, and these values are obtained from the ATREC meridional plane analysis of Section 3.0.

7.2 METHOD SELECTION

Known methods for solving transonic flow fields may be divided into two categories: time-dependent and iterative. Time-dependent methods have achieved much popularity because both the subsonic and supersonic portions of the flow field, in most cases, are solved by the same algorithm. Thus, with a rather simple calculating procedure a difficult mathematical problem is resolved. In the iterative method, however, the calculation formula must reflect the mathematical nature of the equation, and a switch (depending upon the Mach number) to the appropriate formula is required at each calculation point. It is in this way that the different physical characteristics of the subsonic and supersonic regions come into play.

Although there are many variations, the iterative method considered here solves the equation for the unknown fluid dynamic property at each of the net

points by: (1) utilizing a linear approximation to this equation; and (2) solving the resulting system of equations simultaneously. Because of the linear approximation, this process is repeated several times (usually between 3 and 10) before convergence is obtained.

In contrast to solving the field simultaneously, time-dependent methods compute the wave motion of a disturbance as it travels from one part of the flow field to the other. A steady-state result is obtained only after all wave reflections have dissipated to a relatively small level. Although the time-dependent method of updating the flow properties can be likened to an iteration process, clearly the most rapid solution will be obtained when the flow field variables are all corrected simultaneously and when this correction is not limited by (computationally) slow wave transits. Therefore, as a rapid analysis tool, the iterative method is most attractive.

Of the many different representations of the fluid dynamic equations, the number which can be solved by the iterative method across the transonic region are, perhaps, limited. Here the simplest and most general forms of the equations are chosen, namely, those which apply along streamlines (ψ = constant lines) and those which apply along lines which are orthogonal to the streamlines (ξ = constant lines).

Across the streamlines, the continuity and momentum equations are:

Continuity:

$$\partial A = \frac{\partial \Psi}{\rho V} \qquad (\xi = \text{Constant}) \qquad (230)$$

Momentum: (in a rotating coordinate system, see Section 7.12)

$$\frac{1}{2}\frac{\partial V^2}{\partial n} = -V^2 C - T\frac{\partial S}{\partial n} + (2\omega Vr + V^2 \sin \beta_m) \sin \phi \quad (\xi = \text{Const}) \qquad (231)$$

Along the streamlines the energy and momentum equations are:

Momentum:

$$\frac{DS}{Ds} = 0 \qquad (\Psi = \text{Constant}) \qquad (232)$$

Energy:

$$\frac{DI}{Ds} = 0 \qquad (\Psi = \text{Constant}) \qquad (233)$$

where:

$$I = H - r\omega Cu$$

and the independent variables s and n are the distances measured along and across the streamlines in the transformed coordinate system; ϕ is the stream surface slope in the meridional plane.

The solution method is an extension of the standard streamline curvature method. It may be briefly described as follows: First, an approximate grid of streamlines and orthogonal lines is assumed (refer to Figure 26); second, the curvature of the streamlines at each of the grid points is evaluated; third, the momentum equation is integrated along a line normal to the streamlines to obtain velocity, and the continuity equation is integrated to determine the "correct" streamline positions (for the assumed curvature field). These are indicated by the "x" in Figure 26. Fourth, an adjustment (δn) is computed by considering (1) the difference between the computed and assumed streamline positions and (2) the effect of the implied curvature modification in the integrated momentum equation. Finally, the streamlines are repositioned by the δn values.

Because the movement of any one grid point alters the velocity at nearby points through a change in curvature, it is highly desirable to account for these interrelating point adjustments simultaneously. The utilization of a simultaneous solution procedure, employed here, is not part of the classical streamline curvature method (References 7, 8, 9). In comparison, the classical method yields calculation times which are very slow, especially for a closely spaced calculation grid. In concept, the set of simultaneous equations for the normal streamline adjustments is formulated from the finite difference equivalent of the following equation:

$$\frac{\partial^2(\delta n)}{\partial \Psi^2} + \frac{(1-M^2)}{(\rho V)^2} \frac{\partial^2(\delta n)}{\partial s^2} = F \qquad (234)$$

where:

δn = Required streamline adjustment in the normal direction

Ψ = Stream function

s = Curvilinear distance along a given streamline

M = Mach number

ρV = Flow per unit area

F = Driving (or error) function derived from the solution to the integral continuity and normal momentum equations

This equation is derived in Section 7.11 for the special case of isentropic two-dimensional planar flow. (These limiting assumptions are utilized only to maintain simplicity of illustration; they are not part of the computer program.) From a mathematical point of view, the above equation is similar to the small perturbation form of the velocity potential equation employed by Murman and Cole (Reference 10).

1. **Assume a Crude Grid**

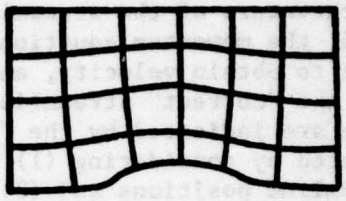

2. **Evaluate Curvature**

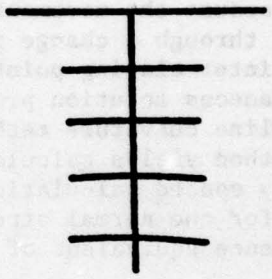

3. **Integrate the Cross-Stream Momentum Equation and the Continuity Equation to Determine the "Correct" Streamline Positions.**

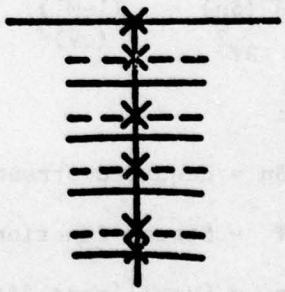

4. **Solve the Matrix Equation for δn and Move the Grid Points.**

Figure 26. Solution Technique.

$$\frac{\partial^2 \Phi}{\partial y^2} + (1-M^2) \frac{\partial^2 \Phi}{\partial x^2} = 0 \qquad (235)$$

$$\frac{v}{a} << 1, \; M \approx \frac{u}{a}$$

In either case, it is possible to numerically solve the equations for either subsonic flow or supersonic flow by changing the finite difference star from a subsonic representation to a supersonic representation as illustrated in Figure 27. Notice that the supersonic representation includes no points downstream of the cross-stream line, reflecting the physical reality that disturbances downstream will not be felt upstream. The type dependent finite difference representation is directly related to the coefficient $(1-M^2)$, and, because this coefficient is zero at unity Mach number, the switch from one star to the other is performed smoothly.

One difficulty which arises when the flow outside of the blade row becomes supersonic is that matrix relaxation techniques, commonly used for transonic flow, fail. Figure 28 is the typical grid downstream of a blade row. The points B and B´ represent the same point relative to the blade row. In supersonic flow the iteration scheme must proceed from upstream to downstream points. There is no way to relax the matrix equations at A and B such that they are in the correct order because B is downstream of A, and B´ is upstream of A. For this reason a direct matrix solution is used.

In summary, the features which make the streamtube curvature method an efficient analysis tool are:

- No additional complexities arise for a rotating blade row.
- The intrinsic grid facilitates a subsonic/supersonic type dependent finite difference representation for transonic flow.
- Rapid convergence is obtained through the use of an implicit correction equation.
- The inclusion of blade surface curvatures in the algorithm gives an accurate solution even with a coarse grid.

7.3 CALCULATION OUTLINE

The operations performed by the CASC program may be outlined as follows:

1. Define an approximate grid of streamlines and orthogonals.
2. Compute the streamline angles, curvatures, and curvilinear distances.

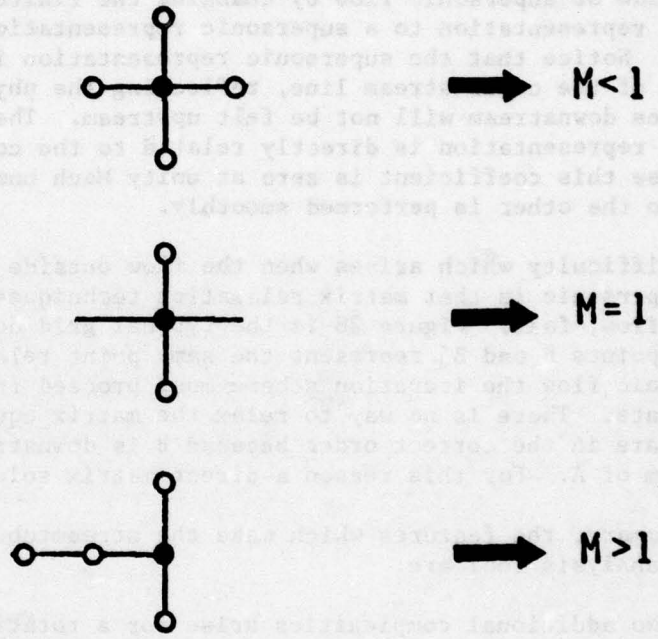

Figure 27. Finite Difference Stars for Subsonic and Supersonic Flow.

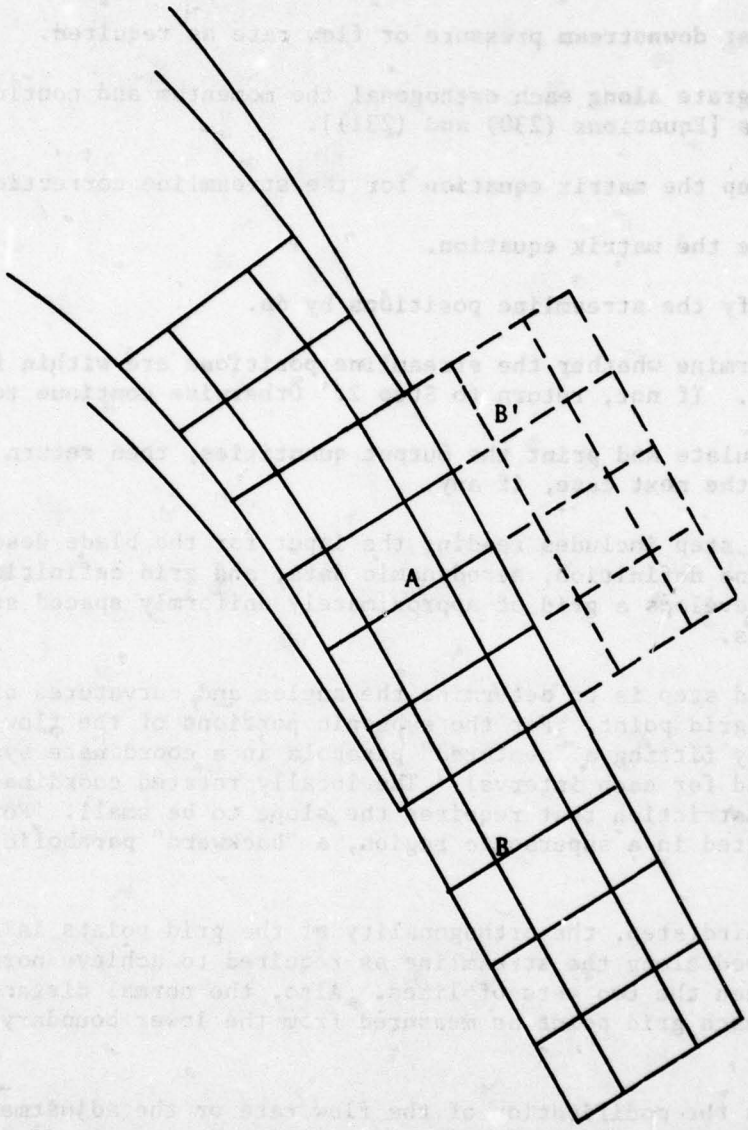

Figure 28. Grid Structure.

3. Compute the orthogonal line angles and move the grid points along the streamlines to obtain orthogonality.

4. Adjust downstream pressure or flow rate as required.

5. Integrate along each orthogonal the momentum and continuity equations [Equations (230) and (231)].

6. Set up the matrix equation for the streamline correction, δn.

7. Solve the matrix equation.

8. Modify the streamline positions by δn.

9. Determine whether the streamline positions are within final tolerance. If not, return to Step 2. Otherwise continue to Step 10.

10. Calculate and print the output quantities; then return to Step 1 for the next case, if any.

The first step includes reading the input for the blade description, meridional plane definition, aerodynamic data, and grid definition. The program then develops a grid of approximately uniformly spaced streamlines and orthogonals.

The second step is to determine the angles and curvatures of the streamlines at each grid point. For the subsonic portions of the flow field, this is performed by fitting a "centered" parabola in a coordinate system which is locally rotated for each interval. The locally rotated coordinate system removes the restriction that requires the slope to be small. For grid points which are located in a supersonic region, a "backward" parabolic fit is employed.

In the third step, the orthogonality of the grid points is checked and points are moved along the streamline as required to achieve normal intersections between the two sets of lines. Also, the normal distance, n, is computed for each grid point as measured from the lower boundary of the orthogonal.

Step 4 is the modification of the flow rate or the adjustment of the downstream pressure. If the cascade is choked, the program finds the maximum flow that will pass at the choked station. The flow is reset to the new value and the boundary conditions are set to keep the same upstream flow angle and downstream pressure. If the cascade is not choked, the program will attempt to adjust the downstream pressure such that the suction surface trailing edge pressure is equal to the pressure surface trailing edge pressure.

Step 5 is the solution of the flow field equations. The momentum equation, derived in the next section, is integrated across the streamlines to

give the velocities. The velocity, total temperature, and total pressure then allow determination of the density at each grid point, and the inverse product of density and velocity is integrated to find flow area.

$$A_2 - A_1 = \int_{\Psi_1}^{\Psi_2} \frac{\partial \Psi}{\rho V} \tag{236}$$

In the "uncovered" portion of the flow field, the integration is carried out along an "extended" orthogonal which spans the distance between the upstream (or downstream) pressure boundary and the blade surface. (See Figure 29. Note that an extended orthogonal will cross the same streamlines several times.) From the pressure boundary condition, the momentum and continuity equations can be integrated directly; no iteration is required.

On the other hand, in the "covered" portion of the blade passage the pressure level is not known as a boundary condition. Instead, the velocity (or pressure) level is chosen by iteration so that the area across the passage computed from Equation (236) agrees with the geometric area. When the program detects that an orthogonal is "choked", i.e., can not pass the required flow, the iteration process proceeds until the maximum flow possible passes across that orthogonal. The fact that the orthogonal choked is noted by the program and is used later.

In steps 6 and 7, the proper adjustment of the streamline positions is determined, and in Step 8, the grid points are moved in the normal direction by this computed adjustment.

7.4 CALCULATION GRID SYSTEM

The blade-to-blade plane, in which the equations of motion are solved, is obtained by rotating a streamline (as depicted in the meridional plane) about the axis of the machine. This streamline cuts the blade and defines the two-dimensional blade section which is to be analyzed. The coordinates of the blade section are θ (radians) for the tangential direction and n (length units) for the meridional direction. Because these two coordinates have different units, they are inappropriate for plotting the section and for determining the intrinsic (orthogonal) blade-to-blade calculation grid. Consequently, the CASC program utilizes transformed m',θ coordinates where m' is a transformed meridional dimension and has units of radians. It is recommended that these or normalized m',θ coordinates be used for blade layouts and for defining the input to CASC.

In the m',θ plane the blade turning angles are properly depicted and the equations of motion for a nonrotating blade row are the same as the equations for planar flow with X,Y coordinates. This is demonstrated in Section 7.13.

The CASC calculation grid is composed of streamlines and orthogonals. The orthogonals are identified by ξ_1 (or XI1) which increase in increments of

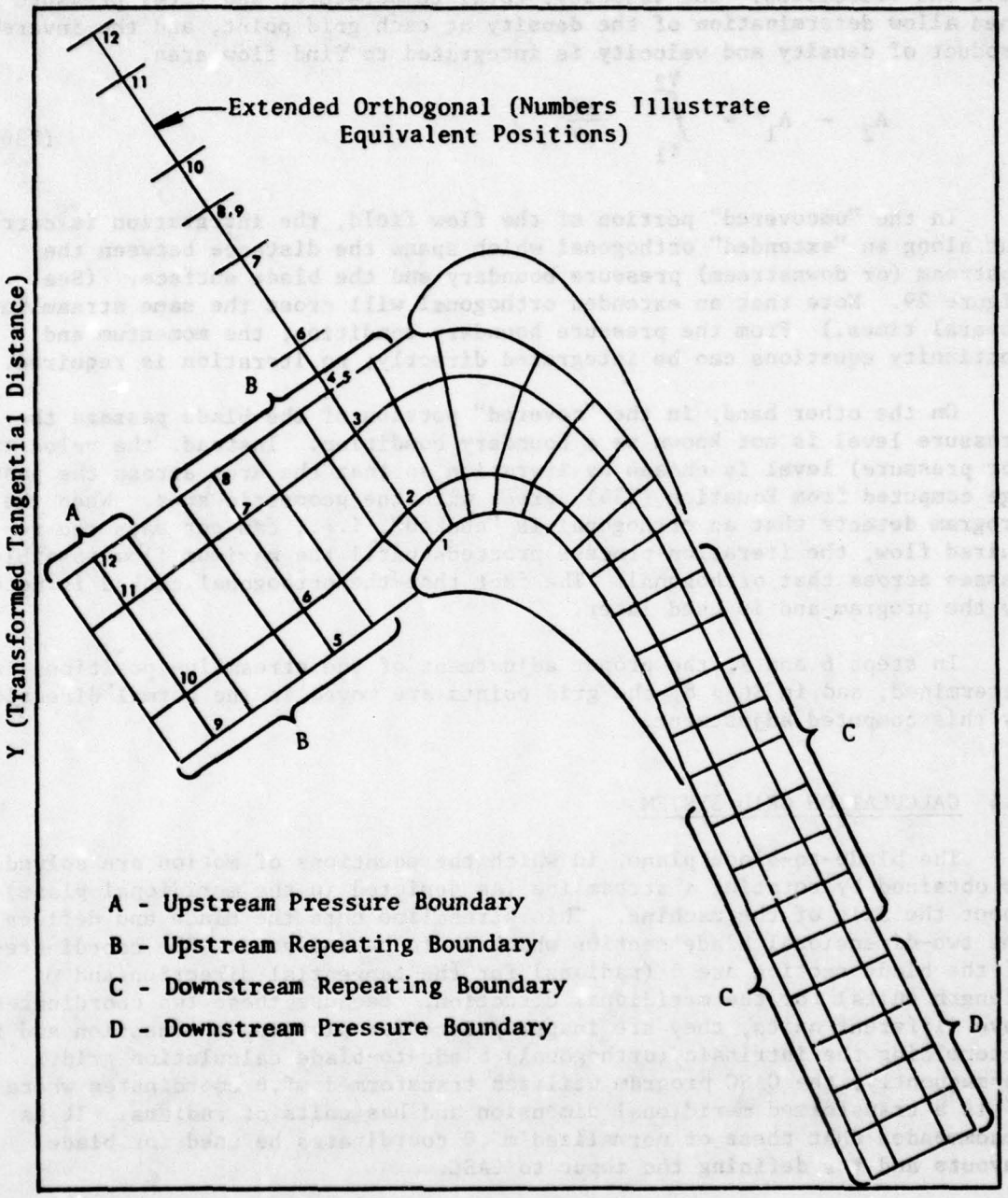

Figure 29. Illustration of CASC Computational Grid and Orthogonal Boundary Conditions.

1 from the first orthogonal upstream to the last orthogonal downstream. The streamlines are identified by ξ_2 (or XI2) which increase from the streamline coincident with the suction surface to the streamline coincident with the pressure surface.

At different steps in the calculation it is necessary for the points to be arranged in different ways. In the normal view, indicated in Figure 29, the points are arranged by streamlines. But for the orthogonalization step and for the solution to governing equations, the points are arranged along extended orthogonal lines. One such line, shown in Figure 29, begins on the blade surface and ends on a pressure boundary. This procedure simplifies the enforcement of the passage-to-passage repeating conditions.

7.5 CURVATURE, ANGLE AND DISTANCE ALONG STREAMLINES

7.5.1 Beam Fit for Angles and Curvilinear Distance

The second step in the calculation procedure outlined in Section 7.3 is the determination of the streamline curvature, angle, and cumulative curvilinear length at each grid point. An accurate and rapid method for accomplishing this is to fit a draftsman's spline or, equivalently, to use the formulas which apply to a beam loaded at discrete points. The classical relation applicable here is that the moment, M, varies linearly, or:

$$\frac{d^2y}{dx^2} = \frac{M}{EI} = bx \qquad (237)$$

The numeric procedure used in the CASC program utilizes locally rotated cubic polynomials between each grid point and is described in Reference 11. The BEAM subroutine described in that reference is used to fit all of the streamlines and to compute the angle and curvilinear distances of the grid points.

7.5.2 Streamline Curvature

To be consistent with the physical character of the flow, two different formulas for evaluating curvature are needed. Specifically, when the flow is subsonic at some point m, the curvature may be determined by fitting a curve through points which are both upstream and downstream of point m. But when the flow is supersonic, the streamline curvature at m cannot be influenced by points downstream. Therefore, the curve fit can include only points m, m-1, m-2, m-3 etc.

For simplicity, a three-point parabolic fit is used for both subsonic and supersonic points. A central three-point fit is used below Mach number 0.95, and a backward three-point fit is used above Mach number 1.05. To avoid a possible difficulty because of the discontinuity in curvature at unity Mach number, a linear weighting of both formulas is used in the Mach number range of 0.95 to 1.05.

In earlier versions of the CASC program, curvature in the subsonic portions of the flow field was obtained by the beam fit described in Section 7.5.1. However, the current three-point formula significantly reduces the bandwidth of the matrix streamline correction equation of Section 7.8, and the resultant loss of accuracy is found to be negligible.

7.5.3 Streamline End Conditions

The boundary condition on the streamline ends is either (1) angle boundary condition (for near axial flow), or (2) curvature boundary condition (otherwise). For the typical CASC grid illustrated in Figure 29, the boundary condition utilized on the ends of the streamlines is that the curvature is set equal to that of a uniform circumferential annular flow. The angle of the upstream and downstream streamlines is then determined through the flow field solution by the pressure level imposed on the pressure boundaries (regions A and D in Figure 29). However, when either the upstream or downstream streamlines become aligned with the axial direction (as is discussed in Section 7.7.1), the length of the pressure boundary reduces to zero. For this situation, the angle boundary condition is then applied directly to the streamlines.

Either of these boundary conditions is calculated from the known flow rate and the known angular momentum:

$$r \, \Delta\theta \, h \, \rho \, V_m = k_1 \tag{238}$$

$$r \, Cu = r \, (V_u + \omega r) = k_2 \tag{239}$$

The values k_1 and k_2 are determined from the user's input aerodynamic properties and/or from the adjusted flow rate and downstream pressure levels determined in Step 4 (see Section 7.3). The boundary condition formulas are derived below.

The tangential relative velocity and meridional relative velocity can be found at any axial location from equations (238) and (239), the energy equation, and the meridional plane lamina thickness (h). Then the streamline angle is

$$\beta_m = \tan^{-1} \frac{V_u}{V_m} \tag{240}$$

The streamline curvature is calculated from equations (238) and (239) using the definition of β_m in equation (240). First express V_m as:

$$V_m = \frac{k_1}{r \Delta\theta h \rho} \tag{241}$$

where:

k_1 = flow rate

h = streamtube height

$\Delta\theta$ = pitch in radians.

From equation (239) and the definition of Vu,

$$Vu = Cu - \omega r \tag{242}$$

where ω = angular velocity, Equation (239) can be rewritten

$$Vu = \frac{k_2}{r} - \omega r \tag{243}$$

Substituting equations (241) and (243) into equation (240) yields:

$$\tan \beta = \left(\frac{k_2}{r} - \omega r\right) \frac{hr\Delta\theta\rho}{k_1} \tag{244}$$

Differentiating equation (244) with respect to arc distance s' we obtain:

$$\sec^2 \beta_m \frac{\partial \beta_m}{\partial s} = (k_2 + \omega r^2) \frac{\Delta\theta\rho h}{k_1} \left[\frac{1}{h}\frac{\partial h}{\partial s} + \frac{1}{\rho}\frac{\partial \rho}{\partial s} + \frac{2\omega r}{k_2+\omega r^2} \frac{\partial r}{\partial s}\right] \tag{245}$$

Then from the definition of curvature, written as:

$$C = \frac{\partial \beta_m}{\partial s}$$

and the differential relationship:

$$\frac{\partial}{\partial s} = \cos \beta_m \frac{\partial}{\partial m}$$

where β_m is the angle between the meridional direction and the s direction, the expression for curvature is

$$C = \cos^3 \beta_m (k_2+\omega r^2) \frac{\Delta\theta\rho h}{k_1} \left[\frac{1}{h}\frac{\partial h}{\partial m} + \frac{1}{\rho}\frac{\partial \rho}{\partial m} + \frac{2\omega r}{k_2+\omega r^2} \frac{\partial r}{\partial m}\right] \tag{246}$$

By using equations (238) and (239), this simplifies to

$$C = -\cos^2\beta_m \sin\beta_m \left[\frac{1}{h}\frac{\partial h}{\partial m} + \frac{1}{\rho}\frac{\partial \rho}{\partial m} + \frac{2\omega r}{k_2+\omega r^2} \frac{\partial r}{\partial m} \right] \quad (247)$$

7.5.4 Stagnation Point End Condition

Even though there is no grid point at the leading edge stagnation point, the location of this point must be known to get an accurate curvature for the first point upstream of the leading edge. It is a requirement in the CASC program that the leading edge be rounded and that a complete numerical description of the leading edge shape be supplied. At the stagnation point, the streamlines are required to turn a 90° corner. Two coincident stagnation streamlines are employed. One turns up and goes over the body; the other turns down and goes below. The location of the stagnation point is found iteratively. As shown on Figure 30, the point is moved along the contour so that the intersection angle with the body surface is 90°. The streamline angle at the stagnation point is found by utilizing the beam fit.

7.5.5 Airfoil Surface Curvatures

For grid points that lie on the airfoil surface, the curvatures are calculated from the input boundary coordinate pairs and angles. The proper interval is found and a cubic interpolation is used to find the curvature at the grid point.

The curvature at the trailing edge point is calculated as if it were not on the blade surface. The resulting curvature best represents the physical realities of the flow at a blunt trailing edge.

7.6 POSITIONING THE ORTHOGONALS

The cross-stream momentum and continuity equations are written in a direction normal to the streamlines. Hence, before these equations are applied, it is necessary to move the grid points along the streamlines to obtain orthogonality. This is easily accomplished as follows (refer to Figure 31). In each region a boundary streamline is chosen as a "control" streamline. Along this line a uniform spacing between orthogonals is chosen. To correct the nonorthogonality, the points on each orthogonal are first fitted with a spline (using the procedure of Section 7.5.1) to obtain the angles ϕ_2. The angle deviation from the streamline normals is then integrated with respect to the cross-stream distance n, from the control streamline to the point in question, to obtain the relative movement D_s. The points are then moved to the new positions along the streamline. The coordinates, ϕ_1 angles, curvatures, and cumulative s-distances are modified as appropriate. The constant of integration, A_{DS}, positions the orthogonal on a control streamline so that a reference position is maintained.

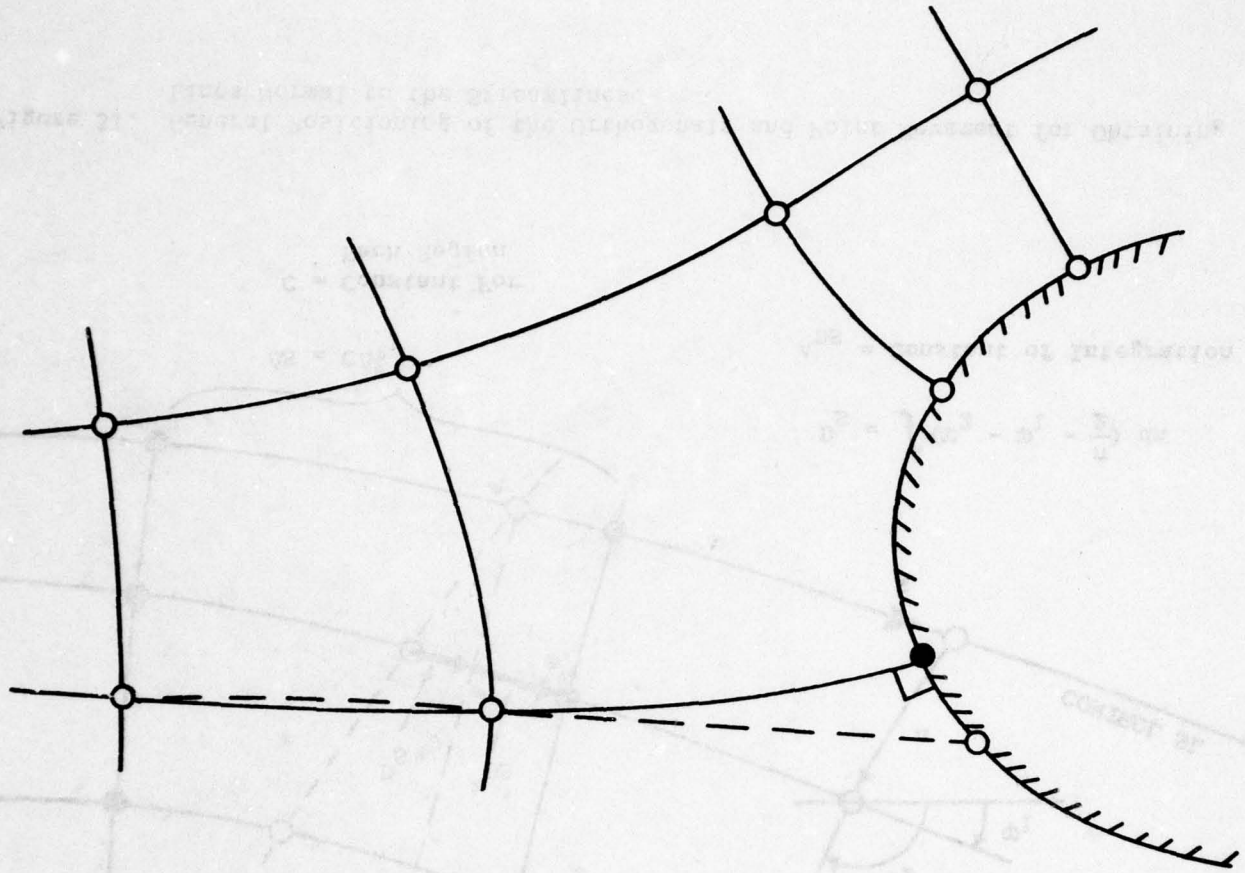

● Points Repositioned in the Streamline Curvature Calculation Routine

Figure 30. Stagnation Point Iteration.

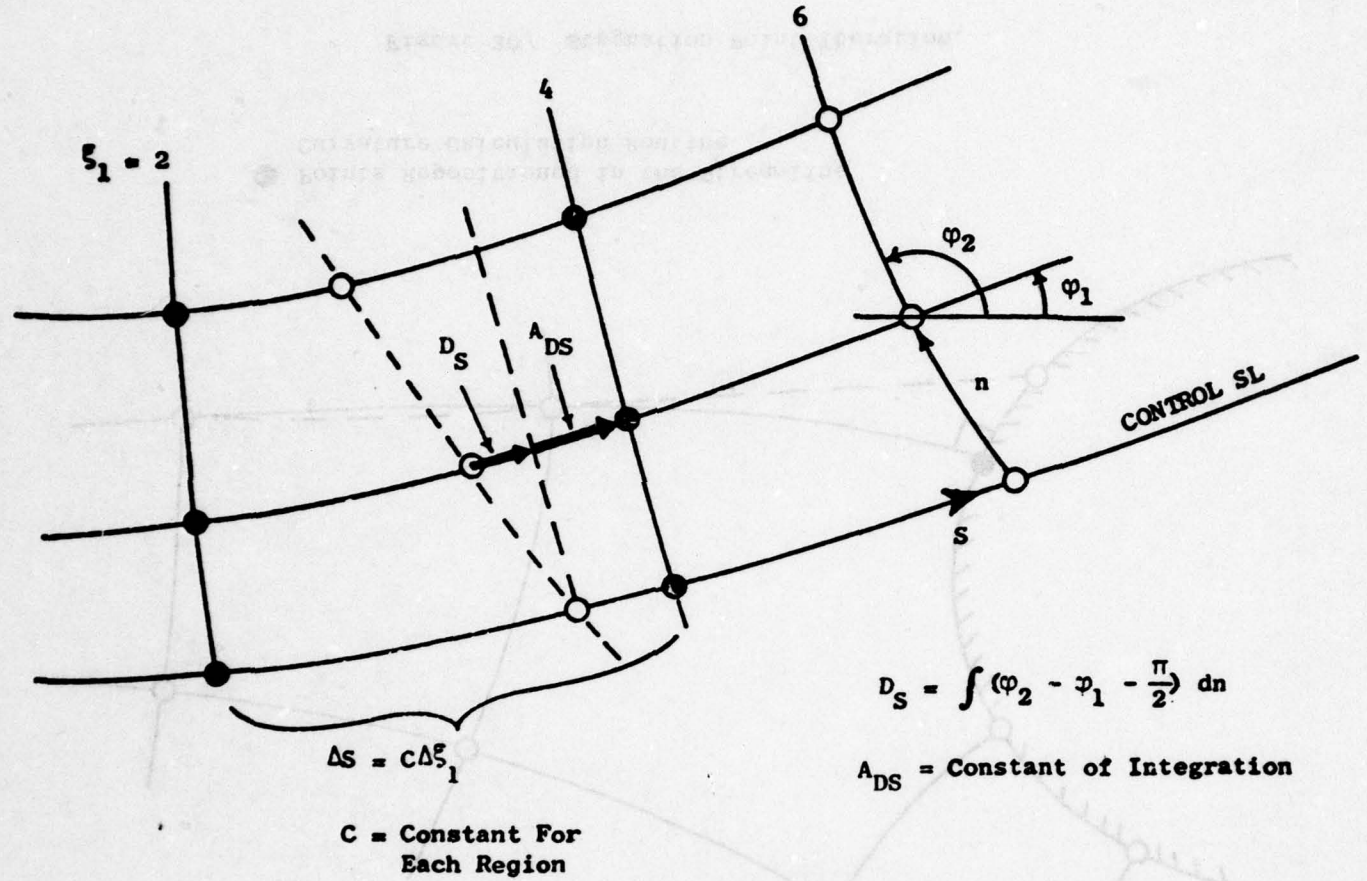

Figure 31. General Positioning of the Orthogonals and Point Movement for Obtaining Lines Normal to the Streamlines.

7.7 INTEGRATION OF CONTINUITY AND MOMENTUM EQUATIONS

In this section the numerical procedure for integrating the full non-isentropic and variable energy form of the equations of motion is developed. Only a portion of this comprehensive derivation is required; however, for completeness, the formulation for general flow properties is retained.

The basic equations of the CASC program are:

Momentum:

$$\frac{1}{2}\frac{\partial V^2}{\partial n} = -V^2 C + \frac{V^2}{2}\sin\beta_m \sin\phi + \frac{\partial I}{\partial n} - T\frac{\partial S}{\partial n} + 2r\omega V \sin\phi \tag{231}$$

Continuity:

$$\partial A = \frac{\partial \psi}{\rho V} \tag{230}$$

Equation (230) is the Crocco form of the momentum equation containing the variables I and S (rothalpy and entropy) and including effects of a rotating coordinate system. The entropy term can be modified for greater engineering convenience by defining

$$Q = e^{\frac{-\Delta S}{R}} = \frac{P_T'}{P_{T_i}'} \tag{248}$$

where P_T' is the relative total pressure and P_{T_i}' is the ideal relative total pressure:

$$P_{T_i}' = P_{T_1}' \left[(I + \frac{1}{2} r^2 \omega^2)/(I_1 + \frac{1}{2} r_1^2 \omega^2)\right]^{\frac{\gamma}{\gamma-1}} \tag{249}$$

Subscript 1 refers to the upstream reference condition. The resulting momentum equation is:

$$\frac{1}{2}\frac{\partial V^2}{\partial n} = V^2\left(-C + \frac{\sin\beta_m \sin\phi}{2}\right) + \frac{\partial I}{\partial n} + T\frac{R\partial \ln Q}{\partial n} + 2r\omega V \sin\phi \tag{250}$$

The above momentum equation is integrated by parts. First we rewrite equation (250) as:

$$\frac{1}{2} dV^2 = \frac{1}{2} V^2 (-2C + \sin\beta_m \sin\phi)\, dn + dI + TR d\ln Q + 2r\omega V \sin\phi\, dn \tag{251}$$

The formula for integrating by parts is:

$$dv = -\frac{v}{u} du + \frac{1}{u} d(u v) \tag{252}$$

By comparing equation (252) with equation (251), it follows that

$$v = \frac{1}{2} V^2 \tag{253}$$

$$\frac{du}{u} = (2C - \sin \beta_m \sin \phi)\, dn \tag{254}$$

and

$$\frac{1}{u}\, d(uv) = dI + T R\, d \ln Q - 2r\omega V \sin \phi\, dn \tag{255}$$

Since the streamline curvature, streamline angle, and meridional plane angle are assumed to be known, equation (254) can be integrated from the first to the k^{th} streamline to obtain

$$u_k = e^{\int (2C - \sin \beta_m \sin \phi)\, dn} \tag{256}$$

Equation (255) is then integrated to yield an expression for the product of u and the velocity squared.

$$\frac{1}{2} u_k V_k^2 - \frac{1}{2} U_{k+1} V_{k+1}^2 = \int_{k+1}^{k} u(dI + TRd \ln Q - 2r\omega V \sin \phi\, dn) \tag{257}$$

Equation (257) represents the integration across one stream tube bounded by streamlines k and k+1. The integration is performed from the top toward the bottom because, frequently, the velocity is known on the top boundary since the blades are oriented suction surface up. The finite difference form of equation (257) employed in the computer program is:

$$u_k V_k^2 - u_{k+1} V_{k+1}^2 = \sqrt{u_k u_{k+1}} \left[2(I_k - I_{k+1}) + (T_k R_k + T_{k+1} R_{k+1}) \right.$$
$$\left. (\ln Q_k/Q_{k+1}) - 2\omega r (V_k \sin \phi_k + V_{k+1} \sin \phi_{k+1})(n_k - n_{k+i}) \right] \tag{258}$$

This numerical expression is solved by a successive approximation procedure to update the right-hand side until the computed fractional velocity change (on each streamline) is less than 4.0×10^{-6}.

The numerical integration of the momentum equation, then, is a two-step process. The first step is the integration of equation (256). The second

step is the integration of equation (257). In equation (256), the integral of curvature is evaluated by fitting a second-order polynominal in each interval. (The second derivative of that polynomial is established by a least square fit to the nearby points.) Implied in the integration is the fact that total temperature and total pressure are known as a function of the streamline index k and, hence, as a function of the cross-stream distance n. This is in slight contradiction to the streamwise momentum and energy equations, equations (232), since total properties are correctly related only to the cumulative flow rate ($\psi = W$). However, this slight error is automatically corrected in the later stages of the iteration when the assumed streamline positions are effectively coincident with the true streamlines.

As noted above, the integration starts from the top boundary and proceeds down. The velocity can be found on the pressure boundary by simultaneously satisfying one-dimensional continuity and conservation of angular momentum. If the pressure boundary is on the lower end of the orthogonal, the velocity on the upper end is iterated on until the lower velocity is matched. For internal channels, this outer boundary velocity is found iteratively as will be discussed below.

Following the momentum equation, the continuity equation is integrated by the algorithm:

$$A_{k+1} - A_k = \frac{W_{k+1} - W_k}{\langle \rho V \rangle} \tag{259a}$$

The average value of mass flow per unit area, in the denominator of equation (259a), may be approximated two ways:

$$\langle \rho V \rangle = \frac{1}{2} \left[(\rho V)_k + (\rho V)_{k+1} \right] \tag{259b}$$

$$\langle \rho V \rangle = \left[(\rho V)_k \ (\rho V)_{k+1} \right]^{\frac{1}{2}} \tag{259c}$$

If the variation of (ρV) between streamlines is small, then the two expressions give similar results. Although equation (259b) is somewhat faster to compute, equation (259c) has been found more reliable for some special cases. Consequently, an approximation to equation (259c) is employed in the computer code.

If the cumulative cross-stream areas are being computed for an internal station, it is required that the last area, A_N, equal the geometric area of the passage at that location. To accomplish this, the value of velocity V_N used as an initial condition in the momentum integration is varied. Figure 32 shows a typical variation of A_N with V_N. Obviously, there are two solutions, one for the subsonic branch and another for the supersonic branch. The subsonic branch is used except when a throat is detected in the internal region which is not at the trailing edge. The indicator SSDF is then used to select the branch for the remaining internal stations.

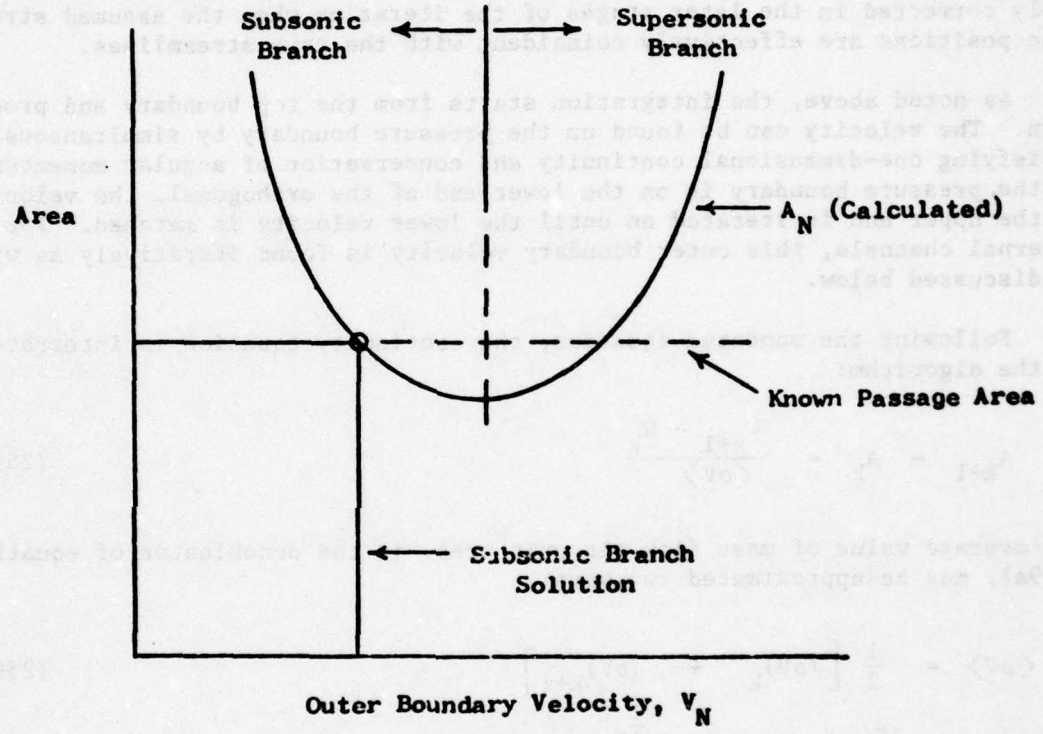

Figure 32. Illustration of Method for Choosing Outer Boundary Velocity in a Confined Passage.

A third possibility is that the geometric passage area is below the minimum computed area, A_N. In this case, the flow is said to be choked, and the flow is adjusted so that the minimum calculated area will be exactly equal to the geometric area.

7.7.1 Near Axial Flows

As the inlet or exit flow angle approaches zero, the grid as shown in Figure 29 becomes intractable because the extent of the pressure boundary becomes small and the orthogonals which originate on the blade do not go upstream. When this situation occurs the grid is changed to that indicated in Figure 33. The orthogonals end and begin on the stagnation streamline at the same axial location. The boundary conditions on the ends of the orthogonal are:

1. The spacing between the end points is one transformed pitch.

2. The velocity at each station end must be equal.

A slight error is introduced by this grid arrangement as the orthogonals are not actually normal to the streamlines; this error is proportional to the cosine of the angle of nonorthogonality.

7.7.2 Wakes from Blunt Trailing Edges

Because it is much easier to obtain a valid numerical solution if the flow streamlines are smooth and the curvatures are not excessive, a "dead" region is allowed to exist behind a trailing edge which has thickness. As shown in Figure 34, the thickness of the dead region is gradually reduced to zero as one proceeds downstream. The derivative, db/ds, has a nominal value of 0.1.

To include the wake displacement effect, the wake area is added to the right-hand side of equation (259a) if a channel boundary streamline is crossed. In this way the cumulative streamtube flow area includes the wake displacements. No correction is required in the momentum equation because pressure continuity is always enforced across a slip line.

7.8 STREAMLINE CORRECTION EQUATION

7.8.1 General Formulation

In the CASC calculation procedure, we start with an estimate of the streamline positions, that is, a set of x_o, y_o. For the second iteration cycle, x_o, y_o will be the coordinates determined by the first iteration, and so forth. These assumed streamline coordinates are used to compute the cumulative width of the stream tubes (n_o), curvature, velocity, and density and, then, a second set of cumulative stream tube widths (n_x). This is illustrated in the following listings:

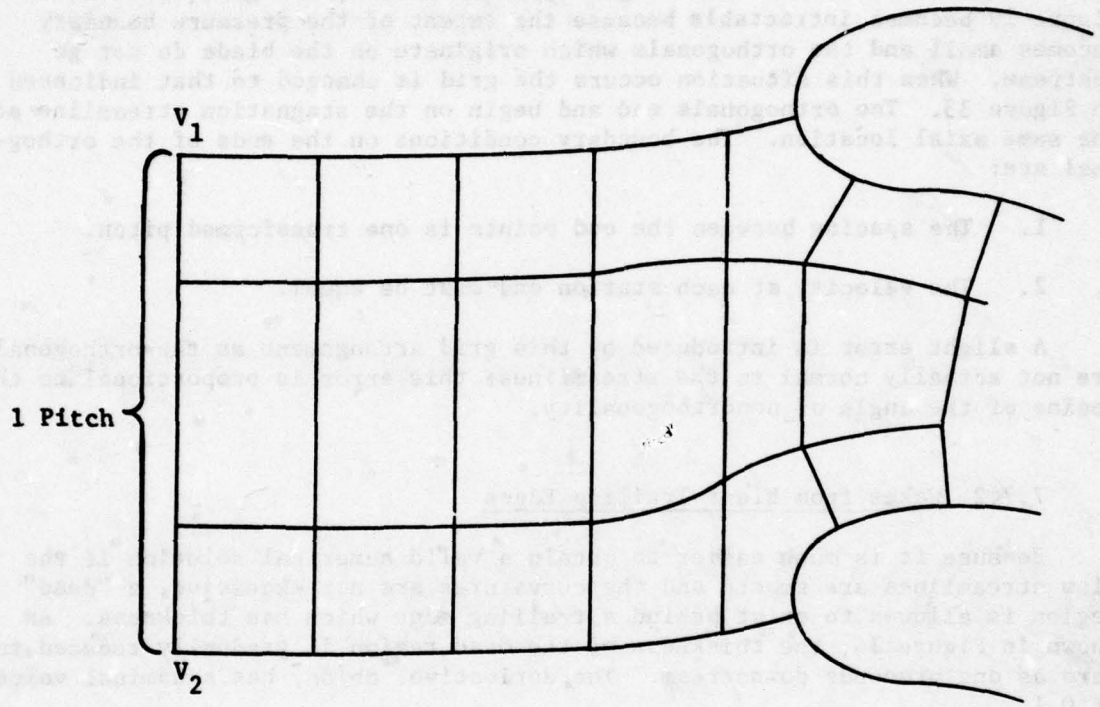

$$V_1 = V_2$$

Figure 33. Grid for Axial Flows.

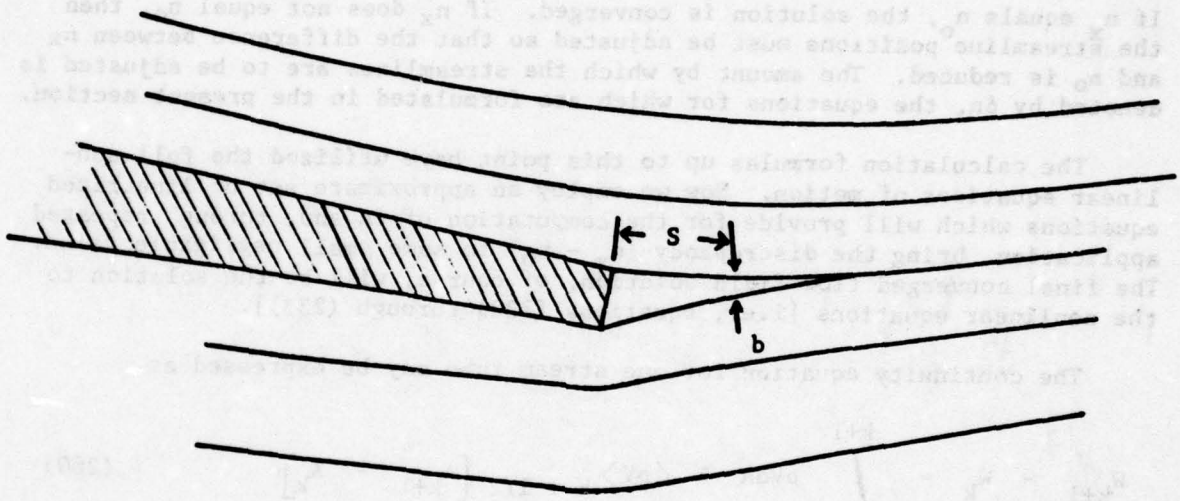

Figure 34. Trailing Edge Region.

Given	Operation	Compute
x_o, y_o	Streamline curve fitting	C_o
x_o, y_o	Orthogonal line curve fitting	n_o, A_o
C_o, n_o	Momentum equation	V_o
V_o	Energy, entropy, and equation of state	ρ_o
ρ_o, V_o	Continuity equation	A_x, n_x

If n_x equals n_o, the solution is converged. If n_x does not equal n_o, then the streamline positions must be adjusted so that the difference between n_x and n_o is reduced. The amount by which the streamlines are to be adjusted is denoted by δn, the equations for which are formulated in the present section.

The calculation formulas up to this point have utilized the full nonlinear equations of motion. Now we employ an approximate set of linearized equations which will provide for the computation of δn and, through repeated application, bring the discrepancy $(n_x - n_o)$ to some small negligible value. The final converged flow field solution, of course, will be the solution to the nonlinear equations [i.e., equations (230) through (233)].

The continuity equation for one stream tube may be expressed as

$$W_{k+1} - W_k = \int_k^{k+1} \rho V dA \equiv \langle \rho V \rangle_{k+1/2} \left[A_{k+1} - A_k \right] \tag{260}$$

where:

$A = \int rhdn$

$\langle \rho V \rangle_{k+1/2}$ = average flow per unit area for the stream tube bounded by the k and k+1 streamlines

h = stream tube height

r = radius

For two adjacent stream tubes:

$$\frac{A_{k+1} - A_k}{W_{k+1} - W_k} = \frac{1}{\langle \rho V \rangle_{k+1/2}} \tag{261}$$

$$\frac{A_k - A_{k-1}}{W_k - W_{k-1}} = \frac{1}{\langle \rho V \rangle_{k-1/2}} \tag{262}$$

The previous two equations are subtracted to obtain the second difference for A, defined as:

$$\frac{\Delta^2 A}{\Delta W} \equiv \frac{A_{k+1} - A_k}{W_{k+1} - W_k} - \frac{A_k - A_{k-1}}{W_k - W_{k-1}} \tag{263}$$

$$\frac{\Delta^2 A}{\Delta W} = \frac{1}{\langle \rho V \rangle_{k+1/2}} - \frac{1}{\langle \rho V \rangle_{k-1/2}} \tag{264}$$

Variables A, ρ, and V (i.e., those without subscripts) will be used in this section to represent the "corrected" (or true solution) values. Thus, equation (264) represents the "correct" solution.

An equivalent expression can be written to represent the continuity equation which was used to predict the x-subscripted areas from the velocities and densities associated with the assumed streamlines. That is:

$$\frac{\Delta^2 A_x}{\Delta W} = \frac{1}{\langle \rho_o V_o \rangle_{k+1/2}} - \frac{1}{\langle \rho_o V_o \rangle_{k-1/2}} \tag{265}$$

Equations (264) and (265) are now substituted into the following identity:

$$\frac{\Delta^2 (A - A_o)}{\Delta W} + \frac{\Delta^2 A_x}{\Delta W} - \frac{\Delta^2 A}{\Delta W} \equiv \frac{\Delta^2 (A_x - A_o)}{\Delta W} \tag{266}$$

to obtain:

$$\frac{\Delta^2 (A - A_o)}{\Delta W} - \left[\frac{1}{\langle \rho V \rangle_{k+1/2}} - \frac{1}{\langle \rho_o V_o \rangle_{k+1/2}}\right] + \left[\frac{1}{\langle \rho V \rangle_{k-1/2}} - \frac{1}{\langle \rho_o V_o \rangle_{k-1/2}}\right] = \frac{\Delta^2 (A_x - A_o)}{\Delta W} \tag{267a}$$

The difference between the "correct" value and the value associated with the assumed streamlines is denoted by δ ( ). In particular:

$$\delta A = A - A_o$$

$$\delta n = n - n_o$$

$$\delta V = V - V_o$$

$$\delta \left[\frac{1}{\rho V}\right] = \frac{1}{\langle \rho V \rangle} - \frac{1}{\langle \rho_o V_o \rangle}$$

$$\delta C = C - C_o$$

Then equation (267a) can be rewritten:

$$\frac{\Delta^2 \delta A}{\Delta W} - \delta\left(\frac{1}{\rho V}\right)_{k+1/2} + \delta\left(\frac{1}{\rho V}\right)_{k-1/2} = \frac{\Delta^2 (A_x - A_o)}{\Delta W} \qquad (267b)$$

This equation represents a difference correction form of the continuity equation.

To eliminate the ρV terms in equation (267b), the momentum equation is introduced. In regions where the rotationality is zero, the momentum equation is:

$$\frac{dV}{V} = -Cdn \qquad (268)$$

As illustrated in Figure 35, the outer boundary of the field is denoted as the N^{th} streamline. Integration of equation (268) from the k^{th} to the N^{th} streamline yields:

$$\ln V_N - \ln V_k = -\int_k^N C dn \qquad (269)$$

For the assumed curvatures, C_o, the momentum equation is:

$$\ln V_{oN} - \ln V_{ok} = -\int_k^N C_o dn \qquad (270)$$

Equation (269) is subtracted from Equation (270), and it is assumed that the lengths of the orthogonals from k to N are not appreciably different.

$$\ln\left(\frac{V}{V_o}\right)_k - \ln\left(\frac{V}{V_o}\right)_N = \int_k^N (C - C_o) dn \qquad (271)$$

Since $V = V_o + \delta V$ we use:

$$\ln\left(\frac{V}{V_o}\right) = \ln\left(1 + \frac{\delta V}{V_o}\right) \simeq \frac{\delta V}{V_o} \qquad \left(\frac{\delta V}{V_o} << 1\right)$$

as a first-order linear approximation, and equation (271) can be written as follows:

$$\left(\frac{\delta V}{V_o}\right)_k - \left(\frac{\delta V}{V_o}\right)_N = \int_k^N \delta C \, dn \qquad (272)$$

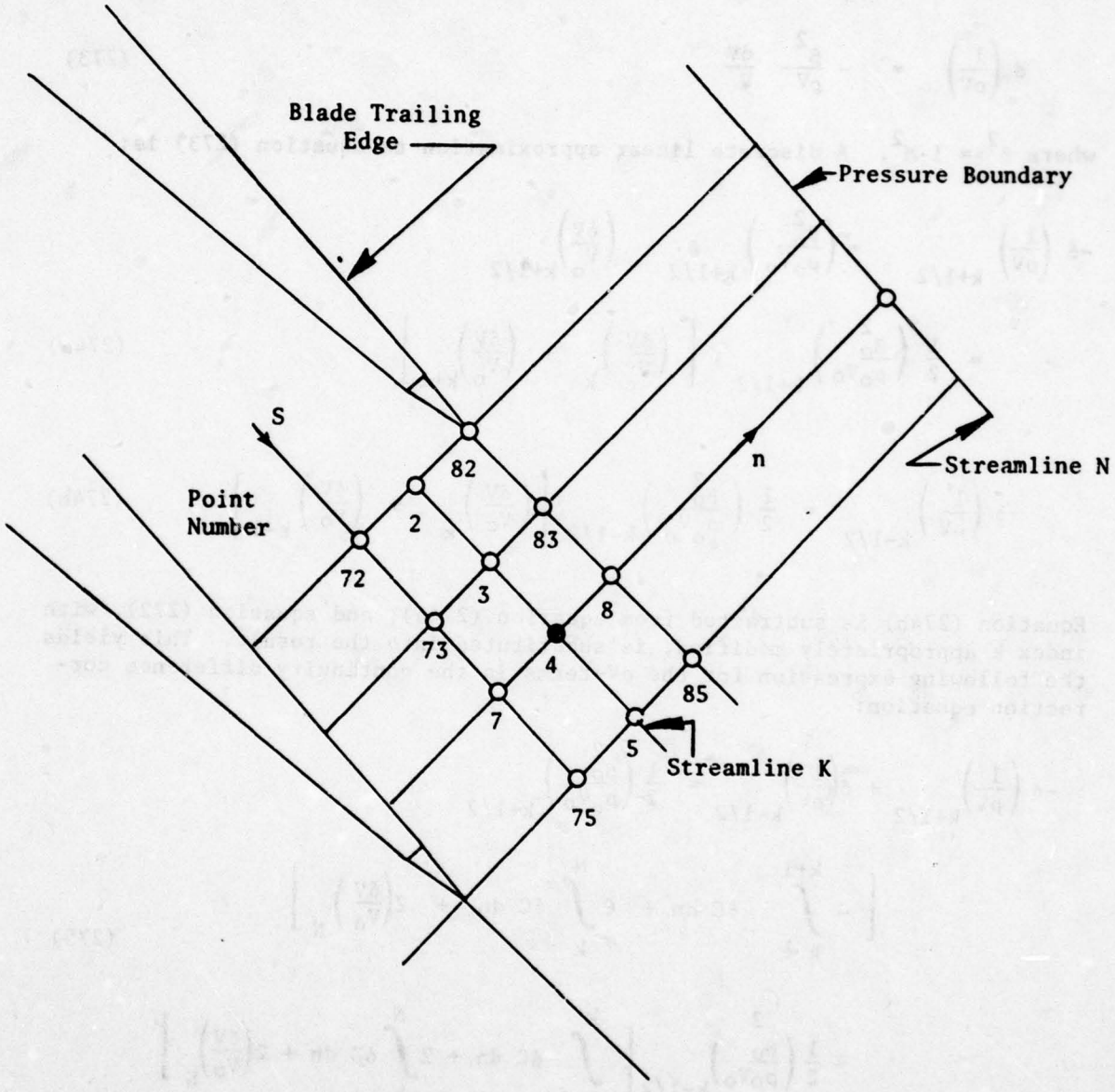

Figure 35. Streamline Subscript Notation and Point Numbering.

Equation (272) is the difference correction form of the momentum equation.

For any given streamline the flow is isentropic, and it can be shown that:

$$d\left(\frac{1}{\rho V}\right) = -\frac{\beta^2}{\rho V}\frac{dV}{V} \tag{273}$$

where $\beta^2 = 1-M^2$. A discrete linear approximation to equation (273) is:

$$-\delta\left(\frac{1}{\rho V}\right)_{k+1/2} = \left(\frac{\beta_o^2}{\rho_o V_o}\right)_{k+1/2}\left(\frac{\delta V}{V_o}\right)_{k+1/2}$$

$$= \frac{1}{2}\left(\frac{\beta_o^2}{\rho_o V_o}\right)_{k+1/2}\left[\left(\frac{\delta V}{V_o}\right)_k + \left(\frac{\delta V}{V_o}\right)_{k+1}\right] \tag{274a}$$

$$-\delta\left(\frac{1}{\rho V}\right)_{k-1/2} = \frac{1}{2}\left(\frac{\beta_o^2}{\rho_o V_o}\right)_{k-1/2}\left[\left(\frac{\delta V}{V_o}\right)_k + \left(\frac{\delta V}{V_o}\right)_{k-1}\right] \tag{274b}$$

Equation (274b) is subtracted from equation (274a), and equation (272), with index k appropriately modified, is substituted into the result. This yields the following expression for the ρV-terms in the continuity difference correction equation:

$$-\delta\left(\frac{1}{\rho V}\right)_{k+1/2} + \delta\left(\frac{1}{\rho V}\right)_{k-1/2} = \frac{1}{2}\left(\frac{\beta_o^2}{\rho_o V_o}\right)_{k+1/2}$$

$$\left[-\int_k^{k+1}\delta C\,dn + 2\int_k^N \delta C\,dn + 2\left(\frac{\delta V}{V_o}\right)_N\right]$$

$$-\frac{1}{2}\left(\frac{\beta_o^2}{\rho_o V_o}\right)_{k-1/2}\left[\int_{k-1}^{k}\delta C\,dn + 2\int_k^N \delta C\,dn + 2\left(\frac{\delta V}{V_o}\right)_N\right] \tag{275}$$

Rearranging the above and substituting a numerical approximation for the integral terms gives:

$$-\delta\left(\frac{1}{\rho V}\right)_{k+1/2} + \delta\left(\frac{1}{\rho V}\right)_{k-1/2} = -1/4 \left[\left(\frac{\beta_o^2}{\rho_o V_o}\right)_{k+1/2} (n_{k+1}-n_k)(\delta C_{k+1}+\delta C_k)\right.$$

$$\left. + \left(\frac{\beta_o^2}{\rho_o V_o}\right)_{k-1/2} (n_k-n_{k-1})(\delta C_k+\delta C_{k-1})\right]$$

$$+ \left[\left(\frac{\beta_o^2}{\rho_o V_o}\right)_{k+1/2} - \left(\frac{\beta_o^2}{\rho_o V_o}\right)_{k-1/2}\right]\left[\int_k^N \delta C \, dn + \left(\frac{\delta V}{V_o}\right)_N\right] \tag{276}$$

The second term on the right hand side is generally small and can be neglected. For convenience, the first term is approximated as follows:

$$-\delta\left(\frac{1}{\rho V}\right)_{k+1/2} + \delta\left(\frac{1}{\rho V}\right)_{k-1/2} \simeq - B_k \delta \bar{C}_k \tag{277}$$

where:

$$B_k = 1/4 \left[\left(\frac{\beta_o^2}{\rho_o V_o}\right)_{k+1/2} (n_{k+1}-n_k) + \left(\frac{\beta_o^2}{\rho_o V_o}\right)_{k-1/2} (n_k-n_{k-1})\right] \tag{278a}$$

$$\delta\bar{C}_k = \frac{W_{k+1}-W_k}{W_{k+1}-W_{k-1}} (\delta C_{k+1}+\delta C_k) + \frac{W_k-W_{k-1}}{W_{k+1}-W_{k-1}} (\delta C_k+\delta C_{k-1}) \tag{278b}$$

Substituting equation (277) into (267b) yields:

$$\frac{\Delta^2(\delta A)}{\Delta W} - B\delta\bar{C}_k = \frac{\Delta^2(A_x-A_o)}{\Delta W} \tag{279}$$

Equation (279) is the desired correction equation. The coefficient B is based on the flow properties calculated from the assumed curvatures. They are known quantities. The unknown quantities are δA and δC. Each of these must be expressed in terms of δn.

Since $\delta A = rh\,\delta n$, the first term in equation (279) can be written

$$\frac{\Delta^2(\delta A)}{\Delta W} = \frac{r_{k+1}\,h_{k+1}\,\delta n_{k+1} - r_k h_k \delta n_k}{W_{k+1} - W_k} - \frac{r_k h_k \delta n_k - r_{k-1} h_{k-1} \delta n_{k-1}}{W_k - W_{k-1}} \tag{280}$$

The second term is composed of terms like:

$$-\delta C_k \approx \frac{D^2(\delta n_k)}{D\,s^2} \tag{281}$$

where s is the curvilinear distance measured along the kth streamline.

The curvature correction for any streamline is obtained by a LaGrange interpolation formula. The form of the expression is:

$$\frac{D^2(\delta n)}{D\,S^2} = G_2\,\delta n_2 + G_3\,\delta n_3 + G_4\,\delta n_4 + G_5\,\delta n_5 \tag{282}$$

where the numbering scheme is shown in Figure 35. For a field point in the subsonic region:

$$G_2 = 0 \tag{283a}$$

$$G_3 = \frac{2}{(S_4-S_3)(S_5-S_3)} \tag{283b}$$

$$G_4 = \frac{-2}{(S_5-S_4)(S_4-S_3)} \tag{283c}$$

$$G_5 = \frac{2}{(S_5-S_4)(S_5-S_3)} \tag{283d}$$

And for a supersonic point:

$$G_2 = \frac{2}{(S_4-S_2)(S_3-S_2)} \tag{284a}$$

$$G_3 = \frac{-2}{(S_4-S_3)(S_3-S_2)} \tag{284b}$$

$$G_4 = \frac{2}{(S_4-S_2)(S_4-S_3)} \tag{284c}$$

$$G_5 = 0 \tag{284d}$$

With equations (280), (281), and (282) substituted into equation (279), there results a set of equations for the variables $\delta n_{i,k}$ where i is an orthogonal line index and k is the streamline index. These equations, together with the boundary condition equations presented below, form a solvable set of linear simultaneous equations.

7.8.2 Upstream and Downstream Streamline Boundaries

Two situations arise at the upstream and downstream boundaries depending on whether or not the flow is near axial. Normally the curvature of the streamline is predefined by the boundary conditions. This eliminates any curvature connections in equation (282). Equation (279) then reduces to

$$\frac{\Delta^2(\delta A)}{\Delta W} = \frac{\Delta^2(A_x - A_o)}{\Delta W} \tag{285}$$

whose solution is

$$\delta A = A_x - A_o \tag{286}$$

When the flow is near axial, an angle boundary condition is employed. The correction at the boundary is

$$\frac{\delta n_j - \delta n_{j+1}}{\Delta s} = \Delta\beta \tag{287}$$

where $\Delta\beta$ is the angle error in the previous iteration and Δs is the streamwise grid spacing.

7.8.3 Body Surface Points

The correction equation for the grid points on a body contour is trivial. The streamlines are already correctly positioned so;

$$\delta n = 0 \tag{288}$$

for each such point.

7.8.4 Pressure Boundary

The techniques of Section 7.8.1 can also be applied to obtain the correction equation for the Nth streamline. This development will be just briefly outlined here. Let k = N and assume equation (261) is replaced by zero. Then equation (263) will be replaced by

$$\frac{\Delta A}{\Delta W} = -\frac{A_k - A_{k-1}}{W_k - W_{k-1}} \tag{289}$$

and equation (267b), the continuity correction equation, becomes:

$$\frac{\Delta \delta A}{\Delta W} + \delta\left(\frac{1}{\rho V}\right)_{k-1/2} = \frac{\Delta(A_x - A_o)}{\Delta W} \tag{290}$$

Again following the previous section for the evaluation of the second term of equation (290) results in

$$\frac{\Delta \delta A}{\Delta W} - \frac{1}{2}\left(\frac{\beta_o^2}{\rho_o V_o}\right)_{k-1/2}\left[\int_{k-1}^{k} \delta C \, dn + 2\left(\frac{\delta V}{V_o}\right)_N\right] = \frac{\Delta(A_x - A_o)}{\Delta W}$$

or approximately

$$\frac{\Delta \delta A}{\Delta W} - \left(\frac{\beta_o^2}{\rho_o V_o}\right)_{k-1/2}\left[\frac{(n_k - n_{k-1})(\delta C_k + \delta C_{k-1})}{4} + \left(\frac{\delta V}{V_o}\right)_k\right] = \frac{\Delta(A_x - A_o)}{\Delta W} \tag{291}$$

Remember that k is the index of the streamline along the pressure boundary. Generally, no correction is made to the velocity on this boundary, so

$$\left(\frac{\delta V}{V_o}\right)_k = 0$$

and the correction equation reduces to:

$$\frac{\Delta \delta A}{\Delta W} - \frac{1}{2} B_N (\delta C_N + \delta C_{N-1}) = \frac{\Delta(A_x - A_o)}{\Delta W} \tag{292}$$

where

$$B_N = \frac{1}{2}\left(\frac{2}{\beta_o \rho_o V_o}\right)_{k-1/2} (n_k - n_{k-1})$$

$$\frac{\Delta\delta A}{\Delta W} = -\frac{r_k h_k \delta n_k + r_{k-1} h_{k-1} \delta n_{k-1}}{W_k - W_{k-1}}$$

7.9 MATRIX SOLUTION PROCEDURE

Iterative methods have been used previously to obtain the solution of the matrix of equations which arise from the numerical representation of the correction equations. When the flow becomes supersonic downstream of the blade row, the standard iterative methods fail as mentioned in Section 7.2.

Therefore, a group of subroutines termed the Crout Factorization - Block Diagonal system (hereafter referred to as CFBD) have been developed to provide an economical and reliable solution of the sets of equations.

The irregular structure of the nonzero elements of the matrix requires relatively complicated organization to obtain an efficient and accurate solution. Furthermore, in transonic flow regimes the finite-difference equations are unsymmetric. For those regimes where iterative methods are suitable, the use of direct methods eliminates the uncertainties of choice of overrelaxation parameters. With proper organization and use of random disc storage capabilities, direct methods are efficient in solving the linear systems produced in the CASC analysis.

The efficiency of a direct solution scheme is related to the bandwidth of the matrix. Unfortunately, the relationships between the grid points which are required to enforce the cascade repeating condition along the stagnation streamlines lead to large bandwidths. Consequently, for the matrix solution a different numbering system is used which orders the points by increasing meridional distance. This has resulted in reducing the bandwidths by a factor of two in some cases.

The CFBD system operates on the region of the matrix which is slightly larger than the region of nonzero elements. A square subregion of the matrix is read into core, factored, and then returned to disc. In an example involving 238 unknowns, such a subregion varies from 14 x 14 to 35 x 35. In contrast, a commercially available system (the LEQT 1B routine of the International Mathematical and Statistical Libraries, Incorporated, 1974) requires a core storage of 53 x 238 for the same example and does not take advantage of the fact that the bandwidth varies.

The upper and lower profiles of the block diagonal matrix are independent. CFBD establishes the working subregions so as to accommodate both upper and lower profiles with minimal increase in the number of arithmetic operations to be performed.

7.10 STREAMLINE ADJUSTMENT

To adjust the streamline position, the coordinates are moved in the normal direction by the computed δn's.

$$x^{p+1} = x^{p} - C_{v} \delta n \sin \beta_{m} \tag{293}$$

$$y^{p+1} = y^{p} + C_{v} \delta n \cos \beta_{m} \tag{294}$$

The streamline angles, β_m, are those found from the curve fits of Section 7.5.1. The superscript p is the iteration sequence number, and C_v is a convergence factor.

When the flow is near axial, equation (294) becomes

$$y^{p+1} = y^{p} + C_{v} \delta n \tag{295}$$

and x is assumed to remain unchanged.

The new values of x and y then form the basis for the next iteration or for the solution which is printed out. The next step in the procedure is to again compute the curvatures and from these compute the velocities and flow balance errors.

The preceding sections have described the procedures utilized in the CASC module. The following sections are supplementary. The streamline curvature correction equation concept, the basic blade-to-blade equations of motion, and the chosen coordinate frame are detailed in Sections 7.11 through 7.13. The CASC nomenclature is summarized in Section 7.14.

7.11 SECOND-ORDER STREAMLINE CURVATURE EQUATIONS FOR ISENTROPIC PLANAR FLOW

In this section the second-order equation which describes the shape of the streamline is derived. An orthogonal system is chosen. The variable n is a measure of the distance across the streamlines and s is the distance along a streamline. The partial differential operator $\hat{\partial}$ indicates that the direction of differentiation is normal to the streamline. The operator D indicates that the direction of differentiation is along a streamline. The basic equations are:

Continuity:

$$\rho V \, \partial n = \partial \Psi \tag{296}$$

Crocco Form of Normal Momentum Equation for Irrotational Flow:

$$\frac{\partial V}{\partial n} = -CV \tag{297}$$

where:

V = velocity

ρ = density

C = streamline curvature = $-\frac{\partial \beta m}{\partial s}$

s = streamwise coordinate

n = cross-stream coordinate

βm = streamline angle measured from the meridional direction

Equation (296) is differentiated as follows:

$$\frac{\partial n}{\partial \Psi} = \frac{1}{\rho V} \tag{298}$$

$$\frac{\partial^2 n}{\partial \Psi^2} = -\frac{1}{\rho V}\left(\frac{1}{V} + \frac{1}{\rho}\frac{\partial \rho}{\partial V}\right)\frac{\partial V}{\partial n}\frac{\partial n}{\partial \Psi} \tag{299}$$

Equation (298) is substituted into equation (299) and the result rearranged:

$$\frac{\partial^2 n}{\partial \Psi^2} + \frac{1}{(\rho V)^2}\left(1 + \frac{V}{\rho}\frac{\partial \rho}{\partial V}\right)\frac{1}{V}\frac{\partial V}{\partial n} = 0 \tag{300}$$

Now equation (297) is substituted into equation (300):

$$\frac{\partial^2 n}{\partial \Psi^2} - \frac{1}{(\rho V)^2}\left(1 + \frac{V}{\rho}\frac{\partial \rho}{\partial V}\right)C = 0 \tag{301}$$

Equation (301) is the desired second-order equation for n, where the curvature is analogous to a derivative of the form (D^2n/Ds^2). Since the flow is isentropic, the coefficient in parentheses may be expressed as follows:

$$1 + \frac{V}{\rho}\left(\frac{\partial \rho}{\partial V}\right)_S = 1 - M^2 \tag{302}$$

thus, the equation reduces to:

$$\frac{\partial^2 n}{\partial \Psi^2} - \frac{1-M^2}{(\rho V)^2} C = 0 \qquad (303)$$

Clearly, the elliptic and hyperbolic nature of the equation is evident when the Mach number is less than and greater than unity, respectively.

Equation (301) is now written in the following abbreviated form:

$$\frac{\partial^2 n}{\partial \Psi^2} - B C = 0 \qquad (304)$$

where:

$$B = \frac{1}{(\rho V)^2} \left(1 + \frac{V}{\rho} \frac{\partial \rho}{\partial V}\right)$$

The equation in its present form cannot be applied directly to obtain a solution for n because of the difficulty of relating the radius of curvature to the second streamwise derivative of n. Instead, it is used to calculate the streamline adjustments (in the cross-stream direction) for an assumed streamline pattern.

To illustrate, we consider an assumed set of streamlines which pass through the small circles in the following sketch.

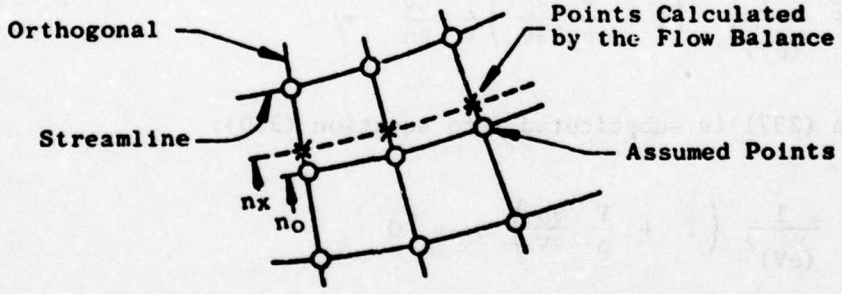

By a curve-fitting process, the values of streamline angle and curvature, C_o, are determined. (The circle points are also orthogonalized. That is, they are moved along the streamlines so that the "orthogonal lines" are truly normal to the given streamlines.) Equations (296) and (297) are integrated along the orthogonal lines, assuming that the value of C_o is valid, and from this "flow balance" the x-positions of the streamline are determined. We have then satisfied the following equation:

$$\frac{\partial^2 n_x}{\partial \Psi^2} - B\,C_o = 0 \tag{305}$$

The "o" subscript denotes values related to the assumed streamline positions and curvatures. The "x" subscript refers to the streamline position as calculated by the continuity equation. The true solution to equation (304) is sought; "true solution values" are unsubscripted.

Equation (305) is subtracted from equation (304). The result is:

$$\left(\frac{\partial^2 n}{\partial \Psi^2} - \frac{\partial^2 n_x}{\partial \Psi^2}\right) + B\left(-C + C_o\right) = 0$$

The adjustment to be made in streamline position is $\delta n = n - n_o$. Hence, the above can be written:

$$\frac{\partial^2 (\delta n)}{\partial \Psi^2} + B\left(-C + C_o\right) = \frac{\partial^2 (n_x - n_o)}{\partial \Psi^2} \tag{306}$$

Finally, we note that:

$$-C + C_o = \frac{D\beta}{D_s} - \frac{D\beta_o}{D_s} \tag{307}$$

$$\approx \frac{D(\beta - \beta o)}{D_s}$$

$$\approx \frac{D}{Ds}\left[\frac{D}{D_s}(\delta n)\right] = \frac{D^2(\delta n)}{Ds^2}$$

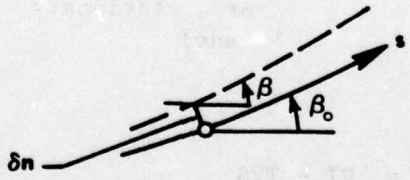

So the differential equation becomes:

$$\frac{\partial^2 (\delta n)}{\partial \Psi^2} + B\,\frac{D^2(\delta n)}{Ds^2} = F \tag{308}$$

where:

$$B = \frac{1-M^2}{(\rho V)^2}$$

$$F = \frac{\partial^2}{\partial \Psi^2}(n_x - n_o)$$

7.12 DERIVATION OF MOMENTUM EQUATION FOR ROTATING COORDINATE SYSTEM

For a frame of reference rotating with constant angular velocity $\vec{\omega}$ about the z-axis, Newton's second law of motion gives, for a frictionless fluid,

$$\frac{D\bar{V}}{Dt} - \omega^2\bar{r} + 2\bar{\omega} \times \bar{V} + \frac{1}{\rho}\nabla P = 0 \qquad (309)$$

This equation together with the law of conservation of energy:

$$T \nabla S = \nabla h_e - \frac{1}{\rho}\nabla P \qquad (310)$$

the vector identity:

$$\frac{D\bar{V}}{Dt} - \frac{\partial \bar{V}}{\partial t} = \bar{V} \cdot \nabla\bar{V} = \nabla\frac{V^2}{2} - \bar{V} \times (\nabla \times \bar{V}) \qquad (311)$$

and the definition of rothalpy:

$$I \equiv h_e + \frac{V^2}{2} - \frac{\omega^2 r^2}{2} \qquad (312)$$

(note $U = \omega = 0$ for a stationary blade)

results in:

$$\bar{V} \times (\nabla \times \bar{V}) - 2\bar{\omega} \times \bar{V} = \nabla I - T\nabla S \qquad (313)$$

for a steady flow. The components in cylindrical coordinate directions (r, z, θ) are as follows:

r direction

$$V_\theta\left(\frac{V_\partial}{r} + \frac{\partial V_\theta}{\partial r} - \frac{\partial V_r}{r\partial\partial}\right) + V_z\left(\frac{\partial V_z}{\partial r} - \frac{\partial V_r}{\partial z}\right) - 2\omega V_\theta = \frac{\partial I}{\partial r} - \frac{T\partial S}{\partial r} \qquad (314)$$

θ direction

$$V_z\left(\frac{\partial V_r}{r\partial\theta} - \frac{\partial V_\theta}{\partial z}\right) - V_r\left(\frac{V_\theta}{r} + \frac{\partial V_\theta}{\partial r} - \frac{\partial V_r}{r\partial\theta}\right) + 2\omega V_r = \frac{\partial I}{r\partial\theta} - T\frac{\partial S}{r\partial\theta} \tag{315}$$

z direction

$$-V_r\left(\frac{\partial V_z}{\partial r} - \frac{\partial V_r}{\partial z}\right) - V_\theta\left(\frac{\partial V_z}{r\partial\theta} - \frac{\partial V_\theta}{\partial z}\right) = \frac{\partial I}{\partial z} - T\frac{\partial S}{\partial z} \tag{316}$$

To obtain a set of intrinsic equations in the blade-to-blade plane, the following coordinate transforms are introduced. First, in the meridional plane the distance m is defined as the distance along a projected streamline. p is defined as the distance perpendicular to the projected streamline. The z, r, θ and m, p, θ differential distances are then related by:

$$\frac{\partial}{\partial m} = \sin\phi\frac{\partial}{\partial r} + \cos\phi\frac{\partial}{\partial z} \tag{317a}$$

$$\frac{\partial}{\partial p} = \cos\phi\frac{\partial}{\partial r} - \sin\phi\frac{\partial}{\partial z} \tag{317b}$$

where ϕ is the inclination of the stream surface of revolution as measured in the meridional plane. However, variations perpendicular to the stream surfaces are assumed to be small and are neglected. Thus by assumption:

$$\frac{\partial(\ )}{\partial p} = 0 \tag{317c}$$

It then follows that:

$$\frac{\partial}{\partial z} = \cos\phi\frac{\partial}{\partial m} \tag{317d}$$

$$\frac{\partial}{\partial r} = \sin\phi\frac{\partial}{\partial m} \tag{317e}$$

New velocity components are also defined:

$$V_m = \sin\phi V_r + \cos\phi V_z \tag{317f}$$

$$V_p = \cos \phi \, V_r - \sin \phi \, V_z = 0 \tag{317g}$$

Introducing equations (317d) through (317g) into equations (314), (315), and (316), after first premultiplying equation (314) by sin ϕ and premultiplying equation (316) by cos ϕ and summing, results in:

$$V_m \left[\frac{1}{r} \frac{\partial V_m}{\partial \theta} - \frac{1}{r} \frac{\partial (rV_\theta)}{\partial m} - 2 \omega \sin \phi \right] = \frac{\partial I}{r \partial \theta} - T \frac{\partial S}{r \partial \theta} \tag{318}$$

$$V_\theta \left[\frac{1}{r} \frac{\partial (rV_\theta)}{\partial m} - \frac{1}{r} \frac{\partial V_m}{\partial \theta} + 2 \omega \sin \phi \right] = \frac{\partial I}{\partial m} - T \frac{\partial S}{\partial m} \tag{319}$$

These equations represent the two-dimensional momentum equations in the blade-to-blade m,θ plane. The intrinsic form is obtained by introducing a second transformation which rotates and aligns the coordinates in the blade-to-blade plane with the velocity vector. A distance s is defined to be in the direction of the velocity vector which is at an angle β_m from the meridional direction. The distance n is measured perpendicular to s. We choose s and n to be in the same units as θ (radians). Thus, the differential distances are related by:

$$\frac{1}{r} \frac{\partial}{\partial s} = \cos \beta_m \frac{\partial}{\partial m} + \sin \beta_m \frac{1}{r} \frac{\partial}{\partial \theta} \tag{320a}$$

$$\frac{1}{r} \frac{\partial}{\partial n} = -\sin \beta_m \frac{\partial}{\partial m} + \cos \beta_m \frac{1}{r} \frac{\partial}{\partial \theta} \tag{320b}$$

$$\frac{\partial}{\partial \theta} = \sin \beta_m \frac{\partial}{\partial s} + \cos \beta_m \frac{\partial}{\partial n} \tag{321a}$$

$$\frac{\partial}{\partial m} = \cos \beta_m \frac{1}{r} \frac{\partial}{\partial s} - \sin \beta_m \frac{1}{r} \frac{\partial}{\partial n} \tag{321b}$$

The total velocity component, V_s is defined:

$$V_s = V_m \cos \beta_m + V_\theta \sin \beta_m \tag{322a}$$

$$0 = -V_m \sin \beta_m + V_\theta \cos \beta_m \tag{322b}$$

Substituting equations (321a), (321b), (322a), and (322b) into equation (318) and (319) yields:

$$\frac{\partial I}{\partial s} - T \frac{\partial S}{\partial s} = 0 \tag{322}$$

$$\frac{1}{2}\frac{\partial V^2}{\partial n} = V^2\frac{\partial \beta_m}{\partial s} + (2r\omega V + V^2 \sin\beta_m)\sin\phi + \frac{\partial I}{\partial n} - T\frac{\partial S}{\partial n} \tag{323}$$

Within the blade row, I is constant and the streamline curvature is defined:

$$C \equiv -\frac{\partial \beta_m}{\partial s} \tag{324}$$

Thus, the final equations are expressed:

$$\frac{1}{2}\frac{\partial V}{\partial n} = -V^2 C + (2r\omega V + V^2 \sin\beta_m)\sin\phi - T\frac{\partial S}{\partial n}$$

$$\frac{\partial S}{\partial s} = 0$$

7.13 CONFORMAL BLADE-TO-BLADE PLANE COORDINATES

CASC utilizes an intrinisic coordinate system where the grid is composed of streamlines and normals to streamlines. Specifically the Crocco momentum equation is integrated normal to the streamline direction. Therefore, it is most convenient to work in a coordinate frame where the streamwise grid lines depict the proper flow angles. The tangent of the local flow angle is given by

$$\tan\beta_m = \frac{rD\theta}{D_m} = \frac{V_\theta Dt}{V_m Dt} \tag{325}$$

where $rD\theta$ and Dm are incremental distances over which a particle travels in time Dt. To eliminate the appearance of the coefficient r in the above equation we may define a new variable

$$dm' = \frac{dm}{r} \tag{326}$$

so that the ratio of distances is simply:

$$\frac{V_\theta\, Dt}{V_m\, Dt} = \frac{D\theta}{Dm'} \tag{327}$$

More generally, we may choose

$$dX = \frac{r^*}{r}\, dm \tag{328a}$$

$$dY = r^*\, d\theta \tag{328b}$$

where X and Y are transformed meridional and tangential coordinates. r^* is either an arbitrarily chosen reference radius or the inverse of the m', θ normalizing factor as presented in Section 9.4.1 of the User's Manual.

Thus, when the blade section is plotted in X, Y (or m', θ) coordinates:

- The blade surface angles are correct (i.e., the blade shape is not distorted, but is locally scaled), and
- The blade pitch is the same from leading edge to trailing edge.

An advantage of the X, Y coordinate frame is that, for a vane, the equations of motion are the same as for a rectilinear cascade. Hence, when the 3-D vane section is viewed in this coordinate frame, the engineer's 2-D aerodynamic experience/intuition is applicable. To illustrate this latter point we consider equation (318) of the previous section. For constant rothalpy and entropy the equation, after multiplying by r, reduces to:

$$\frac{1}{r}\,\frac{\partial(rV_m)}{\partial\theta} - \frac{\partial(rV\theta)}{\partial m} = 2r\omega \sin\phi \tag{329}$$

It can be rewritten as:

$$\frac{1}{r}\,\frac{\partial}{\partial\theta}\left[\frac{r}{\rho h}\,\rho h\, V_m\right] - \frac{\partial}{\partial m}\left[\frac{r}{\rho h}\,\rho h\, V_\theta\right] = 2r\omega \sin\phi \tag{330}$$

Now define the stream function, ψ:

$$\rho h V_m \equiv \frac{1}{r}\,\frac{\partial\psi}{\partial\theta} \tag{331a}$$

$$-\rho h V_\theta \equiv \frac{\partial\psi}{\partial m} \tag{331b}$$

Introduction of equation (331) into (330) gives

$$\frac{1}{r}\,\frac{\partial}{\partial\theta}\left[\frac{r}{\rho h}\,\frac{1}{r}\,\frac{\partial\psi}{\partial\theta}\right] + \left[\frac{\partial}{\partial m}\,\frac{r}{\rho h}\,\frac{\partial\psi}{\partial m}\right] = 2\, r\, \omega \sin\phi \tag{332}$$

This is the stream function equation in the m,θ coordinate system for blade-to-blade flow.

When the independent variables are transformed through use of equations (328a) and (328b), Equation (332) becomes

$$\frac{\partial}{\partial X}\left(\frac{1}{\rho h}\frac{\partial \Psi}{\partial X}\right) + \frac{\partial}{\partial Y}\left(\frac{1}{\rho h}\frac{\partial \Psi}{\partial Y}\right) = 2\left(\frac{r}{r^*}\right)^2 \omega \sin \phi \qquad (333)$$

For a vane, the right hand side is zero, and in this case the above equation are identical to the 2-D stream function equation for a rectilinear geometry with a lamina thickness variation. Thus, the transformations in equations (328a) and (328b) determine the equivalent 2-D blade configuration.

7.14 NOMENCLATURE

Symbols

A	Flow area measured normal to the streamline
b	Wake thickness
B_1, B_2	Coefficients in the streamline correction equation
C	Curvature, = - $d\beta_m/ds$
Cu	Absolute tangential velocity
Cv	Convergence factor
G	Curvature influence coefficients
h	Streamtube height normal to meridional plane streamline; lamina thickness
h_e	Static enthalpy
H	Total absolute enthalpy
I	Rothalpy
k	Streamline number
k_2	Angular momentum constant
m	Curvilinear meridional plane distance
m'	Transformed meridional distance, radians
M	Mach number

μ	Cross-stream distance, radians
p	Perpendicular distance
P	Static pressure
P_T	Total pressure
Q	Total pressure ratio, PT/PT_{ideal}
r	Radius
R	Gas constant
s	Streamwise distance, radians
S	Entropy
t	Time
T	Temperature
u	Axial component of velocity/integration by parts variable
U	Wheel speed (ωxr)
v	Normal component of velocity/integration by parts variable
V	Relative velocity
W	Flow rate
z	Axial distance
β	Streamline angle
β^2	$1-M^2$
δ	Difference between correct value and assumed value
$\Delta\theta$	Blade pitch in radians
θ	Tangential coordinate, radians
ξ	Orthogonal index
ρ	Density
Ψ	Stream function
ω	Angular velocity

Superscripts

p	Iteration counter

Subscripts

u	Tangential direction
m	Meridional direction
o	Assumed location
x	Calculation location

8.0 BLADE HEAT LOAD CALCULATION

8.1 INTRODUCTION

The HTCOEF module calculates the turbine blade row heat load. This heat load must be known if the blade row average metal temperature is to be defined for various cooling air flow rates. This calculation is accomplished with inputs of geometry and gas stream boundary conditions. The heat load includes not only that due to forced convection, but also combustor and nonluminous gas radiation.

The heat load is evaluated by defining the radiation heat flux and the local heat transfer coefficient around the midspan airfoil surface. The heat transfer coefficient distribution is made up of three parts: (1) the leading edge which is evaluated by using a cyclinder in cross-flow laminar heat transfer coefficient analysis, (2) the pressure side which is evaluated with either a laminar or turbulent flat plate analysis, and (3) the suction side which is also evaluated with either a laminar or turbulent flat plate analysis. There is an option to correct any of the above analyses with an input correction factor if this is considered necessary.

The radiation, which is made up of combustor dome radiation and nonluminous gas radiation, is usually restricted to the first-stage nozzle but the nonluminous heat flux can be evaluated at any stage. The input consists of the view factor and beam length of the combustor and the local flowpath, along with the gas properties and combustor inlet temperature.

8.2 TECHNICAL BACKGROUND

In an air-cooled turbine, it is imperative that a detailed thermal analysis of the hot turbine components be performed. The prime purpose of the analysis is calculate the local metal temperatures so that the mechanical life of the components can be calculated. If too much cooling air is used, an excessive penalty associated with using compressor extraction air is incurred. If too little cooling air is used, metal temperatures become excessive and the mechanical life objectives are not met. Thus, it is necessary that the correct cooling air flow rate be established to meet the hot component life objectives. The required cooling airflow rate is determined by the heat load. The heat load is proportional to not only the difference between gas temperature and wall temperature but also the gas side heat transfer coefficient and surface area. The gas temperature is calculated in the GASPRO module, and the metal temperature of the hot components is estimated by the mechanical designer to meet the life objectives. The surface area is physically available from the FLOPTH and CASC outputs. This leaves only the average heat transfer coefficient to be determined. This module was developed to calculate the heat transfer coefficient. Another heat load source on the first-stage vane comes from the hot gas radiation. This radiation heat load is calculated in the program. Also available from the program are detailed heat transfer coefficient and radiation heat flux distributions for detailed analysis.

8.3 PROGRAM OUTLINE

The program consists of taking various inputs from previous modules and then calculating the heat transfer coefficient and radiation distribution around the airfoil. The program is broken down into four major components: the leading edge heat transfer coefficient calculation; the suction and pressure side heat transfer calculation; the radiation heat flux calculation; and the gas property evaluation subroutine.

The leading edge heat transfer calculation procedure consists of calculating the cylinder in cross-flow heat transfer coefficients. A correction based on approach Reynolds number and turbulence intensity can be made if desired. The input consists of the upstream approach gas conditions, wall temperature, and airfoil leading edge radius of curvature. The upstream gas conditions include gas temperature, fuel air ratio, gas pressure, and Mach number (or velocity). The heat transfer coefficient distribution at the leading edge is calculated at 19 equally spaced locations encompassing 160° around the leading edge.

The suction and pressure side heat transfer calculation procedure consists of calculating either a laminar or turbulent heat transfer coefficient along both surfaces. The input required for the heat transfer calculation consists of gas temperature, total pressure, Mach number (or velocity) distribution, average and maximum wall temperature, fuel air ratio, and surface distance from the leading edge stagnation point. The heat transfer coefficients are calculated at the location at which the local surface distance is defined. A correction factor distribution can be applied, if the user desires, for the laminar and turbulent heat transfer coefficients depending on the turbulence, acceleration, or surface curvature. The surface heat transfer coefficient distribution is then integrated over the complete surface to determine the heat load per inch of blade height.

The radiation heat load is calculated in the RAD1 subroutine by first evaluating the combustor radiation heat flux and then adding it to the nonluminous gas radiation in the vane channel. The required input for combustor radiation consists of combustor exit fuel air ratio, view factor, beam length, and combustor inlet air temperature. The required input for the nonluminous gas radiation consists of gas stream total temperature and pressure; Mach number, view factor, beam length distributions, and average wall temperature. The local radiation heat flux distribution is integrated over the surface to determine the radiation heat load per inch of blade height. The radiation heat flux is then added to the convective heat flux to give a total heat load per inch of blade height. The total heat load is the value that will be used in the WCFLOW module to establish the coolant flow versus bulk metal temperature matrix.

All gas properties and boundary layer film properties are evaluated in the SUBCAL subroutine. The SUBCAL subroutine is called at numerous points in the main calculation program and in the RAD1 subroutine to define gas properties for the heat transfer calculations. The properties consist of Prandtl number, viscosity, conductivity, and molecular weight. All the properties are defined as a function of temperature, presssure, and equivalence ratio.

8.4 LEADING EDGE HEAT TRANSFER CALCULATION

The leading edge heat transfer coeficient distribution calculation procedure consists of analyzing the airfoil leading edge as a cylinder-in-cross-flow. A laminar boundary layer flow analysis is used to define the local heat transfer coefficient distribution.

$$h_{cyl} = 1.14(k_*/D)(Re_d)^{0.5}(Pr_*)^{0.4}[1 - (4X_{sp}/\pi D)^3] \quad (334)$$

where:

k_* = Conductivity of the leading edge boundary layer gas based on the average of gas and wall temperature (Btu/hr ft °F)

Re_d = Leading edge Reynolds number based on upstream velocity, and effective leading kinematic velocity of the boundary layer gases which is based on the average of the wall and upstream gas temperatures.

Pr_* = Prandtl number of the boundary layer gas based on the average of the wall and upstream gas temperatures.

X_{sp} = Distance from the leading edge stagnation point to point of calculation (ft).

D = Effective leading edge diameter (ft) or diameter of a cylinder that would represent the airfoil leading edge over approximately a 120° sector as shown in Figure 36.

To accomplish the calculation, it is first necessary to define the quantities that go into the heat transfer coefficient calculation .

The upstream velocity is defined as:

$$V1 = XMI[GAM(GAS)(C2/XMWX) \cdot TS]^{1/2} \quad (335)$$

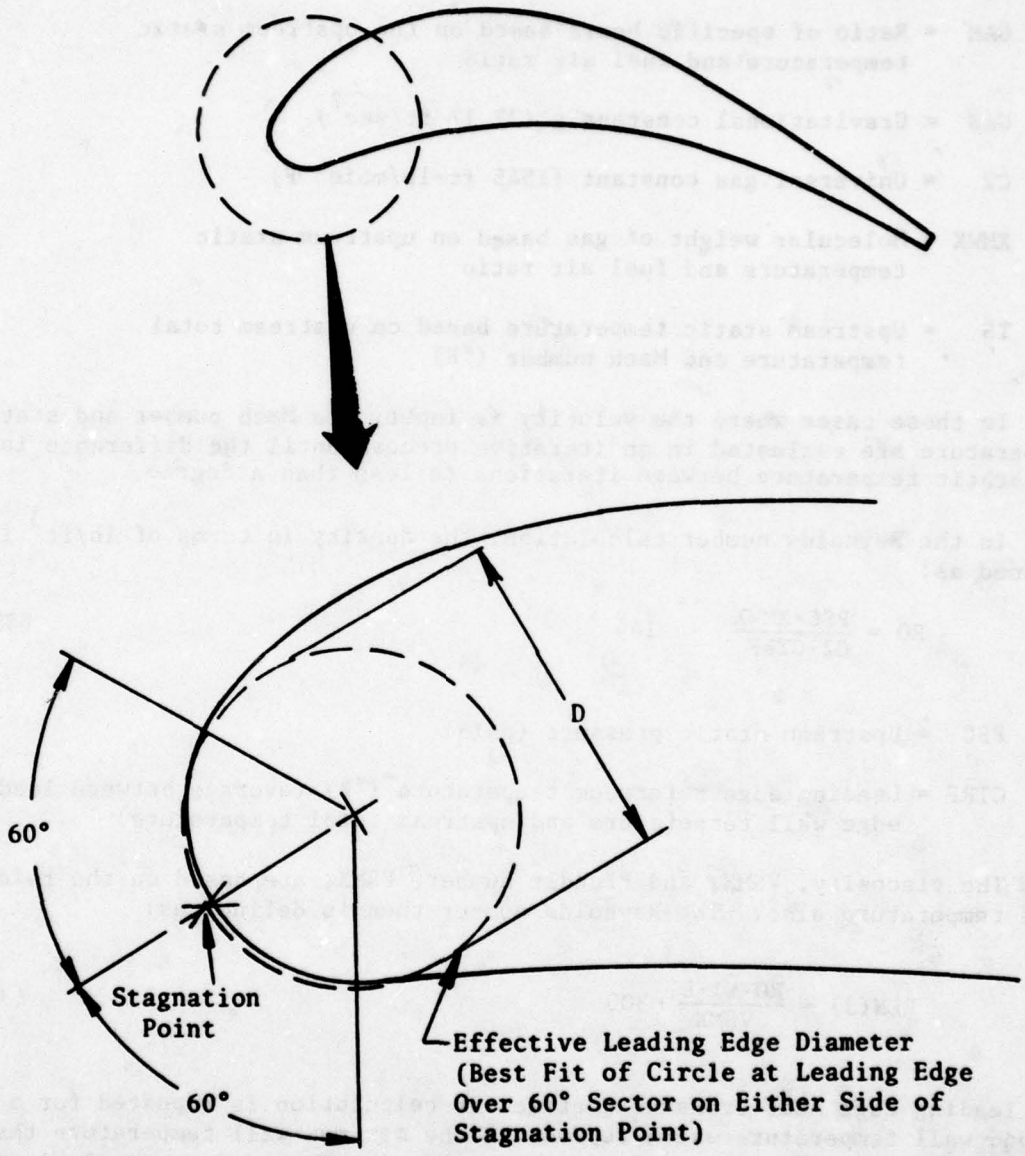

Figure 36. Effective Leading Edge Diameter for Heat Transfer Calculation.

where:

XM1 = Upstream Mach number

GAM = Ratio of specific heats based on the upstream static temperature and fuel air ratio

GAS = Gravitational constant g (32.17 ft/sec^2)

C2 = Universal gas constant (1545 ft-lb/mole °F)

XMWX = Molecular weight of gas based on upstream static temperature and fuel air ratio

TS = Upstream static temperature based on upstream total temperature and Mach number (°R)

In those cases where the velocity is input, the Mach number and static temperature are evaluated in an iterative process until the difference in the static temperature between iterations is less than a degree.

In the Reynolds number calculation, the density in terms of lb/ft^3 is defined as:

$$RO = \frac{PSC \cdot XMWX}{C2 \cdot CTRF} \cdot 144 \qquad (336)$$

PSC = Upstream static pressure (psia)

CTRF = Leading edge reference temperature (°R) (average between leading edge wall temperature and upstream total temperature)

The viscosity, VSMX, and Prandlt number, PRMX, are based on the reference temperature also. The Reynolds number then is defined as:

$$REN(J) = \frac{RO \cdot V1 \cdot D}{VSMX} \cdot 300 \qquad (337)$$

The leading edge heat transfer coefficient calculation is repeated for a second wall temperature which represents the maximum wall temperature that can be expected. The second wall temperature is also used in recalculating the reference temperature CTRF.

The leading edge heat transfer coefficient can be increased depending on the application, turbulence intensity, roughness, or for any other reason. The correction factor built into the program is a function of the leading edge Reynolds number. The corrected heat transfer coefficient is:

$$CHC1(L) = h_{cyl} \cdot CF1 \cdot REN(J)^{CF2} \quad (338)$$

where CF1 and CF2 are empirical correlation coefficients that define the correction to the cylinder in cross-flow calculation procedure. If a fixed correction factor, CF1, is desired, then:

$$CF2 = 0 \quad (339)$$

8.5 PRESSURE AND SUCTION SIDE HEAT TRANSFER CALCULATION

The pressure side and suction side heat transfer calculation procedure differs only in the notation for the variables. Two calculation procedures are available, on either side, a laminar flat plate analysis and a turbulent flat plate analysis. The equation used for both is:

$$H(I,N) = 12 \frac{CI \cdot XKM}{X(I)} \cdot RENO^{XNI} \cdot PRMX^{1/3} \quad (340$$

where:

CI = Empirical coefficient (0.332 for laminar flow and 0.0296 for turbulent flow

XKM = Conductivity of the boundary layer gas based on local reference temperature and static pressure (Btu/hr-ft-° F)

X(I) = Distance from the leading edge stagnation point (inches)

RENO = Local Reynolds number where the characteristic dimension is X(I), the velocity is the local free stream value and the kinematic viscosity is based on the local reference temperature.

XNI = Empirical correlation exponent on RENO (0.5 for laminar flow and 0.8 for turbulent flow)

PRMX = Local Prandtl number of the boundary layer gas based on local reference temperature

The local reference temperature is defined as:

$$TREF(K) = 0.5[TW(N)] + 460 + TSF(I) + 0.22\ PRMX^{1/XNE}\ [T1R - TSF(I)] \quad (341)$$

where:

TSF(I) = Local free stream static temperature (°R)

TW(N) = Wall temperature for which there are two values: the average and maximum expected values (°F)

XNE = Emperical coefficient (2 for laminar flow and 3 for turbulent flow)

T1R = Free stream total temperature (°R)

Once the turbulent or laminar heat transfer coefficients are calculated, they can be corrected by means of a factor, CFA(I), which is the ratio of the corrected to the uncorrected flat plate heat transfer coefficient. The corrected heat transfer coefficient distribution CORH(I,N), is then integrated from leading edge to trailing edge by means of a point-by-point linear integration using the trapezoidal rule and a do loop process.

$$AVGH = AVGH + \left(\frac{CORH1(I-1) + CORH1(1)}{2}\right)\left(\frac{X(I) - X(I-1)}{144}\right) \qquad (342)$$

where:

AVGH = Integral evaluated up to X(I-1)

CORH1 = Corrected heat transfer coefficient evaluated at both (I) and (I-1) locations

X = Distance from stagnation point along surface evaluated at (I) and (I-1) locations.

The first step in the integration uses the stagnation value of the heat transfer coefficient:

$$AVGH = \frac{CHC1(I) + CORH1(I)}{2} \cdot \frac{X(I)}{144} \qquad (343)$$

where CHC1(I) is the stagnation point heat transfer coefficient after it has been corrected. AVGH is used in equation (342) to define the integral. The suction side integral and pressure side integral are summed to give the total integral, AVGHL for laminar flow and AVGHT for turbulent flow.

8.6 RAD1 SUBROUTINE

The RAD1 subroutine calculates the radiation heat flux to the surface of a vane or blade from the nonluminous gas mixture of high temperature product of combustion. The radiation to the first stage vane can be broken down into

two components: the combustor radiation from the flame core, which is significantly higher than the combustor exit maximum peak gas temperature; and the gas radiation to the vane surface in the channels between the vanes. The gas radiation will occur between any gas and the surface but only becomes significant when the gas temperature exceeds 3000° F.

The first step in defining the gas radiation from the combustor is to define the average gas temperature:

$$TCMB = T3 \frac{18400 - 0.60(T3 - 200)}{CP\ (1 + 1/[0.06817\ ERCB])} \tag{344}$$

where:

T3 = Combustor inlet air temperature (°F)

CP = Average specific heat of the products of combustion in raising the temperature from T3 to combustor exit temperature, T1R

ERCB = Average equivalence ratio of the combustion gases

The average combustor equivalence ratio, ERCB, is calculated from the combustor exit maximum peak equivalence ratio, ER, by:

$$ERCB = ER + 0.25(1 - ER) \tag{345}$$

With the combustor temperature, the combustor gas emissivity can be defined:

$$EMS = 1 - EXP\left(\frac{-ATM\ \sqrt{ERCB\ BLD/12}\ (39000)}{TCMB^{1.5}}\right) \tag{346}$$

where:

BLD = Combustor average gas beam length at the vane leading edge (inches)

ATM = Gas pressure in the combustor (atmosphere)

The radiation heat load at the vane leading edge is:

$$RSTG = VFD \cdot EMS \cdot (0.171E\text{-}8) \cdot TCMB^4 \tag{347}$$

where VFD is the view factor of the combustor as seen from the vane leading edge.

The nonluminous gas radiation in the vane passage due to the hot gases between the vanes must also be evaluated. The nonliminous gas radiation calculation is similar to the combustor radiation:

$$EMX(I) = 1 - EXP\left(\frac{-ATM\ \sqrt{ER\ 0.06817 \cdot BLA/12}\ (39000)}{[TSF(I) + 460]^{1.5}}\right) \quad (348)$$

where:

BLA = Local beam length of the gas which is defined from the blade spacing and flowpath height (inches)

TSF(I) = Local gas stream static pressure (°F)

The local nonluminous gas radiation is thus defined as:

$$QGAS = EMX(I) \cdot (0.171E\text{-}8) \cdot [TSF(I) + 460]^4 \quad (349)$$

The combustor dome radiation, RSTG, and passage free stream nonluminous radiation, QGAS, are thus used to define the total gas radiation heat flux to the surface of the vane:

$$RTOT(I) = RSTG \cdot VFA(I) + QGAS \cdot [1 - VFA(I)] \quad (350)$$

where VFA(I) is the local view factor of the combustor gases at each point on the vane surface. When the combustor can no longer be seen from the point at which the heat flux is calculated on the vane surface, the view factor VFA(I) is zero.

The radiation distribution around the vane surface is now integrated to define the total radiation heat flux to the vane surface:

$$AVGQ = AVGQ + \left(\frac{RTOT(I\text{-}1) + RTOT(I)}{2}\right)\left(\frac{X(I) - X(I\text{-}1)}{144}\right) \quad (351)$$

where X(I) is the surface distance from the stagnation point. The pressure surface is integrated to give AVGQP, and the suction side is integrated to give AVGQS. The first element of the integration on either side of the stagnation point is defined as:

$$AVGQ = \left(\frac{RSTG + RTOT(1)}{2}\right)\left(\frac{X(I)}{144}\right) \quad (352)$$

and this is the first value in the integration for both side of the vane that goes into equation (351). The total vane radiation for each inch of blade height is:

$$AVGQ = AVGQS + AVGQP \tag{353}$$

The dimension on the radiation heat load is Btu/ft^2. The equivalent heat transfer coefficient is now defined from the radiation heat load and the difference between the total gas stream temperature and the maximum wall temperature. The total of the integrated laminar heat transfer and integrated equivalent radiation heat transfer is:

$$AVGHL = AVGHL + AVGQ/[T1 - TW(1)] \tag{354}$$

and the total of the turbulent heat transfer and the integrated equivalent radiation heat transfer is:

$$AVGHT = AVGHT + AVGQ[T1 - TW(1)] \tag{355}$$

with the units of Btu/hr-ft^2 - °F/inch of blade height.

8.7 SUBCAL SUBROUTINE

In the main program and subroutine RAD1, there are several places where the thermodynamic gas properties must be defined in order to calculate the heat transfer. These properties are the Prandtl number PRMX, viscosity, VSMX, conductivity, XKM, and molecular weight XMWX. These properties are then used to define all other properties including specific heat, CP, and the ratio of specific heats, GAM.

$$CP = \frac{PRMX \cdot XKM}{VSMX} \tag{856}$$

and

$$GAM = \frac{1}{1 - 1.985/(CP \cdot XMWX)} \tag{357}$$

The thermodynamic properties are defined for air and for the products of combustion of a stoichiometric fuel air ratio mixture. The properties are defined by means of a fourth-order least squares fit baseline temperature function that represents the analytical thermodynamic property information of Reference 12. The Prandtl number, viscosity, and conductivity were least squares fit over a temperature range from 540° R to 5040° R and the molecular weight over a 900° R - 5040° R temperature range. The equation for the Prandtl number of air is:

$$\begin{aligned} FUNPA(T) = {} & 0.69854 + 0.18615(10^{-4})T - 0.14933(10^{-7})T^2 \\ & + 0.46435(10^{-11})T^3 - 0.52452(10^{-15})T^4 \end{aligned} \tag{358}$$

and the Prandtl number of the products of combustion of a stoichiometric fuel-air ratio mixture is:

$$\begin{aligned} FUNPS(T) = {} & 0.73511 - 0.42786(10^{-6})T - 0.16305(10^{-7})T^2 \\ & + 0.70836(10^{-11})T^3 - 0.96944(10^{-15})T^4 \end{aligned} \tag{359}$$

The Prandtl number of any other fuel-air ratio mixture can be defined by interpolating between FUNPA(T) and FUNPS(T). The interpolation was set up to match the analytical model at an equivalence ratio of 0.5. The Prandtl number is thus:

$$PRMX = FUNPA + ER^{0.3446}\ (FUNPS - FUNPA) \tag{360}$$

where ER is the equivalence ratio of the products of combustion mixture.

The viscosity is calculated in a similar way. The temperature function for the viscosity of air is:

$$\begin{aligned} FUNVA(T) = {} & 0.11390(10^{-1}) + 0.70105(10^{-4})T - 0.15266(10^{-7})T^2 \\ & + 0.25340(10^{-11})T^3 - 0.15921(10^{-15})T^4 \end{aligned} \tag{361}$$

and the temperature function for the viscosity of the products of combustion of the stoicmetric fuel air ratio mixture is:

$$\begin{aligned} FUNVS(T) = {} & 0.61999(10^{-2}) + 0.72177(10^{-4})T - 0.1558(10^{-7})T^2 \\ & + 0.27452(10^{-11})T^3 - 0.18909(10^{-15})T^4 \end{aligned} \tag{362}$$

The viscosity of any intermediate equivalence ratio, ER, is thus defined as:

$$VSMX = FUNVA + ER^{0.58427}\ (FUNVS - FUNVA) \tag{363}$$

The molecular weight of the gas is calculated in a similar way. The temperature function for the molecular weight of the air is:

$$FUNMA(T) = 0.28932(10^{2}) + 0.76716(10^{-4})T - 0.59348(10^{-7})T^{2} + 0.18457(10^{-10})T^{3} - 0.19865(10^{-14})T^{4} \quad (364)$$

and the temperature function for the molecular weight of the products of combustion of a stoichmetric fuel air ratio mixture is:

$$FUNMS(T) = 0.28871(10^{2}) + 0.25752(10^{-3})T - 0.22072(10^{-6})T^{2} + 0.76797(10^{-10})T^{3} - 0.93792(10^{-14})T^{4} \quad (365)$$

The molecular weight of the products of combustion mixture at any intermediate equivalence ratio, ER, is thus defined as:

$$XMWX = FUNMA + ER^{1.5726}\ (FUNMS - FUNMA) \quad (366)$$

The conductivity of the gas is more difficult to define since it is a function of both temperature and pressure. Because of this, the gas conductivity temperature function is defined at 20 and 40 atmospheres for an air mixture and for the products of combustion of a stoichmetric fuel air ratio mixture. At the 20-atmosphere pressure, the temperature function for the air mixture is:

$$FUNA2(T) = 0.78796(10^{-2}) + 0.11806(10^{-4})T + 0.66529(10^{-8})T^{2} - 0.25488(10^{-11})T^{3} + 0.31634(10^{-15})T^{4} \quad (367)$$

and the temperature function for the products of combustion of the stoichmetric fuel air ratio mixture is:

$$FUNS2(T) = 0.11783(10^{-1}) - 0.47667(10^{-5})T + 0.25557(10^{-7})T^{2} - 0.98023(10^{-11})T^{3} + 0.12889(10^{-14})T^{4} \quad (368)$$

At the 40 atmosphere pressure conditions, the temperature function for the conductivity of the air mixture is:

$$FUN4A(T) = 0.62113(10^{-2}) + 0.15922(10^{-4})T + 0.33309(10^{-8})T^{2} - 0.1478(10^{-11})T^{3} + 0.19744(10^{-15})T^{4} \quad (369)$$

and the corresponding temperature function for the products of combustion of the stoichmetric fuel air ratio mixture is:

$$FUN4S(T) = 0.90198(10^{-2}) + 0.26335(10^{-5})T + 0.18949(10^{-7})T^{2} - 0.74192(10^{-11})T^{3} + 0.98676(10^{-15})T^{4} \quad (370)$$

The conductivity of the products of combustion of a gas mixture at any intermediate equivalence ratio, ER, for the 20-atmosphere pressure gas is:

$$XKM2 = FUNA2 + ER^{1.0512} (FUNS2 - FUNSA) \quad (371)$$

and the conductivity at any intermediate equivalence ratio for the 40-atmosphere pressure gas is:

$$XKM4 = FUN4A + ER^{1.1163} (FUN4S - FUN4A) \quad (372)$$

The conductivity of the 20- and 40-atmosphere pressure mixtures are used to define the conductivity at any other pressure. If the pressure is below 20 atmospheres:

$$XKM = XKM2 + \left(\frac{ATM-20}{20}\right) \cdot (XKM4 - XKM2) \quad (373$$

but if the pressure is above 20 atmospheres:

$$XKM = XKM2 + \left(\frac{ATM-20}{20}\right)^{0.65896} \cdot (XKM4 - XKM2) \quad (374)$$

The dimension on the conductivity is Btu/hr-ft-°F and the dimension on the viscosity is lb/hr-ft.

9.0 COOLING FLOW RATE PREDICTION

9.1 INTRODUCTION

The WCFLOW module defines the cooling airflow. The cooling airflow is presented not as a single value but, rather, as a matrix of cooling airflows and corresponding average metal temperatures. This approach is necessary since the mission objectives, in terms of life cycle costs and bulk metal temperature, can not be defined at this point in the Turbine Design System.

The WCFLOW cooling airflow estimation module uses the output of HTCOEF, which defines the blade row heat load. The output from FLOPTH and CASC are also used to define the heat transfer surface area.

Several different heat transfer technology levels can be used when defining the cooling airflow/bulk temperature matrix. This allows a complete life cycle cost analysis to be made early in the preliminary design of the turbine.

9.2 TECHNICAL BACKGROUND

High performance jet engines having turbine inlet temperatures which exceed allowable metal temperatures by 500° to 1000° F require a detailed thermal analysis of the turbine. The engine performance is sensitive to coolant airflows required to cool components down to levels which yield the desired hardware life. A compromise between meeting engine performance and hardware life must be made. The tradeoff is difficult and time consuming by conventional methods. Although over-simplified parametric curves may be generated to help define the required cooling airflow for a particular application, a reasonable answer is not achievable until after a detailed design has been made. Thus, the need for a program to calculate the cooling airflow to a blade was identified. WCFLOW uses the heat load on the blade along with the cooling air temperature to calculate the bulk metal temperature.

The bulk metal temperature of the blade cross section is evaluated by first specifying the heat transfer technology level of the cooling system being considered along with the quantity of film that will cover the surface of the airfoil. There are five technology levels to choose from:

1. Simple Convection - e.g., radial hole, single pass.
2. Production Convection - e.g., serpentine passages with turbulence promoters for heat transfer augmentation, and possible single row impingement at the leading edge.
3. Advanced Convection - e.g., impingement baffles with a configuration of multiple rows of small cooling jets.

4. Production Convection with Film - e.g., internal cooling geometry the same as (2) above but with some of the flow ejected on the airfoil surface for film cooling.

5. Advanced Convection with Film - e.g., internal cooling geometry the same as (3) above but with some of the coolant flow ejected on the airflow.

An intermediate film technology level between local film coverage and full film coverage can be accounted for using an additional input. More than one heat transfer technology level can be considered if there is some question as to which to use.

9.3 PROGRAM OUTLINE

The program starts with the definition of the inlet conditions for which the turbine is being designed. The relative blade row inlet "design to" temperature T1 is listed along with the five heat transfer technology levels. The designer then chooses one technology level to be evaluated. The average heat load which was calculated in HTCOEF is listed for the designer's reference. This value can be used or changed. The wall conductivity and thickness are input by the designer after which the blade cross-sectional bulk metal temprature, cooling effectiveness, flow area, and average film effectiveness are presented for each cooling flow rate. This process can be repeated for any other heat transfer technology level.

The programming code is accomplished by treating the blade as a heat exchanger and then defining the overall conductance of the blade. The airflow through the blade, along with the inlet temperature, can be used to establish the cooling airflow exit temperature and, hence, total heat flux to the blade. With the heat flux and wall thickness, the average bulk metal temperature is calculated. Subroutine SIMPLE calculates the bulk metal temperature of a blade without film, and subroutine CONVEC calculates the bulk metal temperature of a film/convection design. The required cooling airflow area in the blade cross section is also calculated using the input value of cooling air pressure and blade row inlet gas stream relative total pressure. This cooling airflow area is then subtracted from the blade cross-sectional area to determine the metal cross-sectional area that is available to handle the mechanical loads.

The bulk cooling effectiveness and average film cooling effectiveness are also printed as a reference when comparing with other designs.

9.4 OVERALL CONDUCTANCE CALCULATION

The calculation procedure starts with the definition of all the necessary peripheral information. This information is then used to calculate the bulk cooling effectiveness.

The calculations start with evaluation of the conductivity of the metal, the wall thickness, and the surface area to give the conduction resistance of the blade wall:

$$DXKA = \frac{12 \cdot DELTX}{COND \cdot (XLSS + XLPS)\ (RTIP - RHUB)} \qquad (375)$$

where:

COND = Average conductivity of the metal in (Btu/hr-ft-° F)

XLSS = Suction side length of the airfoil from the leading edge stagnation point along the surface to the trailing edge (in.)

XLPS = Pressure side length of the airfoil from the leading edge stagnation point along surface to the trailing edge (in.)

RTIP = Radius of the tip section of the airfoil, defined at the airfoil trailing edge (in.)

RHUB = Radius of the hub section of the airfoil, defined at the airfoil trailing edge (in.)

DELTX = Average wall thickness from the outside surface to the closest edge of the cooling circuit (in.)

The heat load on the outside surface of the blade is defined by the input HEAT FLUX/INCH OF AIRFOIL HEIGHT and the blade height.

$$HGAGCA = HGAGIN \cdot (RTIP - RHUB) \qquad (376)$$

The cooling air side boundary conditions are calculated first by taking the input coolant air temperature and defining the properties of the air. These properties include specific heat, CPC, and ratio of specific heats, GAM:

$$CPC = 0.2323 + 3.0333 \cdot 10^{-5}\ TCPICH \qquad (377)$$

and:

$$GAM = 1.410 - 5.666 \times 10^{-5}\ TCPICH \tag{378}$$

where TCPICH is the cooling air temperature (° F) at the airfoil midspan before any convection cooling temperature rise has been added. The average isentropic Mach number in the cooling passage is calculated by:

$$COOLMO = SQRT\left[\frac{22}{(GAM - 1)}\left\{\left(\frac{PCPICH}{P1}\right)^{\left(\frac{GAM-1}{GAM}\right)} - 1\right\}\right] \tag{379}$$

where:

PCPICH = Input cooling air pressure (psia) at the airfoil midspan before any losses are incurred in cooling

P1 = Gas stream relative total pressure at the blade row inlet midspan location (psia)

The cooling airflow WCWG(I) is input as a percent of turbine inlet flow WGAS which is the first stage nozzle inlet gas flow. The product of specific heat and cooling airflow to each blade is then defined as:

$$WCPCBD(I) = \frac{WC(I) \cdot CPC}{FLOAT\ (NBLDS)} \tag{380}$$

where:

$$WC(I) = \frac{WCWG(I)}{100} \cdot WGAS \tag{381}$$

which is the coolant flow to the blade row (lb/sec).

FLOAT (NBLDS) = Number of airfoils in the blade row in floating point mode.

The cooling air heat load is defined by the product of the coolant side average heat transfer coefficient and the effective cooling surface area.

$$HCAC(I) = CAPK \cdot [3600 \cdot WCPCBD(I)] \cdot FINN \qquad (382)$$

where CAPK is a generalized parameter that defines the cooling technology:

	CAPK
Simple Convection (radial hole)	0.6
Production Convection (serpentine cast impingement hole, turbulence promoter)	0.8
Advanced Convection (impingement baffle, fabricated cooling circuit with small impingement holes)	1.0

FINN is the parameter that takes into account the fin effectiveness of ribs that might exist in the blade.

$$FINN = 2.5 \frac{TANH\ (PARAM)}{PARAM} \qquad (383)$$

where

$$PARAM = 3 \cdot DELTX \cdot SQRT \left(\frac{HGAS}{6 \cdot COND \cdot DELTX} \right) \qquad (384)$$

and where HGAS is the average gas side heat transfer coefficient, defined by:

$$HGAS = \left(\frac{HGAGIN \cdot 144}{XLSS + XLPS} \right) \qquad (385)$$

With equations (375), (376), and (382), the overall conductance, UA, can be defined:

$$UA(I) = \frac{1}{\left(\frac{1}{HGAGCA} + DXKA + \frac{1}{HCAC(I)} \right)} \qquad (386)$$

The overall conductance can be used to define the heat flux on a plain convection cooling system or convection/film cooling system.

9.5 SUBROUTINE SIMPLE

This subroutine calculates the bulk metal temperature for an airfoil cooling system that has no film.

$$CAPY = EXP\left(\frac{UAC}{3600 \cdot WCPC}\right) \tag{387}$$

where:

UAC = Overall conductance (Btu/hr-° F)

WCPC = Product of airfoil coolant flow and specific heat (Btu/sec ° F)

This defines the heat exchanger effectiveness which is then used to calculate the cooling air temperature leaving the airfoil, TCO.

$$TCO = T1 - \left(\frac{T1 - TCPICH}{CAPY}\right) \tag{388}$$

where T1 is the relative gas temperature at the inlet to the blade row and is defined by taking the highest value of the radial temperature profile.

The average cooling air temperature is then used to define the specific heat, CPCN:

$$CPCN = 0.2323 + 3.0333 \cdot 10^{-5}\ TCA \tag{389}$$

where:

$$TCA = \frac{TCO + TCPICH}{2} \tag{390}$$

The total heat flux to the airfoil, CAPQUE, is thus calculated by using the specific heat, the weight flow per airfoil, and the cooling air temperature rise:

$$CAPQUE = 3600 \cdot \frac{CPCN}{CPC} \cdot WCPC \cdot (TCO - TCPICH) \tag{391}$$

The specific heat is corrected to reflect the average coolant temperature rather than the inlet temperature.

The total heat flux is now used in conjunction with the gas temperature T1, the gas side heat transfer, and conduction factors to yield a bulk metal temperature, BULKT:

$$\text{BULKT} = \text{T1} - \text{CAPQUE}\left(\frac{1}{\text{HGAGCA}} + \frac{\text{DXKA} \cdot \text{FINN}}{2}\right) \tag{392}$$

This bulk metal temperature can be used to determine the mechanical life of the turbine component being considered.

9.6 SUBROUTINE CONVEC

This subroutine calculates the bulk metal temperature for an airfoil cooling scheme which incorporates film cooling. Two film cooling technologies are input into the program which represent General Electric Company experience. The lower film effectiveness technology represents local film injection such as at the leading edge and the suction and pressure gill locations. The higher technology level represents the average film effectiveness that might be achieved in a full-coverage film cooling design. It is assumed that 40 percent of the cooling air is used for film in the lower film technology design and 70 percent in the higher technology design. Any other film cooling technology level can be accommodated by use of PCTDIF. This represents the percentage difference between local film cooling technology flow rate and full-coverage film flow rate. Thus, the fraction of the cooling air used for film cooling is:

$$\text{WCFWC} = 0.4 + \frac{\text{PCTDIF}}{100} \cdot 0.3 \tag{393}$$

The fraction of the gas stream flow that is then used for film is defined as WCFWG:

$$\text{WCFWG} = \text{WCFWC} \cdot \frac{\text{WCWG1}}{100} \tag{394}$$

where WCWG1 is the blade row cooling airflow expressed as a percentage of the turbine inlet gas flow.

The film cooling correlation parameter CAPP is defined as:

$$\text{CAPP} = \frac{420 \cdot \text{WCFWG} \cdot \text{PICH} \cdot [\cos(\text{BETA1}) + \cos(\text{BETA2})]}{(\text{XLSS} + \text{XLPS})} \tag{395}$$

where:

BETA1 = Blade row inlet relative flow angle measured from the axial direction (degrees)

BETA2 = Blade row exit relative flow angle measured from the axial direction (degrees)

PICH = Blade-to-blade midspan spacing (inches)

A linear interpolation function of two film curves (ETALO and ETAHI) is used to determine the average film effectiveness for both local film injection and full-coverage film injection. The average film effectiveness for the design in question can then be calculated with the use of PCTDIF.

$$\text{FLMETA} = \text{ETALO} + \frac{\text{PCTDIF}}{100} \cdot (\text{ETAHI} - \text{ETALO}) \tag{396}$$

The heat exchanger effectiveness can now be calculated by:

$$\text{CAPY} = (1 - \text{FLMETA}) \cdot \text{EXP}\left(\frac{\text{UAC}}{3600 \cdot \text{WCPC}}\right) \tag{397}$$

The average film temperature, TFILM, can be calculated with the use of equations (396) and (397):

$$\text{TFILM} = \frac{\text{FLMETA} \cdot \text{TCPICH} + \text{CAPY} \cdot \text{T1}}{\text{FLMETA} + \text{CAPY}} \tag{398}$$

This film temperature, along with the average film effectiveness, gas stream temperature, and inlet cooling air temperature, is used to calculate the cooling air temperature leaving the blade:

$$\text{TCO} = \text{T1} - \frac{(\text{T1} - \text{TFILM})}{\text{FLMETA}} \tag{399}$$

Once again, equations (389) and (390) are used to calculate the average specific heat CPCN of the cooling air in the blade. Equation (391) is then used to determine the total heat load CAPQUE to the blade, and the blade cross section bulk metal temperature is evaluated:

$$\text{BULKT} = \text{TFILM} - \text{CAPQUE}\left(\frac{1}{\text{HGAGCA}} + \frac{\text{DXKA} \cdot \text{FINN}}{2}\right) \tag{400}$$

The blade cross-section bulk metal temperature can be used to determine the mechanical life of the turbine component being considered.

9.7 OUTPUT DEFINITION

Besides the blade cross section bulk metal temperature, other parameters are calculated which are either used in the calculation of the mechanical life or listed as reference information. The blade cross section bulk cooling effectiveness is defined for each cooling airflow rate:

$$\text{ETABLK(I)} = \frac{\text{T1 - TBULK(I)}}{\text{T1 - TCPICH}} \tag{401}$$

This is used in comparing one design to another at different coolant and gas stream temperature conditions. The blade cross section area that is required for coolant airflow and hence is not available to handle blade mechanical loads is defined as ACMIN(I):

$$\text{ACMIN(I)} = \frac{2 \cdot \text{WCBLD(I)}}{\text{PCPICH}} \cdot \frac{\text{SQRT [53.35 } \cdot \text{ (TCPICH + 460]}}{ff} \tag{402}$$

where ff is the isentropic flow function and is defined as:

$$ff = \frac{\text{COOLMO } \cdot \text{ SQRT (GAM } \cdot \text{ 32.17)}}{\left(1 + \frac{\text{GAM - 1}}{2} \cdot \text{COOLMO}^2\right)^{\text{(GAM+1)/2 (GAM-1)}}} \tag{403}$$

The cooling air isentropic Mach number COOLMO is calculated using equation (379), and the ratio of specific heats GAM is calculated by equation (378). The blade row inlet relative gas pressure and blade midspan relative cooling air pressure are used to determine the isentropic Mach number. The isentropic flow area is doubled to give ACMIN(I), which is the required flow area to circulate the air through the blade while cooling it.

The film cooling effectiveness for a convection/film cooled design is also printed for reference so that a comparison with experience can be made.

10.0 AIRFOIL PROPERTIES

10.1 INTRODUCTION

The AFPROP module calculates the section properties of an airfoil cross section with cooling hole passages. Specifically, this program will take the coordinate points which describe the airfoil contour and calculate the cross sectional area, the minimum moment of inertia, the maximum moment of inertia, the location of the centroid, and the angle from the axial direction to the minimum moment of inertia axis. If the shapes of the interior cooling passages have not been previously defined, circular or rectangular passages can be added during program execution.

10.2 AIRFOIL CONTOUR DEFINITION

The airfoil contour is described in a clockwise manner by up to one hundred pairs of X and Y values. The last pair of X and Y values must represent the same point as the first pair of X and Y values. X and Y are taken to be positive in the axial and tangential directions, respectively.

10.3 COOLING PASSAGE DEFINITION

Like the outer airfoil contour, the contour of each cooling passage is described by pairs of X and Y coordinates. These coordinates, however, must be given in a counterclockwise manner and must be limited in number to twenty-five or less. The last pair of X and Y values must be a repetition of the first pair. Any airfoil may have as many as ten cooling passages.

If the user so wishes, circular or rectangular cooling passages can be added by the program. To add a circular passage, the X and Y coordinates of the passage center are specified along with the radius of the passage. The AFPROP module will then determine twenty-five equally spaced coordinate pairs describing the passage in a counterclockwise manner.

To add a rectangular passage, the X and Y coordinates of the passage center are specified along with the length and width of the passage as well as the angle between the X axis and the orientation axis of the rectangle. Figure 37 shows this geometry. The AFPROP module will then determine the coordinate pairs of the four corners.

10.4 AREA, CENTROID, AND MOMENT OF INERTIA CALCULATIONS

Once the contour of the airfoil section has been defined in terms of X and Y coordinate pairs, the section properties are calculated. As is shown in Figure 38, a trapezoidal element is the building block of these calculations.

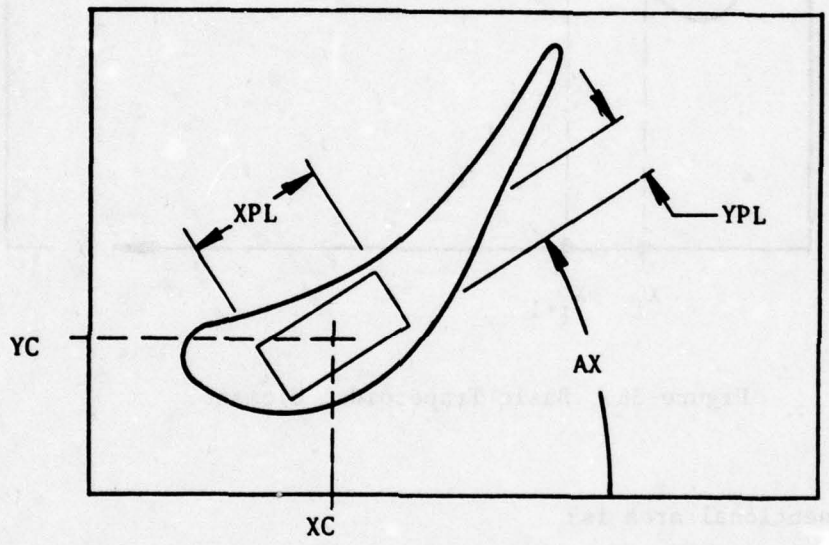

Figure 37. Rectangular Cooling Passage.

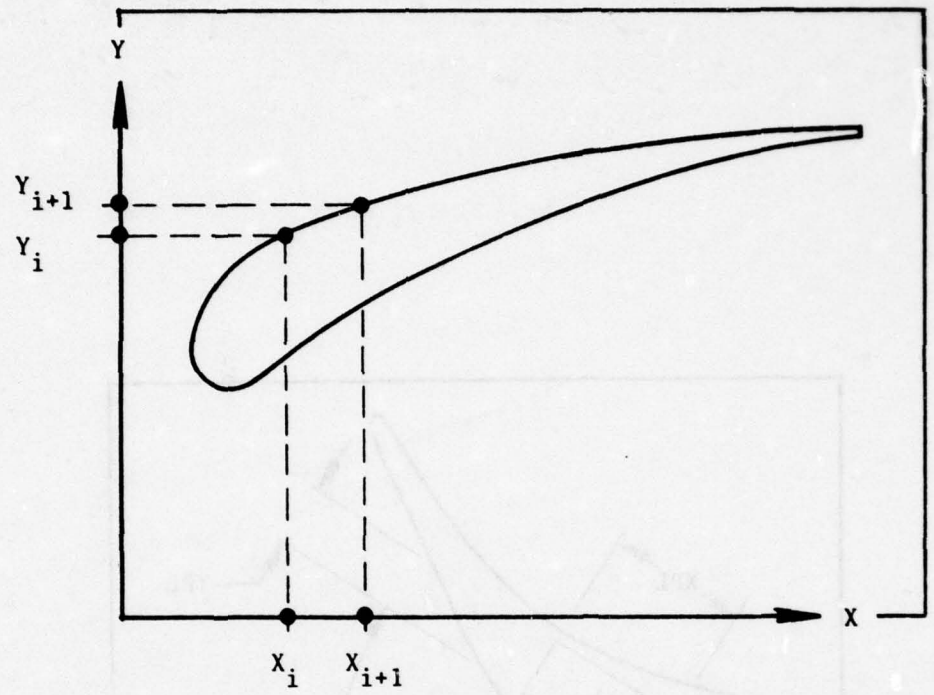

Figure 38. Basic Trapezoidal Element.

The cross-sectional area is:

$$A = \sum_{i=1}^{N} A_i \tag{404}$$

The center of gravity is at:

$$\bar{X} = \frac{\sum_{i=1}^{N} A_i \bar{X}_i}{A} \tag{405}$$

$$\bar{Y} = \frac{\sum_{i=1}^{N} A_i \bar{Y}_i}{A} \tag{406}$$

The moments of inertia about the centroidal axial and tangential axes are:

$$I_{AA} = \sum_{i=1}^{N} I_{XX_i} - A\bar{Y}^2 \tag{407}$$

$$I_{TT} = \sum_{i=1}^{N} I_{YY_i} - A\bar{X}^2 \tag{408}$$

The product of inertia is:

$$I_{AT} = \sum_{i=1}^{N} I_{XY_i} - A\overline{XY} \tag{409}$$

The angle, in radians, from the axial axis to the least moment of inertia axis is:

$$\alpha = \frac{1}{2}\left[\pi + \tan^{-1}\left(\frac{2\ I_{AT}}{I_{TT} - I_{AA}}\right)\right] \tag{410}$$

The least moment of inertia is:

$$I_{min.} = \frac{I_{AA} + I_{TT}}{2} + \frac{I_{AA} - I_{TT}}{2} \cos(\alpha) - I_{AT} \sin(\alpha) \tag{411}$$

10.5 DETERMINING THE STRESS CALCULATION POINTS

This module will determine the location of three points on the airfoil outer contour at which stresses will be calculated by the ASTRES module. Figure 39 shows these points on a typical airfoil section with its principal axes.

Point 1 is that point near the trailing edge which is the farthest from the least moment of inertia axis. Point 2 is that point on the suction surface which is the farthest from the least moment of inertia axis. Point 3 is that point near the leading edge which is the farthest from the least moment of inertia axis.

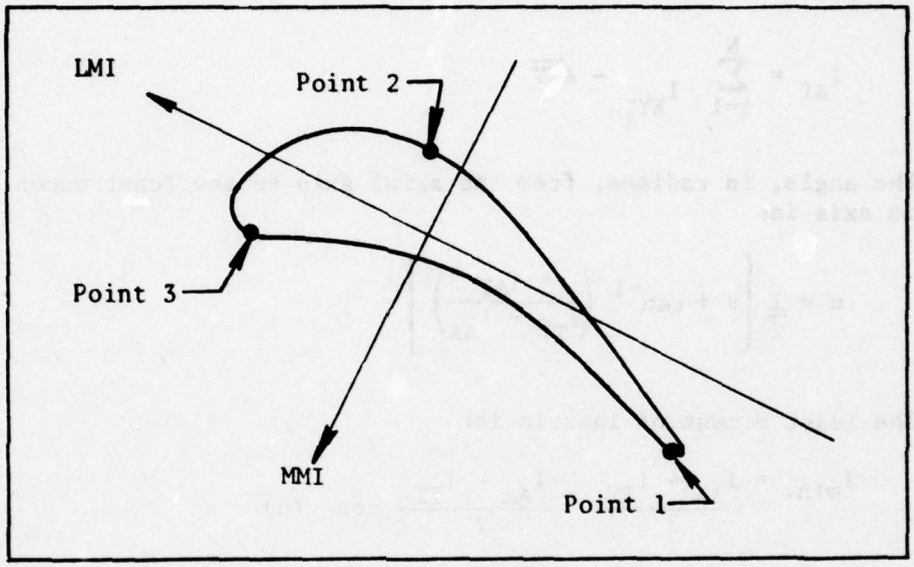

Figure 39. Stress Calculation Points.

11.0 AIRFOIL STRESS

11.1 INTRODUCTION

The ASTRES module calculates the stress present in the airfoil section of a turbine blade or vane. If a blade is being analyzed, the user specifies the allowable stress at the root, pitch, and break point, and the program will calculate the required airfoil areas at these locations. Capability exists to account for the presence of a tip shroud. If a vane is being analyzed, the user will input the boundary conditions, and the module will calculate the stress due to the gas load. This program will also make preliminary calculations as to the amount of vane ballooning.

At the time that the ASTRES module is executed, the actual operating temperature of the blade or vane is not known. Thus it is not possible to accurately know the value of the elastic modulus, since it decreases with temperature. The elastic modulus, in turn, controls the magnitude of deflections which then vary with temperature; thus, this module will not calculate deflections. Instead, values of strain will be calculated at the temperatures for which material properties are given.

11.2 BLADE STRESS CALCULATIONS

If the airfoil being analyzed is a turbine blade, a calculation of the centrifugal stress will be made. The input file to the module contains the user-specified values of the stress at the root, pitch, and break point. If a tip shroud is to be used, the input file will contain its weight as well as the radius of its center of gravity.

The radius of the break point is found by moving radially inward from the tip, with the cross-sectional area remaining constant, until reaching the radius at which the centrifugal stress is equal to the specified value. Between the break point and the pitch, the cross-sectional area varies linearly. The pitch area is calculated so that the stress at the pitch is equal to the specified value. Between the pitch and the root, the airfoil cross-sectional area varies linearly. The area of the root is calculated so that the centrifugal stress at the root is equal to the specified value.

11.3 VANE BENDING STRESS CALCULATIONS

The stress experienced by a turbine vane is primarily due to the gas load on that vane. This module will make an approximate calculation of this stress in the following manner.

The AFPROP module calculated the section properties for the pitch section of the vane. For a bending analysis, however, the section properties

must be known all along the length of the vane. These properties will be approximated by scaling the pitch section properties.

$$I_{min.,i} = I_{min.,p} \, (T_i/T_p)^3 \, (C_i/C_p) \tag{412}$$

where: T_i = maximum thickness at the ith section

C_i = chord at the ith section

$$I_{max.,i} = I_{max.,p} \, (C_i/C_p)^3 \, (T_i/T_p) \tag{413}$$

$$A_i = A_p \, (C_i/C_p) \, (T_i/T_p) \tag{414}$$

The aerodynamic portion of TDS determined the gas loading as components in the axial and tangential directions. A bending analysis is performed separately for each of these directions. The moments of inertia are transformed to moments of inertia about the axial and tangential axes. Between each of the radial spanwise locations is modeled a beam having properties equal to the average of the properties at each of its ends. The gas loading is also averaged along this beam. Ten beams constitute the entire vane the ends of which can have any boundary conditions desired. These ten beams and their respective loads undergo a finite element analysis which results in a listing of the external forces on each member. Following this is a table of the radial stress at each of the three contour points at each of the eleven spanwise locations.

11.4 VANE BALLOONING CALCULATIONS

In preparation for the vane ballooning time calculations of the MISLIF module, the ASTRES module calculates the elastic deformation as well as the effective stress at the center of the panel experiencing the ballooning. Since the actual temperature of the panel is not yet known, the deflection will be calculated at each temperature for which material properties have been supplied. The panel is modeled as a plate, fixed on all four sides, with a uniform pressure on its surface. The length of the panel is equal to the span of the vane while the width is input by the user along with the pressure difference and panel thickness.

12.0 MISSION LIFE

12.1 INTRODUCTION

The MISLIF module calculates the life of a turbine airfoil subjected to a specific mission. The heart of the module is a relatively simple rupture damage, but to execute this calculation, much conditioning of the data supplied by other modules must be done. The module also performs several auxiliary calculations such as vibratory allowable stresses and vane ballooning.

12.2 DEFINITIONS

Life is synonomous with stress rupture life. It is expressed in hours of mission operation.

Damage or rupture damage is time on mission leg divided by rupture life at mission leg conditions. Damage multiplied by 100 is the percent life used per mission leg. Damage is also used to mean accumulated damage.

Mission Leg is a steady-state operating condition that is present during some portion of an aircraft flight (e.g., takeoff, climb, etc.).

Accumulated Damage is the value that results from summing the damage for each mission leg.

Stress is the physical load per unit area as seen by microscopic elements of material.

Pseudostress is the stress that would result in a part if no yielding of the material could occur. Below the material's yield point, pseudostress and stress are identical.

12.3 MISSION RUPTURE LIFE CALCULATIONS

MISLIF is dimensioned to do a damage calculation for

- 11 airfoil locations
- 6 different cooling flow values
- 7 different cooling technology levels

or 462 values of damage. If more than one mission leg is involved, the damage accumulated for each leg by technology level, cooling flow, and location is

$$\text{Accumulated Damage} = \sum_{\#\ \text{Legs}} \text{Damage on Leg} \tag{415}$$

This is based on Miner's Rule of Damage Accumulation. To perform damage calculations, one needs:

- Temperature
- Stress
- Length of time on leg

12.4 TEMPERATURE SCALING

From the heat transfer modules, the following are known:

- Gas temperature distributions
- Corresponding T_3 and T_4
- Zeta factor for use on vanes
- Pitch section metal temperatures

$$\text{ZETA} = \frac{T_{Gas} - T_{Avg}}{T_{Peak} - T_{Avg}} \tag{416}$$

where: T_{Gas} = actual gas temperature

T_{Avg} = average gas temperature

T_{Peak} = peak gas temperature

If ZETA = 1.0, the gas peak temperature profile is chosen to be the actual gas temperature profile.

If ZETA = 0, the gas average temperature profile is chosen to be the actual gas temperature profile.

Solving equation (416) for the actual gas temperature profile yields:

$$T_{Gas} = T_{Avg} + \text{ZETA}\,[T_{Peak} - T_{Avg}] \tag{417}$$

The gas profile temperature effectiveness is calculated to be:

$$\eta_{GP} = \frac{T_4 - T_{Gas}}{T_4 - T_3} \qquad \text{for a vane} \qquad (418)$$

and:

$$\eta_{GP} = \frac{T_4 - T_{TB}}{T_4 - T_3} \qquad \text{for a blade} \qquad (419)$$

where T_{TB} is the blade row inlet relative gas temperature.

The WCFLOW module determined the average bulk metal temperature at the pitch, T_{BULKP}. The pitch metal temperature effectiveness is:

$$\eta_M = \frac{T_{Gas} - T_{BULKP}}{T_{Gas} - T_3} \qquad (420)$$

This value is assumed to remain constant along the span of the airfoil. With these calculations accomplished, the module can now calculate metal temperatures for any mission leg, cooling flow, technology level, or airfoil section:

$$T_{Gas} = T_4 - \eta_{GP} [T_4 - T_3] \qquad (421)$$

$$T_{Bulk} = T_{Gas} - \eta_M [T_{Gas} - T_3] \qquad (422)$$

If the airfoil is uncooled, the metal temperature is the same as the gas temperature.

12.5 STRESS SCALING

The ASTRES module calculated stresses in an airfoil only for the design point of the turbine. If the mission profile consists of operating points at other than the design point, the stresses at these points must be scaled from the known values. The stresses in a vane are scaled by the ratio of turbine inlet total pressures, while the stresses in a blade are scaled by the ratio of the shaft speeds squared.

These stresses can be increased, by an amount specified by the user, so as to allow for a factor of safety.

Airfoil Type	Factor
Vanes	1.0
Uncooled Blades	1.0
Simple Blade Cooling (No Film)	1.1
Highly Cooled Blades	1.3

12.6 THE YIELD SUBROUTINE

The stress which was determined above could be above the yield point of the material and therefore unsuitable for rupture calculations on vanes. This subroutine is provided to handle this situation.

A stress-strain curve can be approximated on a log-log plot by two straight lines:

$$\sigma = E\,\varepsilon \qquad \text{elastic range} \qquad (423)$$

$$\sigma = C\,\varepsilon^{N} \qquad \text{plastic range} \qquad (424)$$

With two plastic points known, the constants in equation (424) can be determined. The intercept of these two lines is the proportional limit. If the stress in the vane is above the proportional limit, the strain is solved for in equation (423) and substituted into (424).

12.7 DAMAGE AND RUPTURE LIFE CALCULATIONS

For given values of stress and temperature, the module calculates the corresponding Larson-Miller parameter based upon the data in the material data file. The life on any given mission leg is then determined. The life of the airfoil undergoing a number of mission legs is equal to the duration of the mission divided by the sum of the fractions of life used on each mission leg.

12.8 BLADE ALLOWABLE VIBRATORY STRESSES

For a turbine blade, MISLIF will calculate the amount of vibratory stress permissible in the airfoil. This calculation is carried out at the root as well as the spanwise location with the lowest life. The mean stress is considered to be equal to the centrifugal stress. From the material data file, the corresponding values of the single-amplitude alternating stress are determined. If the mean stress is greater than the highest value in the data file, the allowable vibratory stress is set equal to zero.

12.9 VANE BALLOONING ANALYSIS

Cooled turbine vanes are pressure vessels. If a thin-wall panel gets too large, it may creep and bulge under the influence of pressure. This phenomenon is called ballooning.

Under the influence of internal pressure, an elastic deformation, δ_e, occurs at the center of the panel along with an elastic strain, ε_e, and a stress, σ. This analysis makes the assumption that the shape of the deflection does not change as inelastic deformation takes place. If δ_p is the plastic deflection, then:

$$\frac{\delta_p}{\varepsilon_p} = \frac{\delta_e}{\varepsilon_e} \tag{425}$$

The elastic strain and elastic deflection are readily determined by plate theory. Thus if ε_p, as a function of time, can be determined, the plastic deflection will be known. Test data have shown that if pressure is applied to the panel, the stress at the center of the panel will not remain constant but will decrease slightly with time as the panel deforms plastically. With the creep data from the material data file, the module can determine how long it takes for the panel to reach a certain amount of plastic deformation at any given temperature.

13.0 INTEGRATED DATA BASE

13.1 INTRODUCTION

This section serves to explain the purpose and usages of the integrated data base system set up for use with the CDC 6600. A look at the glossary of terms in Section 13.8 may prove helpful. The integrated data base (IDB) is a vehicle for storage and communication of data from many disciplines and many activities on a common ground using a common language. The purpose is to aid the exchange of information used in the design, development, and production of jet engines.

Information normally communicated by paper, which has multidiscipline or multiple user application, may be stored and communicated within the data base. Users from all disciplines and functions, with a need-to-know, may access the data from the base.

13.2 DATA BASE STRUCTURE

The IDB is actually a set of three indexed sequential files. The CDC Record Manager was found to be sophisticated with a flexible structure and flexible data content. The first of the three files contains the list of valid 10-character keys. A set of keys, arranged in a string of six levels, establishes a category or structure under which data can be stored. A blank is a valid key at any level. An abbreviated, yet still unique, numeric key string is generated from the longer alphanumeric string. This string points to a location on the second file which contains the names of the data sets associated with each key structure and their starting locations on the third file where the actual data values are stored.

13.3 DATA BASE FUNCTIONS

The current functions available to the general user are the abilities to store data onto the data base and to retrieve it after it has been stored. A third function, which necessarily precedes the other two, is the initialization of the data base itself.

Data are stored on the data base as a NAMELIST set. This convention is compatible with many present computer programs, especially in the scientific area. Data within the namelist set is identified by variable name. The variables may be scalar or dimensioned. Typing of variables is done according to the FORTRAN convention (I-N are integer, others are real) with the exception that Q-variables are alphanumeric (comments, etc.).

13.4 SECURITY FOR THE DATA BASE

Two passwords are assigned to each namelist as it is stored on the base. Knowledge of the READ password allows a user to access the data for a namelist.

Knowledge of both the READ and WRITE passwords allows a user to edit data for a namelist or add data to the data base. Normally, unsensitive data would be passworded rather loosely; for example, the passwords for namelists for a component, or perhaps an entire engine, could be the same.

The presence of data and its READ password are disseminated on a need-to-know basis. The WRITE password is an item of information which is not disseminated.

13.5 BATCH FUNCTIONS

Three operations can be performed in the batch mode. They are the initialization of the data base files, along with the loading of the master keys; the transfer of data from a buffer file to the IDB; and the retrieval from the IDB to a buffer file.

13.5.1 Initialization of the Data Base

Initialization consists of establishing the three data base files as indexed sequential with the proper file descriptions and loading the master keys onto the first file. The initialization for all three files is only run once. However, if new keys are added to the master list, the key file can be reinitialized and reloaded without disturbing the other two files.

Following are the control card setup to run the initialization and a listing of the key-tree file.

```
COMMAND- FETCH,INITCC,LJKUES

COMMAND- EDITOR

..
YOU HAVE AN EXISTING EDIT FILE
EDIT,INITCC

..L,A

    100=TDS,T20,I050,CMI25000,SICSA. P750587,KUES,X3153
    110=ATTACH,INITDB,INITHS,ID=P750587.
    120=REQUEST,D0,*PF.
    130=REQUEST,D1,*PF.
    140=REQUEST,D2,*PF.
    170=ATTACH,STAPE5,TDSKEYS,ID=LJKUES.
    180=COPYBF(STAPE5,TAPE5)
    190=REWIND(TAPE5)
    220=RFL(60000)
    230=INITDB.
    250=CATALOG,D0,DBFILS,CY=1,RP=365.
    260=CATALOG,D1,DBFILS,CY=2,RP=365.
    270=CATALOG,D2,DBFILS,CY=3,RP=365.
    271=*EOR
    272=*EOF
    273=*EOF
..B

COMMAND- BATCH,INITCC,INPUT,HERE

COMMAND-
```

```
FETCH,TDSKEYS,LJKUES
..EDIT,TDSKEYS
..L,A

1000= $K
1010= KEYA(001)="HPTURB      ",
1020= KEYA(003)="LPTURB      ",
1030= KEYA(005)="            ",
1040= KEYA(007)="FLOPTH      ",
1050= KEYA(009)="VANE01      ",
1060= KEYA(011)="VANE02      ",
1070= KEYA(013)="VANE03      ",
1080= KEYA(015)="VANE04      ",
1090= KEYA(017)="VANE05      ",
1100= KEYA(019)="VANE06      ",
1110= KEYA(021)="VANE07      ",
1120= KEYA(023)="VANE08      ",
1130= KEYA(025)="VANE09      ",
1140= KEYA(027)="VANE10      ",
1150= KEYA(029)="BLAD01      ",
1160= KEYA(031)="BLAD02      ",
1170= KEYA(033)="BLAD03      ",
1180= KEYA(035)="BLAD04      ",
1190= KEYA(037)="BLAD05      ",
1200= KEYA(039)="BLAD06      ",
1210= KEYA(041)="BLAD07      ",
1220= KEYA(043)="BLAD08      ",
1230= KEYA(045)="BLAD09      ",
1240= KEYA(047)="BLAD10      ",
1250= KEYA(049)="            ",
1260= KEYA(051)="DSEC01      ",
1270= KEYA(053)="DSEC02      ",
1280= KEYA(055)="DSEC03      ",
1290= KEYA(057)="ISEC01      ",
1300= KEYA(059)="ISEC02      ",
1310= KEYA(061)="ISEC03      ",
1320= KEYA(063)="ISEC04      ",
1330= KEYA(065)="ISEC05      ",
1340= KEYA(067)="ISEC06      ",
1350= KEYA(069)="ISEC07      ",
1360= KEYA(071)="ISEC08      ",
1370= KEYA(073)="ISEC09      ",
1380= KEYA(075)="ISEC10      ",
1390= KEYA(077)="ISEC11      ",
1400= KEYA(079)="STA011      ",
1410= KEYA(081)="STA012      ",
1420= KEYA(083)="STA013      ",
1430= KEYA(085)="STA014      ",
1440= KEYA(087)="STA021      ",
```

```
1450= KEYA(089)="STA022          ",
1460= KEYA(091)="STA023          ",
1470= KEYA(093)="STA024          ",
1480= KEYA(095)="STA031          ",
1490= KEYA(097)="STA032          ",
1500= KEYA(099)="STA033          ",
1510= KEYA(101)="STA034          ",
1520= KEYA(103)="STA041          ",
1530= KEYA(105)="STA042          ",
1540= KEYA(107)="STA043          ",
1550= KEYA(109)="STA044          ",
1560= KEYA(111)="STA051          ",
1570= KEYA(113)="STA052          ",
1580= KEYA(115)="STA053          ",
1590= KEYA(117)="STA054          ",
1600= KEYA(119)="STA061          ",
1610= KEYA(121)="STA062          ",
1620= KEYA(123)="STA063          ",
1630= KEYA(125)="STA064          ",
1640= KEYA(127)="STA071          ",
1650= KEYA(129)="STA072          ",
1660= KEYA(131)="STA073          ",
1670= KEYA(133)="STA074          ",
1680= KEYA(135)="STA081          ",
1690= KEYA(137)="STA082          ",
1700= KEYA(139)="STA083          ",
1710= KEYA(141)="STA084          ",
1720= KEYA(143)="STA091          ",
1730= KEYA(145)="STA092          ",
1740= KEYA(147)="STA093          ",
1750= KEYA(149)="STA094          ",
1760= KEYA(151)="STA101          ",
1770= KEYA(153)="STA102          ",
1780= KEYA(155)="STA103          ",
1790= KEYA(157)="STA104          ",
1800= KEYA(159)="                ",
1810= KEYA(161)="VERS01          ",
1820= KEYA(163)="VERS02          ",
1830= KEYA(165)="VERS03          ",
1840= KEYA(167)="VERS04          ",
1850= KEYA(169)="VERS05          ",
1860= KEYA(171)="VERS06          ",
1870= KEYA(173)="VERS07          ",
1880= KEYA(175)="VERS08          ",
1890= KEYA(177)="VERS09          ",
1900= KEYA(179)="VERS10          ",
1910= KEYA(181)="VERS11          ",
1920= KEYA(183)="VERS12          ",
1930= KEYA(185)="VERS13          ",
1940= KEYA(187)="VERS14          ",
1950= KEYA(189)="VERS15          ",
```

AD-A066 092 GENERAL ELECTRIC CO CINCINNATI OHIO AIRCRAFT ENGINE GROUP F/G 21/5
TURBINE DESIGN SYSTEM.(U)
NOV 78 R R WYSONG, T C PRINCE, D T LENAHAN F33615-75-C-2073
UNCLASSIFIED R78AEG XXX AFAPL-TR-78-92 NL

3 OF 3
ADA
066092

END
DATE
FILMED
5 79
DDC

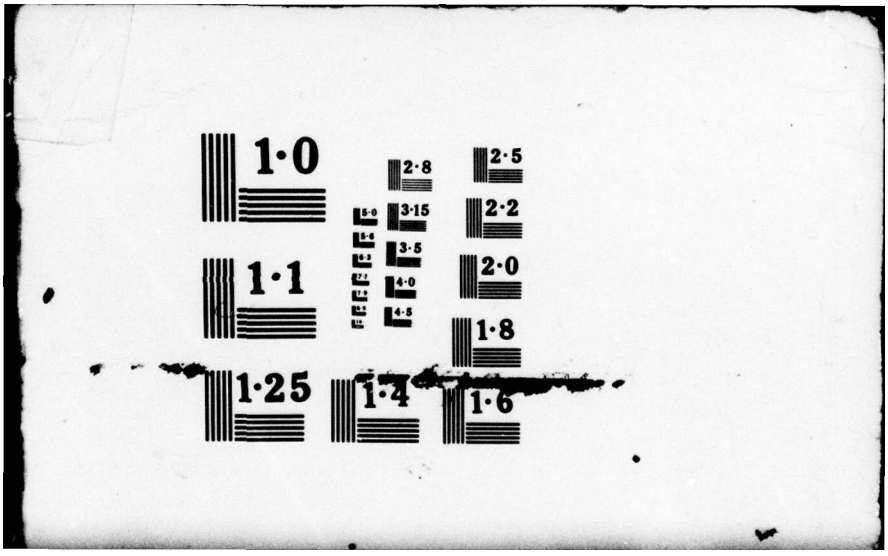
1·0
1·1
1·25
1·4
1·6
1·8
2·0
2·2
2·5
2·8
3·15
3·5
4·0
4·5

```
1960= KEYA(191)="VERS16      ",
1970= KEYA(193)="VERS17      ",
1980= KEYA(195)="VERS18      ",
1990= KEYA(197)="VERS19      ",
2000= KEYA(199)="VERS20      ",
2010= KEYA(201)="VERS21      ",
2020= KEYA(203)="VERS22      ",
2030= KEYA(205)="VERS23      ",
2040= KEYA(207)="VERS24      ",
2050= KEYA(209)="VERS25      ",
2060= KEYA(211)="VERS26      ",
2070= KEYA(213)="VERS27      ",
2080= KEYA(215)="VERS28      ",
2090= KEYA(217)="VERS29      ",
2100= KEYA(219)="VERS30      ",
2110= KEYA(221)="VERS31      ",
2120= KEYA(223)="VERS32      ",
2130= KEYA(225)="VERS33      ",
2140= KEYA(227)="VERS34      ",
2150= KEYA(229)="VERS35      ",
2160= KEYA(231)="VERS36      ",
2170= KEYA(233)="VERS37      ",
2180= KEYA(235)="VERS38      ",
2190= KEYA(237)="VERS39      ",
2200= KEYA(239)="VERS40      ",
2210= KEYA(241)="VERS41      ",
2220= KEYA(243)="VERS42      ",
2230= KEYA(245)="VERS43      ",
2240= KEYA(247)="VERS44      ",
2250= KEYA(249)="VERS45      ",
2260= KEYA(251)="VERS46      ",
2270= KEYA(253)="VERS47      ",
2280= KEYA(255)="VERS48      ",
2290= KEYA(257)="VERS49      ",
2300= KEYA(259)="VERS50      ",
2310= KEYA(261)="VERS51      ",
2320= KEYA(263)="VERS52      ",
2330= KEYA(265)="VERS53      ",
2340= KEYA(267)="VERS54      ",
2350= KEYA(269)="VERS55      ",
2360= KEYA(271)="VERS56      ",
2370= KEYA(273)="VERS57      ",
2380= KEYA(275)="VERS58      ",
2390= KEYA(277)="VERS59      ",
2400= KEYA(279)="VERS60      ",
2410= KEYA(281)="VERS61      ",
2420= KEYA(283)="VERS62      ",
2430= KEYA(285)="VERS63      ",
2440= KEYA(287)="VERS64      ",
2450= KEYA(289)="VERS65      ",
2460= KEYA(291)="VERS66      ",
2470= KEYA(293)="VERS67      ",
```

```
2480= KEYA(295)="VERS68          ",
2490= KEYA(297)="VERS69          ",
2500= KEYA(299)="VERS70          ",
2510= KEYA(301)="VERS71          ",
2520= KEYA(303)="VERS72          ",
2530= KEYA(305)="VERS73          ",
2540= KEYA(307)="VERS74          ",
2550= KEYA(309)="VERS75          ",
2560= KEYA(311)="VERS76          ",
2570= KEYA(313)="VERS77          ",
2580= KEYA(315)="VERS78          ",
2590= KEYA(317)="VERS79          ",
2600= KEYA(319)="VERS80          ",
2610= KEYA(321)="VERS81          ",
2620= KEYA(323)="VERS82          ",
2630= KEYA(325)="VERS83          ",
2640= KEYA(327)="VERS84          ",
2650= KEYA(329)="VERS85          ",
2660= KEYA(331)="VERS86          ",
2670= KEYA(333)="VERS87          ",
2680= KEYA(335)="VERS88          ",
2690= KEYA(337)="VERS89          ",
2700= KEYA(339)="VERS90          ",
2710= KEYA(341)="VERS91          ",
2720= KEYA(343)="VERS92          ",
2730= KEYA(345)="VERS93          ",
2740= KEYA(347)="VERS94          ",
2750= KEYA(349)="VERS95          ",
2760= KEYA(351)="VERS96          ",
2770= KEYA(353)="VERS97          ",
2780= KEYA(355)="VERS98          ",
2790= KEYA(357)="VERS99          ",
2800= KEYA(359)="                ",
2810= KEYA(361)="                ",
2820= KEYA(363)="                ",
2830= KEYA(365)="                ",
2840= KEYA(367)="                ",
2850= KEYA(369)="                ",
2860= KEYA(371)="                ",
2870= KEYA(373)="                ",
2880= KEYA(375)="                ",
2890= KEYS(377)="                ",
2900= KEYS(379)="                ",
2910= KEYS(381)="                "
2920= $
2921=*EOR
2922=*EOF
2923=*EOF
..
```

13.5.2 Data Storage

Two steps are involved in the transfer of data from a computer program to the integrated data base. The first step is to write the data to be transferred onto a permfile. The second step is to move the data from the permfile onto the IDB.

The functions which provide the capability of preparing data files for input to the data base and transferring those files to the data base are WRITNA and STORE, respectively.

WRITNA

This subprogram generates an image of a user's NAMELIST on a permfile which is compatible with the input routines for the data base. The data file is also NAMELIST readable.

STORE

The execution of a STORE job performs the actual transfer of a data file which has been prepared from a call to WRITNA to the data base. The store control card setup and instruction file are prepared through a series of questions and answers in the on-line program called BATCH. Following are the setup and a sample instruction file. For an explanation of the BATCH program, see Section 13.6.1. An explanation of the variables in the instruction file follows the RETRIEVE example.

BATCH-STORE

```
COMMAND- ATTACH,TAPE10,KEYDATA

 PF CYCLE NO. = 001
COMMAND- EDITOR
..EDIT,TAPE10,S
..L,A


   100= KEYS="LPTURB" "VANE01" 4*" "
   110= $TESTNA
   120= INA1= 10*1 RNA1=33.3 QNA1="OUTER" INA2=2 INA3= 2*11
   130= RNA2=6. 7. 9. INA4=4
   140= $
   150= KEYS="LPTURB" "VANE02" 4*""
   160= $TESTNA INA1=4 5 6 77 88 99
   170= QNA1="SECOND NAMELIST - TAPE10" RNA1= 11. 12. 13. 14.
   180= $
..B
COMMAND- ATTACH,BAT,BATHS

 PF CYCLE NO. = 001
COMMAND- BAT

KEY STRUCTURE?  LPTURB


FUNCTION COMPLETE.
FUNCTION DESIRED?BATCH


JOBID,PROGRAM NO.,NAME?  TDS,P750587,KUES


RETRIEVE/STORE?  STORE


FILE NAME,CYCLE NO.?  KEYDATA,1


 NAMELIST = TESTNA   KEY STRUCTURE =
LPTURB    ,VANE01    ,          ,          ,          ,          ,
GO/SKIP/STOP?  GO


READ,WRITE PASSWORDS,ALT-NAME?  VELL,TOWER,TEST01


 NAMELIST = TESTNA   KEY STRUCTURE =
LPTURB    ,VANE02    ,          ,          ,          ,          ,
GO/SKIP/STOP?  GO


READ,WRITE PASSWORDS,ALT-NAME?  VELL,RINGER,TEST03

 END OF DATA FILE.

FUNCTION COMPLETE.
FUNCTION DESIRED?DONE

     STOP
       .754 CP SECONDS EXECUTION TIME
```

13.5.3 Data Retrieval

As in the case of storage, two steps are involved in the retrieval of data. The first step is to transfer the data from the IDB to a permfile. The second is to read the data off the permfile onto a computer program. The functions which provide these capabilities are RETRIEVE and READNA, respectively.

RETRIEVE

The execution of a RETRIEVE job performs the actual transfer of data from the IDB to a permfile. This file is NAMELIST readable. The control card setup and instruction file are prepared through a series of questions and answers in the on-line program BATCH. Below are the control setup and a sample instruction file.

READNA

This subprogram reads the data from the permfile created by RETRIEVE into the NAMELIST variables of the user's computer program.

```
COMMAND- ATTACH,BAT,BATHS

 PF CYCLE NO. = 001
COMMAND- BAT

KEY STRUCTURE?  HPTURB,VANE01,,VERS04

FUNCTION DESIRED?BATCH

JOBID,PROGRAM NO.,NAME?  TDS,P750587,KUES

RETRIEVE/STORE?  RETRIEVE

FILE NAME,CYCLE NO.?  RETOUT,1

NAMELIST NAME,READ PASSWORD,ALT-NAME?TEST01,VELL

NAMELIST NAME,READ PASSWORD,ALT-NAME?TEST03,VELL,TESTA1


NAMELIST NAME,READ PASSWORD,ALT-NAME?DONE

FUNCTION COMPLETE.
FUNCTION DESIRED?DONE

     STOP
       .105 CP SECONDS EXECUTION TIME
```

Namelist "KEYNL" Definition

KEYS	- 6-word array in which the 10-character keys are defined (corresponding to the 6 key levels for the data base). Defines the key structure for the NAMELIST to be stored/ retrieved.
NLNAME	- The name of the namelist to be stored/retrieved.
IPWR	- The read password for the namelist to be stored/retrieved.
IPWW	- The write password for the namelist to be stored.
NSUB	- Sequential occurrence on the buffer file of the "NLNAME" NAMELIST which is to be stored on the data base.
NEWNAM	- Alternate NAMELIST NAME - Store-name used on IDB - Retrieve-name used on buffer file
IPRINT	- If input is zero, no printout of the data stored/retrieved will be generated

13.6 ON-LINE FUNCTIONS

There are two on-line programs. The first, called BATCH, is used to build the control card and instruction files, discussed in Section 13.4, to be used in storing data to or retrieving data from the IDB. The second program, called COMMAND, allows the user direct access to the IDB for querying and editing.

13.6.1 BATCH

When using the on-line BATCH program to build a retrieval setups file, only the program itself must be attached. In the case of a store, both the program and the namelist key and data file created by the user's calls to WRITNA must be attached. The following pages contain examples of both uses of the program.

TAPE8 is the output file created by the on-line BATCH program.

```
EDIT,TAPE8,S

..L,A

   100=TDS  ,T20,I050,CMI 25000,SICSA. P750587,KUES
   110=ATTACH,D0,DBFILS,CY=1.
   120=ATTACH,D1,DBFILS,CY=2.
   130=ATTACH,D2,DBFILS,CY=3.
   140=ATTACH,STORDB,STORHS.
   150=ATTACH,STAPIO,KEYDATA ,CY=  1.
   160=COPYBF(STAPIO,TAPEIO)
   170=REWIND(TAPEIO)
   180=STORDB.
   190=*EOR
   200= $KEYNL
   210= KEYS(1)=10HLPTURB     ,10HVANE01     ,10H           ,10H          ,
   220= KEYS(5)=10H           ,10H           ,
   230= NLNAME=7HTESTNA ,NSUB= 1,
   240= IPWR=6HVELL   ,IPWW=6HTOWER ,NEWNAM=7HTEST01 ,
   250= $
   260= $KEYNL
   270= KEYS(1)=10HLPTURB     ,10HVANE02     ,10H           ,10H          ,
   280= KEYS(5)=10H           ,10H           ,
   290= NLNAME=7HTESTNA ,NSUB= 2,
   300= IPWR=6HVELL   ,IPWW=6HRINGER,NEWNAM=7HTEST03 ,
   310= $
..B

COMMAND- BATCH,TAPE8,INPUT,HERE
```

RETRIEVE

TAPE8 is the output file created by the on-line BATCH program.

```
COMMAND- EDITOR

..EDIT,TAPE8,S

..L,A

   100=TDS   ,T20,I050,CMI25000,STCSA. P750587,KUES
   110=ATTACH,D0,DBFILS,CY=1.
   120=ATTACH,D1,DBFILS,CY=2.
   130=ATTACH,D2,DBFILS,CY=3.
   140=ATTACH,RETRDB,RETRHS.
   150=REQUEST,TAPE10,*PF.
   160=RETRDB.
   170=CATALOG,TAPE10,RETOUT  ,CY=  1,RP=30.
   180=*EOR
   190= $KEYNL
   200= KEYS(1)=10HHPTURB     ,10HVANE01     ,10H           ,10HVERS04     ,
   210= KEYS(5)=10H           ,10H           ,
   220= NLNAME=7HTEST01 ,IPWR=6HVELL  ,NEWNAM=7H        ,
   230= $
   240= $KEYNL
   250= KEYS(1)=10HHPTURB     ,10HVANE01     ,10H           ,10HVERS04     ,
   260= KEYS(5)=10H           ,10H           ,
   270= NLNAME=7HTEST03 ,IPWR=6HVELL  ,NEWNAM=7HTESTA1 ,
   280= $
..B

COMMAND- BATCH,TAPE8,INPUT,HERE
```

13.6.2 COMMAND

In order to run the on-line COMMAND program, the three data base files must be attached along with the program itself. The following pages contain explanations and examples of the functions available. The EDIT functions precede the QUERY functions which are followed by three utility functions. For all EDIT functions both the read and write passwords must be known. Only the read password need be known to perform the QUERY functions.

A special response that is used across most functions is the word END. It is used to move to a higher level question within a function or to leave a function entirely. Its usage is included in the examples.

```
COMMAND- ATTACH,D0,DBFILS,CY=1

COMMAND- ATTACH,D1,DBFILS,CY=2

COMMAND- ATTACH,D2,DBFILS,CY=3

COMMAND- FILE(D0,FO=IS,BFS=320)

COMMAND- FILE(D1,FO=IS,BFS=384)

COMMAND- FILE(D2,FO=IS,BFS=384)

COMMAND- ATTACH,CMD,CMDHS

 PF CYCLE NO. = 003
COMMAND- CMD

KEY STRUCTURE?  HPTURB,VANE01,,VERS04
```

ADD NA performs the EDIT function of adding a namelist, with read and write passwords, to a given key structure.

```
FUNCTION DESIRED?ADD NA

NAMELIST,READ,WRITE PASSWORDS?  TEST01,VELL,TOWER

VARIABLE,DIMENSION?  INT1,8

DATA? 81,82,83,84,85,86,87,88,

VARIABLE,DIMENSION?  REAL,1

DATA? 100.5,

VARIABLE,DIMENSION?  QCHAR,3

DATA? TURBINE DESIGN TEST VARIABLE

VARIABLE,DIMENSION?  END

NAMELIST,READ,WRITE PASSWORDS?  TEST02,SEPT,1977

VARIABLE,DIMENSION?  INT2,1

DATA? 5,

VARIABLE,DIMENSION?  REAL,10

DATA? 1,2,3,4,5,6,7,8,9,10,

VARIABLE,DIMENSION?  Q21,1

DATA? TURBINE

VARIABLE,DIMENSION?  END

NAMELIST,READ,WRITE PASSWORDS?  TEST03,VELL,RINGER

VARIABLE,DIMENSION?  Q31,4

DATA? SAME READ PASSWORD, NEW WRITE PASSWORD.

VARIABLE,DIMENSION?  END

NAMELIST,READ,WRITE PASSWORDS?  END

FUNCTION COMPLETE.
```

ADD VA performs the EDIT function of adding a variable to an existing namelist.

```
FUNCTION DESIRED?ADD VA

NAMELIST,READ,WRITE PASSWORDS?  TEST01,VELL,TOWER

VARIABLE,DIMENSION?  Q2,4

DATA? CHARACTER VARIABLE ADDED THRU ADD VA

VARIABLE,DIMENSION?  END

NAMELIST,READ,WRITE PASSWORDS?  END

FUNCTION COMPLETE.
```

REP VA performs the EDIT function of deleting a variable from a namelist and replacing it with a new variable with the same or different name and dimension.

```
FUNCTION DESIRED?REP VA

NAMELIST,READ,WRITE PASSWORDS?  TEST01,VELL,TOWER

VARIABLE TO BE DELETED?  INT2

VARIABLE,DIMENSION TO BE INSERTED?  INT22,5

DATA? 10,20,30,

DATA? 40,50,

FUNCTION COMPLETE.
```

DEL NA performs the EDIT function of deleting a namelist, with read and write passwords, from a given key structure.

```
FUNCTION DESIRED?DEL NA

NAMELIST,READ,WRITE PASSWORDS?  TEST03,VELL,RINGER


FUNCTION COMPLETE.
FUNCTION DESIRED?LIST

READ PASSWORD?  VELL

NAMELISTS

  TEST01

FUNCTION COMPLETE.
```

DEL VA performs the EDIT function of deleting a variable from an existing namelist.

```
FUNCTION DESIRED?DEL VA

NAMELIST,READ,WRITE PASSWORDS?  TEST02,SEPT,1977

VARIABLE TO BE DELETED?  REAL

VARIABLE TO BE DELETED?  END


FUNCTION COMPLETE.
FUNCTION DESIRED?LIST N

NAMELIST NAME,READ PASSWORD?  TEST02,SEPT


 NAMELIST - TEST02

  INT2     -      1 -
  Q21      -      1 -

FUNCTION COMPLETE.
```

NEWPAS performs the EDIT function of changing either or both passwords of a given namelist.

```
FUNCTION DESIRED?NEWPAS

NAMELIST,CURRENT READ,WRITE PASSWORDS?  TEST01,VELL,TOWER

NEW READ,WRITE PASSWORDS?  VELL,BRIDGE

NAMELIST,CURRENT READ,WRITE PASSWORDS?  END

FUNCTION COMPLETE.
```

LIST performs the QUERY function of listing all namelist names for a given key structure and read password.

```
FUNCTION DESIRED?LIST

READ PASSWORD?  VELL

NAMELISTS

  TEST01
  TEST03

FUNCTION COMPLETE.
```

LIST N performs the QUERY function of listing the structure (variable names and dimensions) of a given namelist under a given key structure and read password.

```
FUNCTION DESIRED?LIST N

NAMELIST NAME,READ PASSWORD?  TEST01,VELL

 NAMELIST - TEST01

  INT1     -     8 -
  REAL     -     1 -
  QCHAR    -     3 -
  Q2       -     4 -

FUNCTION COMPLETE.
```

SCAN performs the QUERY function of listing all namelist names and their structures for a given key structure and read password.

```
FUNCTION DESIRED?SCAN

READ PASSWORD?  VELL

 NAMELIST - TEST01

  INT1     -     8 -
  REAL     -     1 -
  QCHAR    -     3 -
  Q2       -     4 -

 NAMELIST - TEST03

  Q31      -     4 -

FUNCTION COMPLETE.
```

SCAN N performs the QUERY function of listing the structure and data contents of a given namelist under a given key structure and read password. SCAN N also can be used to list the structure and contents of one variable of a namelist. Examples of both uses are shown.

```
FUNCTION DESIRED?SCAN N

NAMELIST NAME,READ PASSWORD,VARIABLE NAME?  TEST02,SEPT


 NAMELIST - TEST02

  INT2    -     1 -
       5,

  REAL    -    10 -
  1.00000E+00,  2.00000E+00,  3.00000E+00,  4.00000E+00,  5.00000E+00,
  6.00000E+00,  7.00000E+00,  8.00000E+00,  9.00000E+00,  1.00000E+01,

  Q21     -     1 -
TURBINE

FUNCTION COMPLETE.

FUNCTION DESIRED?SCAN N

NAMELIST NAME,READ PASSWORD,VARIABLE NAME?  TEST02,SEPT,Q21


 NAMELIST - TEST02

  Q21     -     1 -
TURBINE

FUNCTION COMPLETE.
```

KEYS causes the user's current key structure to be displayed.

```
FUNCTION DESIRED?KEYS

** CURRENT KEY STRUCTURE **

HPTURB    , VANE01    ,           , VERS04    ,           ,

FUNCTION COMPLETE.
```

CATALOG causes all valid keys for a requested level to be displayed. To exit from this function, respond-1 to KEY LEVEL?

```
FUNCTION DESIRED?CATLOG

KEY LEVEL?  2

  * VALID KEYS ARE-

FLOPTH    , VANE01    , VANE02    , VANE03    , VANE04    , VANE05    ,
VANE06    , VANE07    , VANE08    , VANE09    , VANE10    , BLAD01    ,
BLAD02    , BLAD03    , BLAD04    , BLAD05    , BLAD06    , BLAD07    ,
BLAD08    , BLAD09    , BLAD10    ,

KEY LEVEL?  1

  * VALID KEYS ARE-

HPTURB    , LPTURB    ,

KEY LEVEL?  -1

FUNCTION COMPLETE.
```

DONE, when entered at the FUNCTION level, terminates the program.

```
FUNCTION DESIRED?DONE

PROGRAM STOP.
   EXIT
       .430 CP SECONDS EXECUTION TIME
```

13.7 LIMITATIONS

Some current program limits are:

1. Namelist names - 7 characters
2. Passwords - 7 characters
3. Variable names - 7 characters
4. Maximum dimension of a variable being added on-line - 450 words
5. Maximum number of variables in one NAMELIST set in a batch store - 25
6. Maximum size of all data for one NAMELIST set in a batch store - 948 words

13.8 GLOSSARY

For the nonprogramming user, this list should help clarify some of the frequently used terms in this section.

DATA BASE - A structured collection of information on a computer storage device.

MANAGEMENT SYSTEM - The *software* which governs transactions with the data base.

APPLICATION PROGRAMS - Specialized user-generated software which utilizes the functions provided in the management system.

KEY TREE - A logical hierarchy defining the placement of data on the data base.

MASTER CATALOG - A catalog within the data base which contains the entire set of keys available at all levels of the key tree.

KEY - A word or abbreviation of up to 10 characters identifying a logical location within a level of the key tree.

KEY STRUCTURE - A combination of keys which locates a data set on the key tree.

DATA SET - An organized collection of data which is generally related by its applicability to some problem or process.

NAMELIST - A commonly used facility to identify a data set.

FUNCTION - A specific operation on a data set.

14.0 CONCLUSIONS

The foregoing sections of this volume have dealt with the calculation procedures employed in the major modules of the Turbine Design System. They provide a record of the level of effort which is involved in a preliminary design phase of a turbine design project. Furthermore, they provide insights to the system user in understanding and interpreting the results at each step along the way.

It should be clear that the modular arrangement of the system provides the flexibility necessary for the iterative interactions which are natural characteristics of the design process involving multi-discipline requirements and decisions. Having this calculation system in a computer time-sharing environment and coupling it with the input/output data handling features provided, results in a potential for increased engineering productivity and an opportunity for greater in-depth penetration on a new design before having to commit to a final detailed design phase.

REFERENCES

1. Wysong, R.R., "Detail Design of Free Vortex Turbines," M.S. Thesis, 1964, University of Cincinnati. Published as ASTIA AD-8061-9079.

2. Fremont, H.A., et. al., Properties Of Combustion Gases, AGT Div., General Electric Company, 1955.

3. Colley, W.C. Ferguson, D.R., and Smith, M.A., "Development of Emissions for Afterburning Turbine Engines," AFAPL-TR-75-52, October 1975.

4. Powell, H.N. Shaffer, A, and Suciu, S.N., "Properties of Combustion Gases, System: Cr H_{2n} - Air," General Electric Company, 1955.

5. Carnahan, B., Luther, H.A., and Wilkes, J.O., Applied Numerical Methods, John Wiley & Sons, New York, 1969.

6. Giles, G.L., "Digital Computer Programs for Generating Oblique Orthographic Projections and Contour Plots," NASA TN D-7797, Langley Research Center, January 1975.

7. Smith, L.H., Jr., "The Radial-Equilibrium Equation of Turbo-Machinery," Journal of Engineering for Power, Trans. ASME, Series A, Vol. 88, 1966, pp. 1-12.

8. Novak, R.A., "Streamline Curvature Computing Procedures for Fluid Flow Problems," ASME Paper 66--WA/GT-3, 1966.

9. Katsanis, T., "Use of Arbitrary Quasi-Orthogonals for Calculating Flow Distribution in the Meridional Plane of a Turbomachine," NASA TN D-2546, 1964.

10. Murman, E.M., and Cole, J.D., "Calculation of Plane Steady Transonic Flows," AIAA Journal, Vol. 9, No. 1, January 1971, pp. 114-121.

11. Keith, J.S., "BEAM: A Computer Procedure for Fitting a Piecewise Continuous Curve and Evaluating Angle and Curvature," General Electric TM No. 74-679, 9-20-74. (Also contained in Section 5.2.1 of NASA CR-2217, July 1973.)

12. Poferl, D.J. and Svebla, P.A., "Thermodynamic and Transport Properties of Air and its Products of Combustion with ASTM-A-1 Fuel and Natural Gas at 20, 30, and 40 Atmospheres," National Aeronautics and Space Administration Technical Note TN D-7488, December 1973.

*U.S.Government Printing Office: 1979 — 657-002/374